Measurement of the W-boson mass at 7 TeV

Stefano Camarda

CAT physics meeting – 23 Sept 2016

Measurement of the W-boson mass - Overview

- Introduction: motivation and experimental context
- Measurement overview
- Results
- Detailed discussion of the analysis

Precision measurements of EW parameters

- After the measurement of the Higgs mass, all the free parameters of the Standard Model are known
- Relations between electroweak observables can be predicted (almost) at 2-loop level

Precise measurements of the EW parameters allow

- Stringent test of self consistency of the SM
- Look for hints of BSM physics

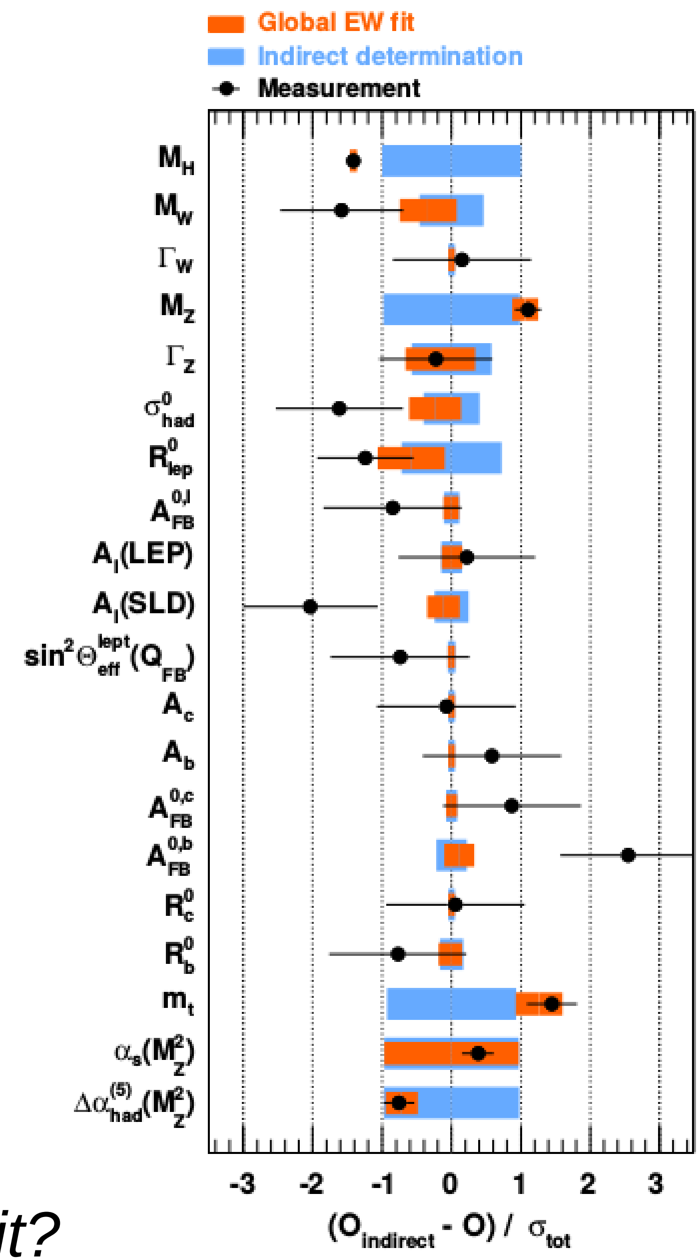

Why is m_W of special importance in the EW fit?

Eur.Phys.J. C74 (2014) 3046

Measurement of the W mass

The EW sector of the SM, relates M_W to α, G_F, and $\sin^2\theta_W$

$$M_W^2 = \frac{\pi\,\alpha_{EM}}{\sqrt{2}\,G_F\,(1 - M_W^2/M_Z^2)\,(1 - \Delta r)}$$

Radiative corrections Δr are dominated by Top and Higgs loops

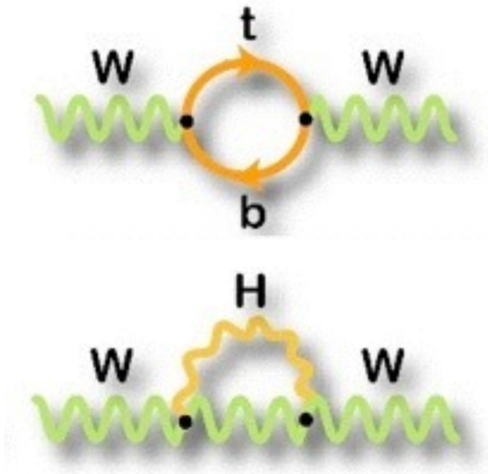

- The relation between M_{top}, M_H and M_W provides a stringent test of the SM
- The comparison between the measured M_H and the predicted M_H is sensitive to new physics

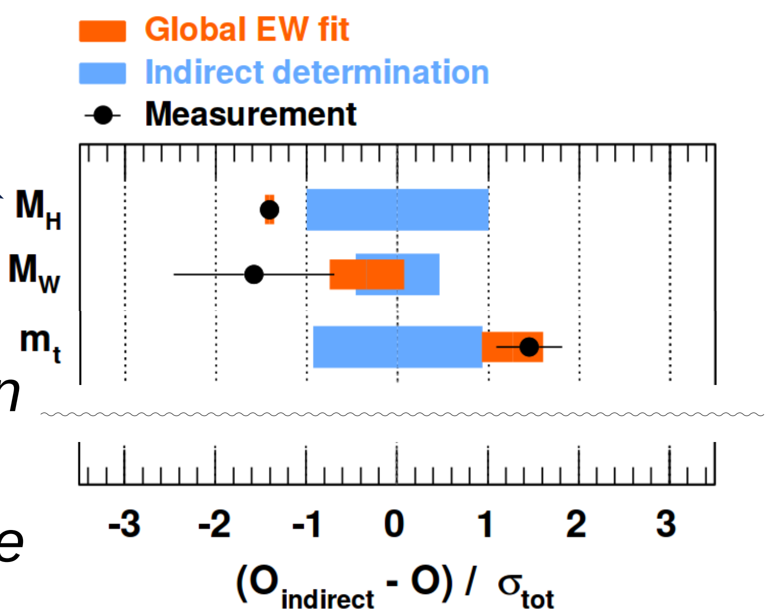

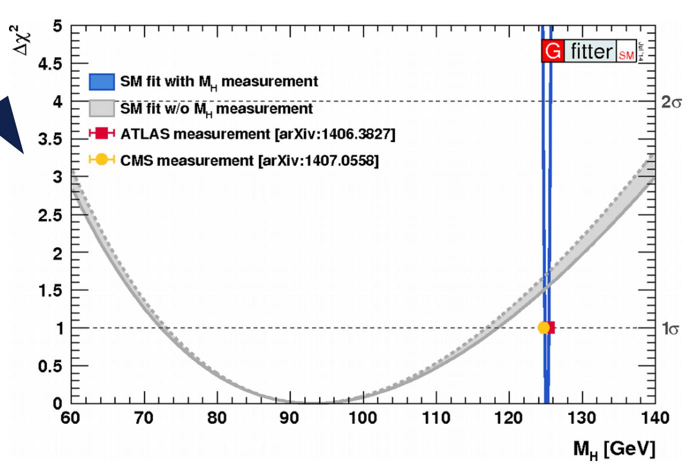

Indirect determination of M_W (±8 MeV) is more precise than the experimental measurement

Call for $\delta M_W^{exp} < 10$ MeV

Experimental measurements at colliders

- The W mass can be measured from:
- Kinematic properties of decay leptons in the final state in $pp \to W \to l\nu$ processes (hadron colliders)
- Direct reconstruction from the final state in $ee \to WW \to qqqq/qql\nu$ (e+e- colliders)
- W-pair production at thresholds (e+e- colliders)

SPS, Tevatron, LHC

LEP best measurements

Limited by stat at LEP, but most precise prospect

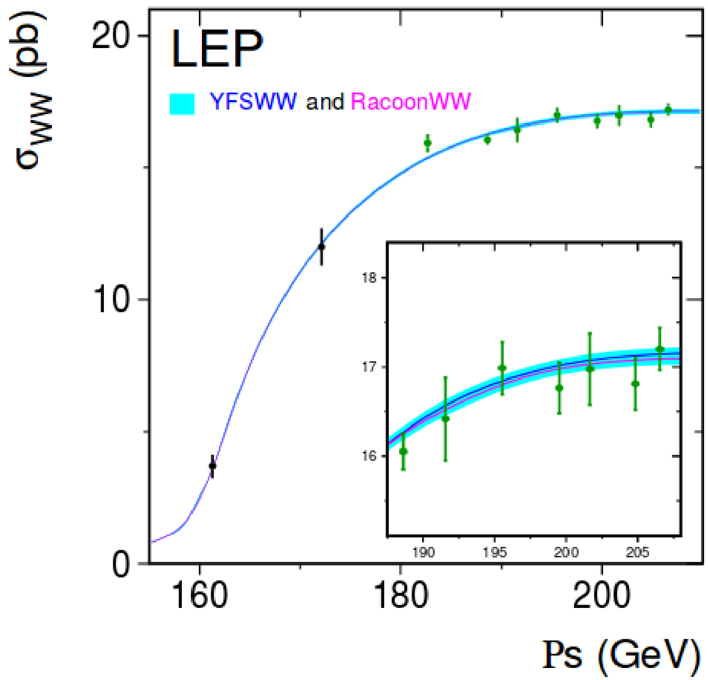

Experimental background – W mass history

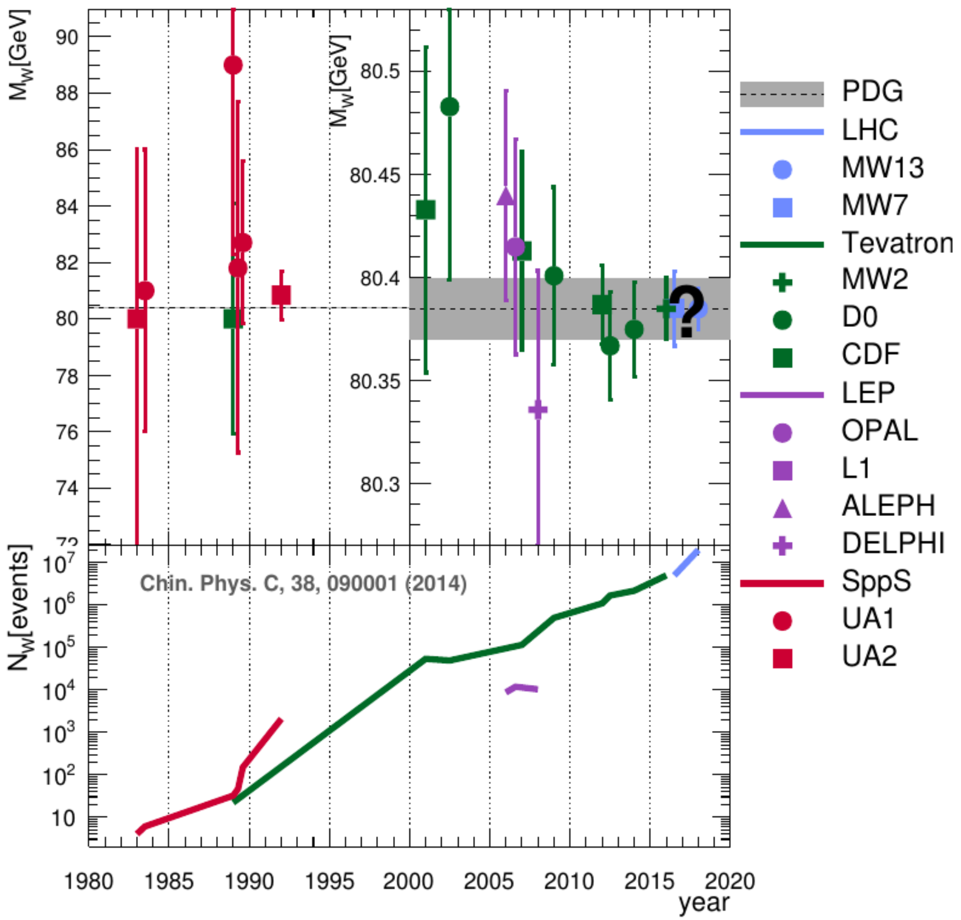

- 1983 CERN SPS – W discovery
- 1983 – UA1

  mW = 81 ± 5 GeV
- 1992 – UA2 (with mZ from LEP)

  mW = 80.35 ± 0.37 GeV
- 2013 – LEP

  mW = 80.376 ± 0.033 GeV
- 2013 – Tevatron

  mW = 80.387 ± 0.016 MeV

Experimental context – W mass status

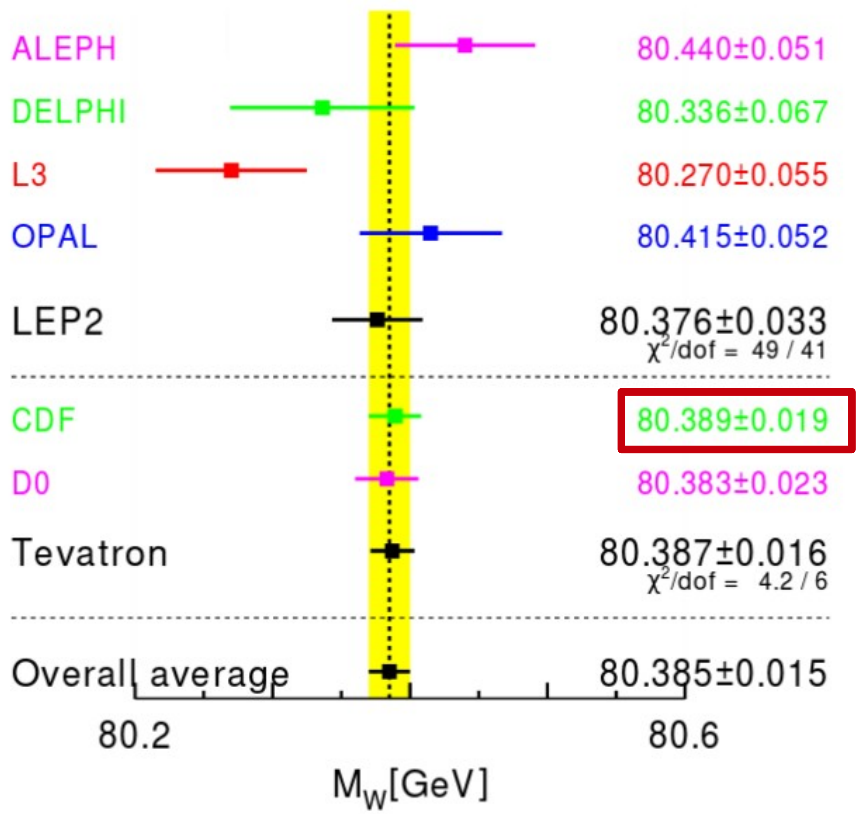

- The world average has an uncertainty of 15 MeV, and is currently dominated by CDF and D0
- This was quite a surprise, The Tevatron was built to discover the top quark, not to do a precise measurement of W mass
- But precision comes at a price: the W-mass measurements at CDF and D0 are known as the longest measurements in HEP, they lasted about 7 years

W mass – future prospects

m_W can be measured at e^+e^- colliders through an energy scan of the WW production threshold

Near threshold, the WW cross section is proportional to the non-relativistic W velocity

$$\sigma(WW) \propto \beta_W$$

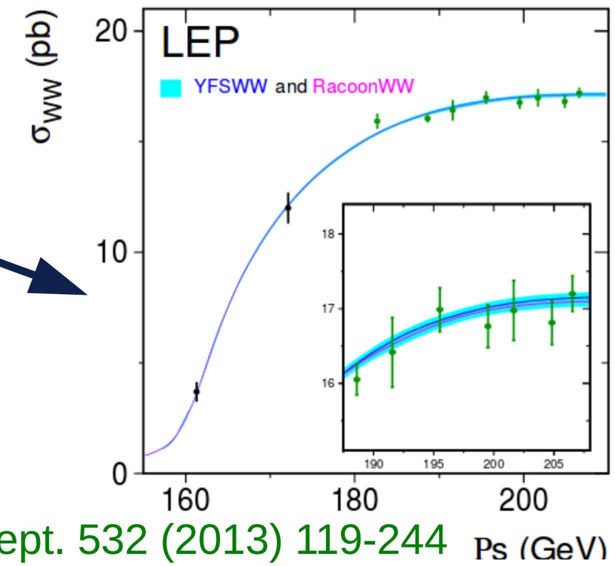

Phys.Rept. 532 (2013) 119-244

arXiv:1306.6352

ILC Giga-Z program

- Energy scan 160 to 170 GeV
- δM_W = 6-7 MeV

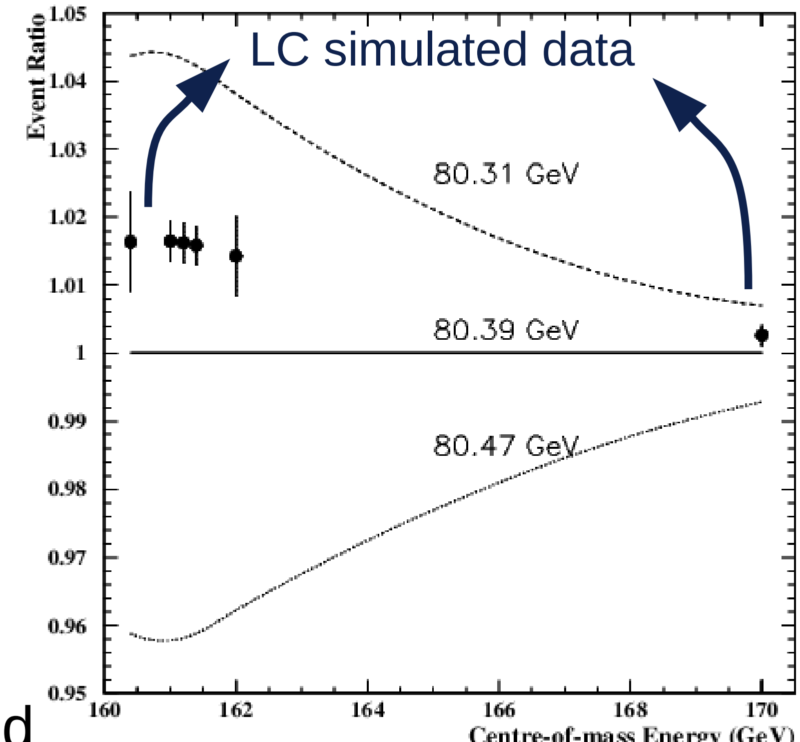

LC-PHSM-2001-009

JHEP 1401 (2014) 164

TLEP OkuW program

- δM_W = 0.5 MeV

  → dominated by statistical uncertainty

Dominant theory uncertainties

- Initial state QED corrections
- Parametrization of cross section near threshold

W mass status – present

80389 ± 19 MeV → current best single measurement (CDF)

80385 ± 15 MeV → world average (PDG)

80358 ± 8 MeV → indirect determination from the EW fit (GFitter)

W mass at the LHC

- The LHC was not built to measure the W mass, but to discover new physics with direct searches
- Indeed, a proton-proton collider is the most challenging enviroment to measure m_W, worse compared to e+e- and proton-antiproton
- The important difference between Tevatron and LHC, is that in $p\bar{p}$ collisions W production is dominated by valence quarks, while in pp the sea quarks and the heavy quarks are important contribution
- This difference affects all aspects of the measurement, detector calibration, transfer from Z to W, PDF uncertainties, W polarisation, modelling of p_T W
- The measurement of m_W at the LHC is extremely challenging and prone to biases due to QCD effects. Need to design the measurement to be "waterproof" from the point of view of detector calibration and physics modelling
- At the same time, the challenge makes it very interesting, and provides a great occasion to test and learn QCD

W mass at the LHC - Psychological profile

Are you?

Optimist

Pessimist

W mass at the LHC - Psychological profile

Are you?

Optimist

Eur. Phys. J. C (2008) 57: 627–651
DOI 10.1140/epjc/s10052-008-0774-4

Special Article - Scientific Note

Re-evaluation of the LHC potential for the measurement of m_W

Nathalie Besson[1], Maarten Boonekamp[1,a], Esben Klinkby[2], Sascha Mehlhase[2], Troels Petersen[2,3]

2008 δm_W = 7 MeV

Pessimist

Eur. Phys. J. C (2010) 69: 379–397
DOI 10.1140/epjc/s10052-010-1417-0

Regular Article - Experimental Physics

$\Delta M_W \leq 10$ MeV/c^2 at the LHC: a forlorn hope?*

M.W. Krasny[1,a], F. Dydak[2], F. Fayette[1], W. Płaczek[3], A. Siódmok[1,3]

2010 δm_W = 100-150 MeV

Measurement strategy

- m_W extracted with template fits to p_T lepton and transverse mass (m_T)
- Physics modelling
- Calibration
- Z-boson cross checks
- Background
- Combination

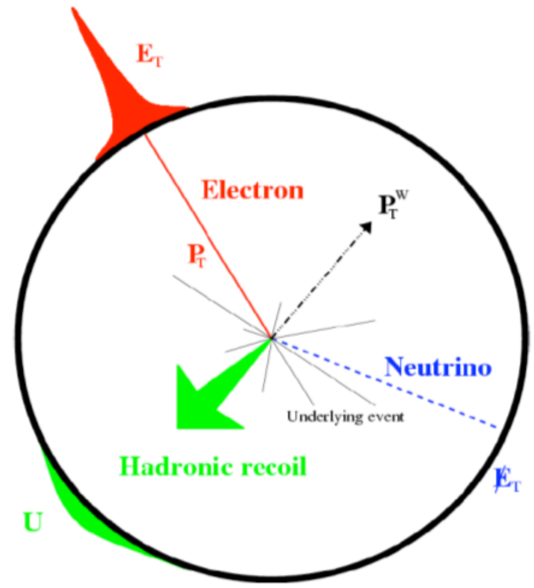

Measurement strategy

- m_W extracted with template fits to p_T lepton and transverse mass (m_T)
- Build the physics modelling by supplementing the MC samples with higher-order corrections and fits to DY ancillary measurements
- Use $Z \rightarrow ll$ events to calibrate the detector response to the energy scales and resolutions of the leptons and of the recoil

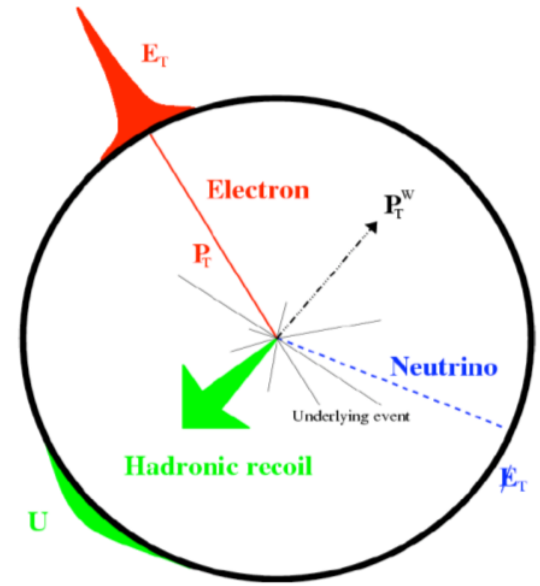

- Validate the physics modelling and the calibration by extracting m_Z from the Z sample
- Estimate and subtract the backgrounds in the W sample
- Extract m_W in several categories and combine

Definitions, Event selection, blinding

- The recoil is the vector sum of the transverse energy of all the calorimeter clusters. u_T is a measure of p_T W

$$\vec{u}_{\mathrm{T}} = \sum_i \vec{E}_{\mathrm{T},i},$$

- upar and uperp are the parallel and perpendicular projections of the recoil on the charged lepton (W events) or on the dilepton p_T (Z events)

- p_T nu is inferred from the momentum imbalance in the transverse plane

$$\vec{p}_{\mathrm{T}}^{\,\mathrm{miss}} = -\left(\vec{p}_{\mathrm{T}}^{\,\ell} + \vec{u}_{\mathrm{T}}\right)$$

- m_W in the MC is blinded by an additive offset of 80399 MeV +- b with b a random number in [-100,100] MeV

Event selection

- p_T lepton > 30 GeV
- $|\eta|$ lepton < 2.4
- m_T > 60 GeV
- $p_T$miss > 30 GeV
- u_T < 30 GeV

Measurement strategy - categories

- A crucial aspect of the measurement design is the categorisation
- The importance of categories is twofold
  - Validate detector calibration and physics modelling
  - Improve accuracy
- The various set of categories are sensitive to different experimental and theoretical biases, the consistency of m_W across categories validates our knowledge of the detector and of QCD
- The measurement is ready for unblinding only when all the categories yield consistent values of m_W
- The experimental and theoretical uncertainties have different correlation or anticorrelation patterns, the categorisation allows to constrain them, and increase the sensitivity to m_W

Measurement strategy - categories

- Categories used for the combination (28 in total)
  - p_T lepton – m_T
  - Electrons – muons
  - $|\eta|$ lepton bins
  - W+ – W-
- Categories used for cross checks
  - Average $\langle\mu\rangle$ (pile-up)
  - Recoil u_T (measure of the p_T of the W-boson)
  - upar (projection of the recoil on the charged lepton)

Measurement strategy – categories p_T lepton – m_T

p_T lepton is almost insensitive to the recoil, and very sensitive to p_TW modelling, polarisation, PDFs

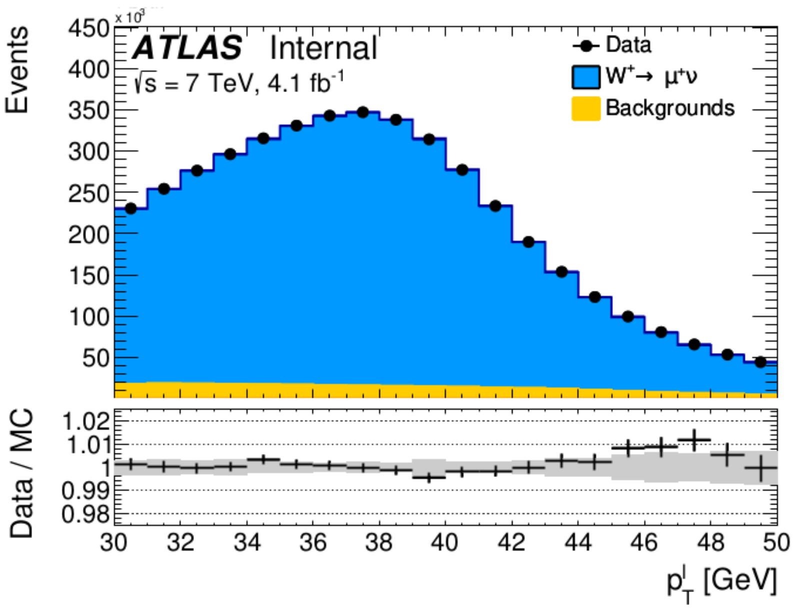

m_T is sensitive to the recoil, and less sensitive to p_TW modelling, polarisation, PDFs

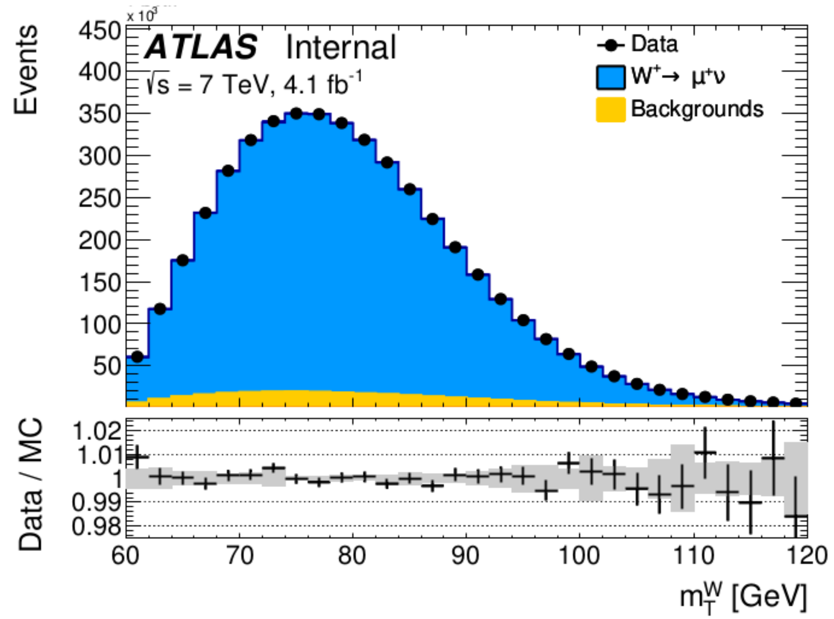

- Biases in the QCD modelling would produce discrepancies between p_T lepton and m_T determinations of mW
- Biases in the recoil calibration affects m_T, but leaves p_T lepton almost invariant

Measurement strategy – categories e – μ

- Electron and muon decay channels independently test
  - Muon momentum and electron energy calibrations
  - Efficiencies scale factors
  - Multijet background estimation

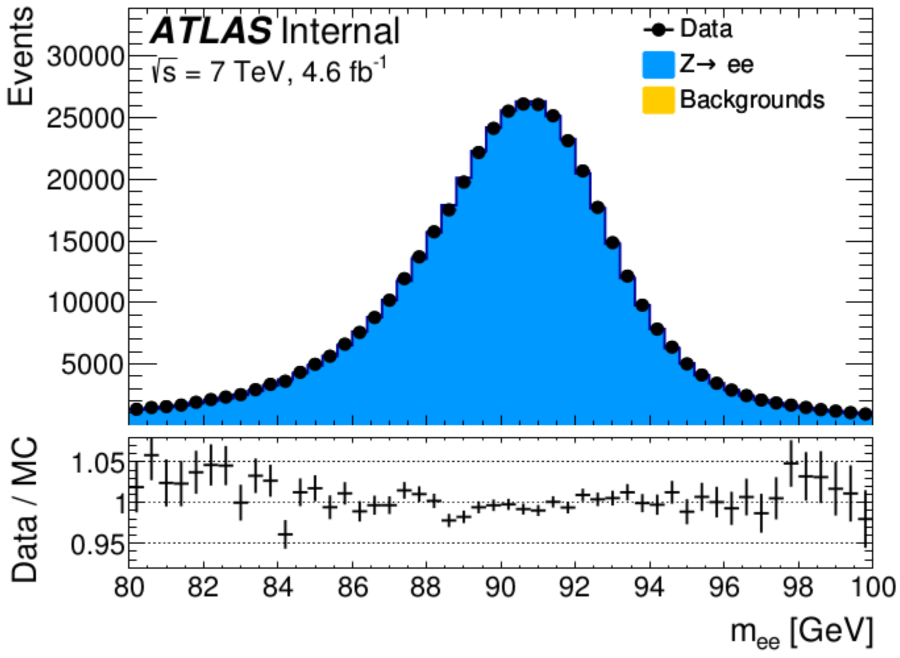

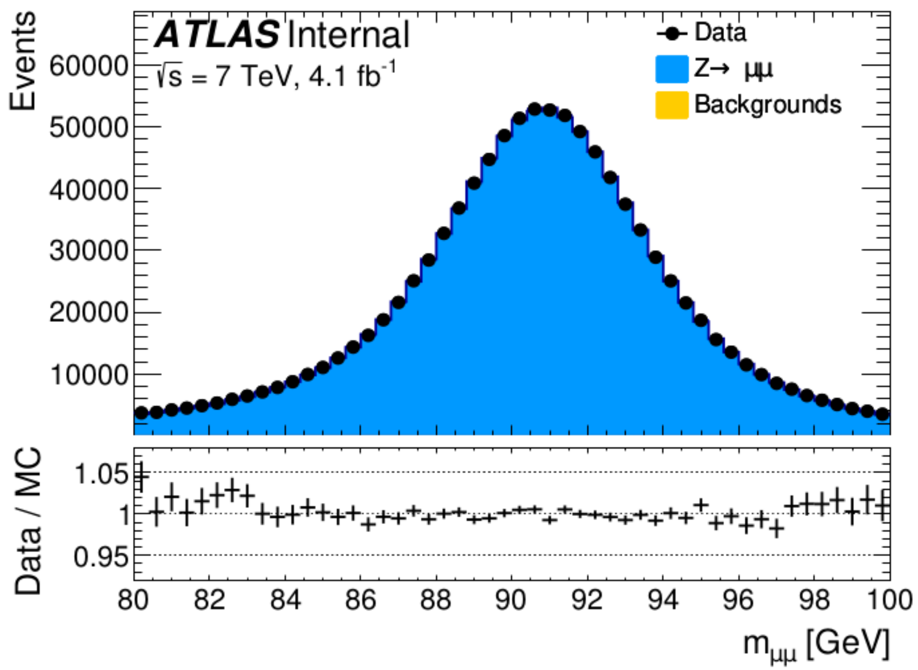

Measurement strategy – categories W+ – W-

- Positively- and negatively-charged W bosons and |η| lepton bins
  - W+ and W- have different helicity states, and are produced by different valence and sea quark flavours in the initial state
  - Charm-initiated production is relatively larger for W-
  - |η| lepton bins are sensitive to PDFs
- Biases in the modelling of the W polarisation or of heavy-quark-initiated production would produce discrepancies between W+ and W- determinations of m_W
- Some of the PDF uncertainties are anticorrelated between W+ and W-, and between |η| bins. The combination constrains PDF uncertainties

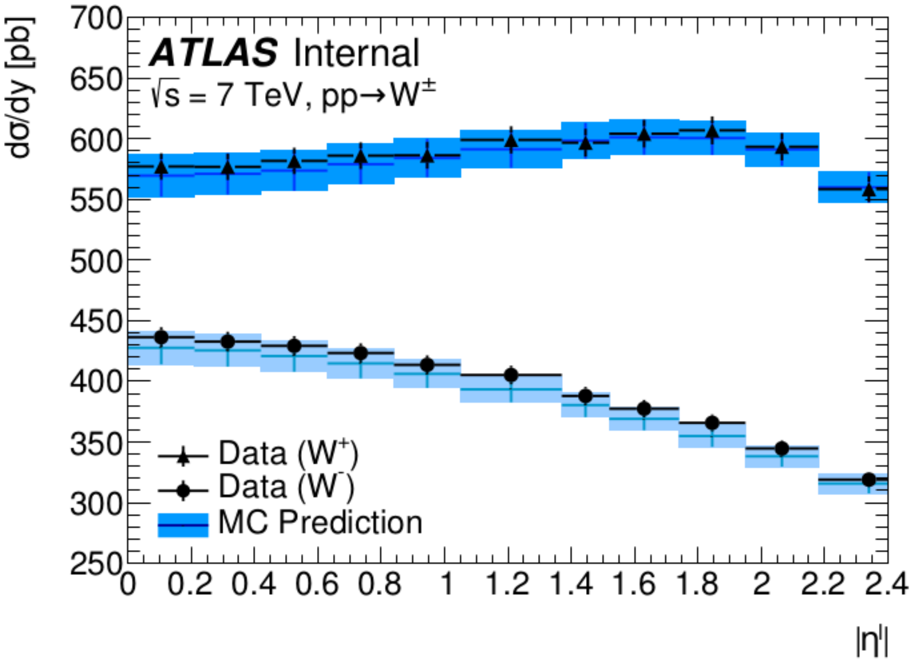

Measurement strategy - categories

- Average <μ> → Validate recoil and leptons calibration
- Recoil bins (u_T) → Validate p_T W modelling and recoil calibration
- Upar bins → Validate p_T W modelling

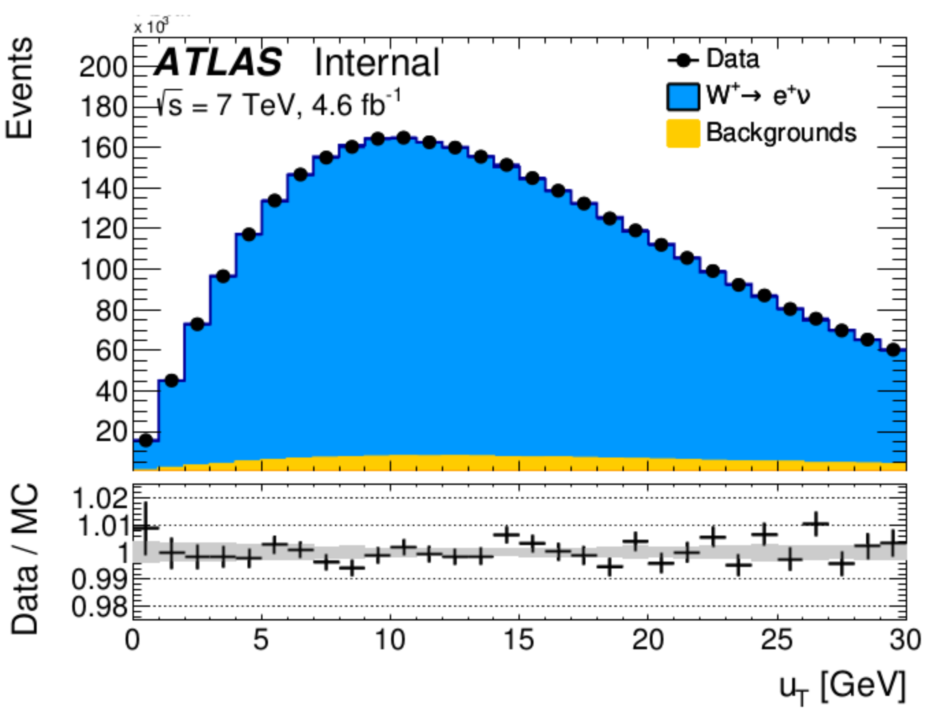

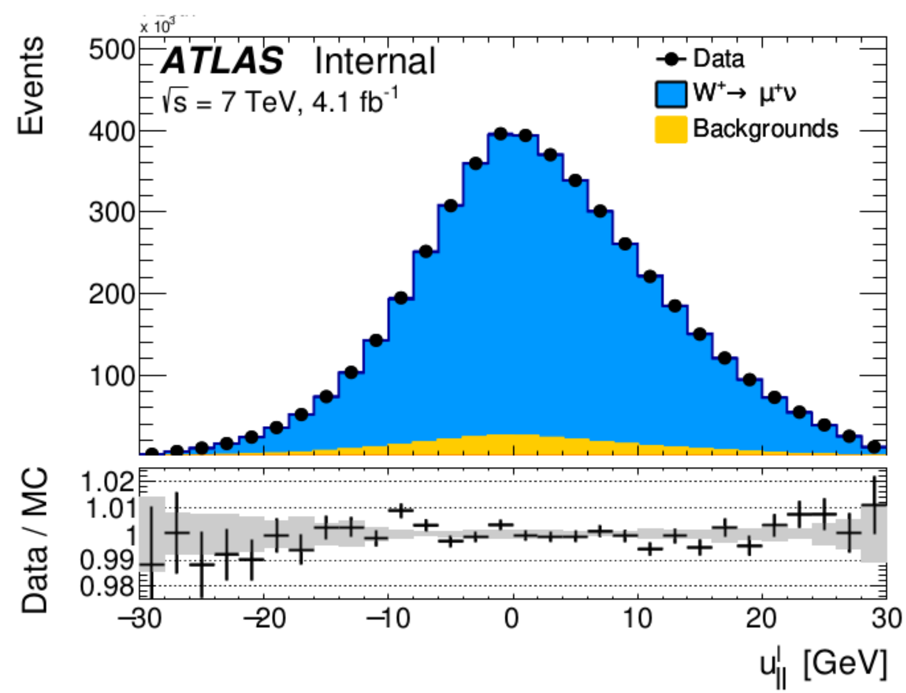

Measurement strategy – categories e – μ

- Status as of December 2015: 50 MeV discrepancy between electrons and muons

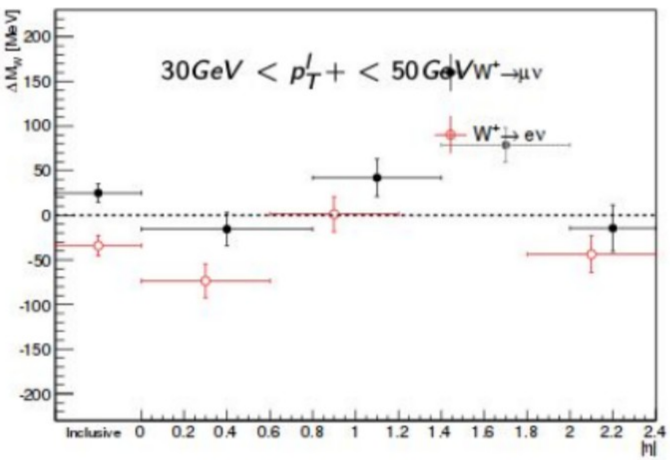

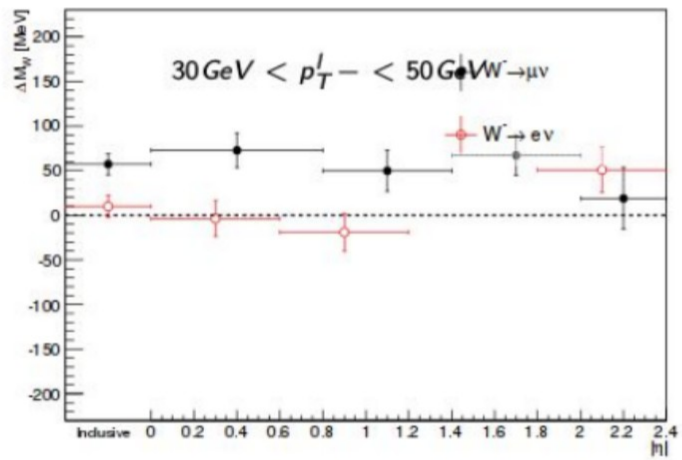

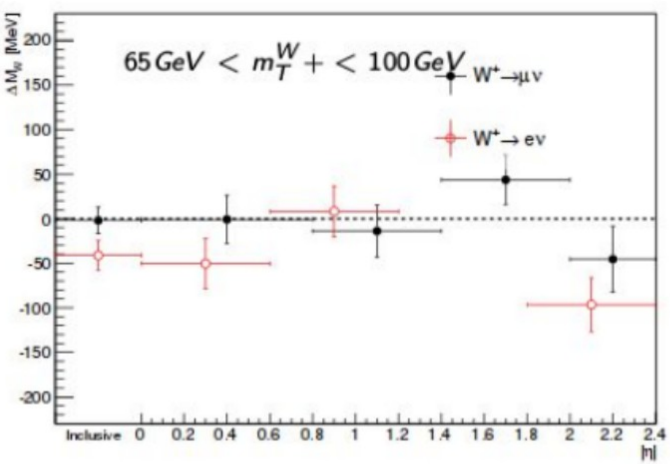

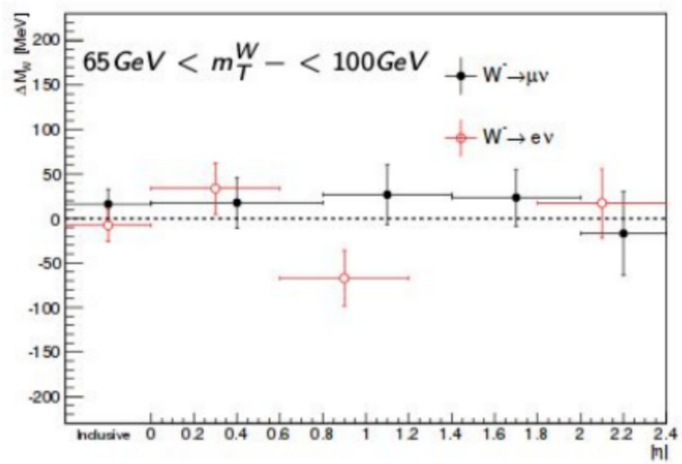

Measurement strategy – e m categories

- Discrepancy solved by SFmiss, and phi-dependent calibration

- Z-background events contribute to the W samples if one lepton is reconstructed, and the other lepton fails the lepton veto requirement
- The number of reconstructed and selected Z-background events in data and MC can be expressed as

$$N_{\mathrm{MC}} \propto \epsilon_{\mathrm{MC}}(1-\epsilon_{\mathrm{MC}}); \quad N_{\mathrm{data}} \propto \epsilon_{\mathrm{data}}(1-\epsilon_{\mathrm{data}}) \qquad (1)$$

- The MC background estimation needs to be corrected for $\mathrm{SF} = \epsilon_{\mathrm{data}}/\epsilon_{\mathrm{MC}}$ and for $\mathrm{SFMiss} = (1-\epsilon_{\mathrm{data}})/(1-\epsilon_{\mathrm{MC}})$

Large effect in the muon channel (30-40 MeV), small effect in the electron channel (~ 2 MeV) due to the larger value of the efficiency for the muons

- With SFMiss correction (red), without SFMiss correction (blue)

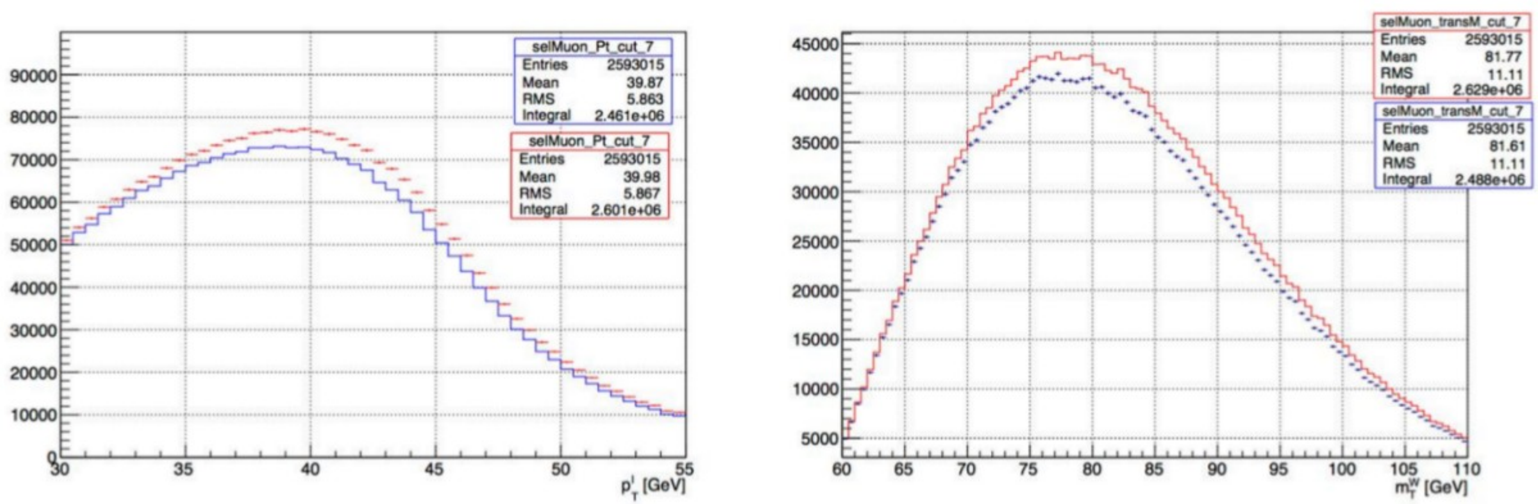

Physics modelling overview

- Factorise the fully-differential DY cross section in 4 terms

$$\frac{d\sigma}{dp_1\,dp_2} = \left[\frac{d\sigma(m)}{dm}\right]\left[\frac{d\sigma(y)}{dy}\right]\left[\frac{d\sigma(p_T,y)}{dp_T\,dy}\left(\frac{d\sigma(y)}{dy}\right)^{-1}\right]\left[(1+\cos^2\theta)+\sum_{i=0}^{7}A_i(p_T,y)P_i(\cos\theta,\phi)\right]$$

Breit-Wigner

NNLO pQCD

Parton Shower

Use ancillary measurements to constrain and validate the modelling

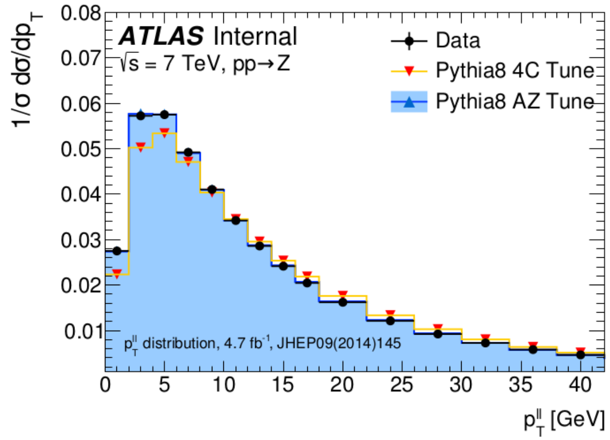

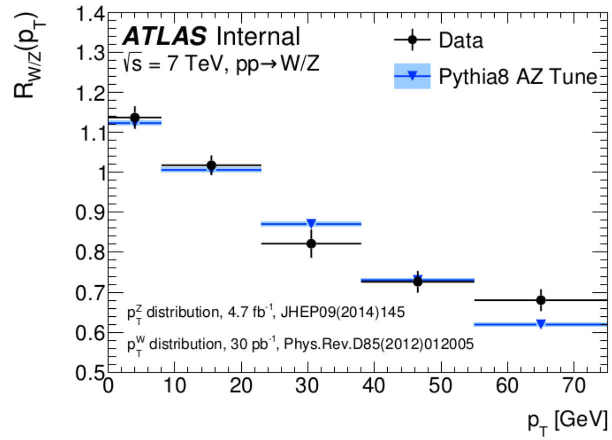

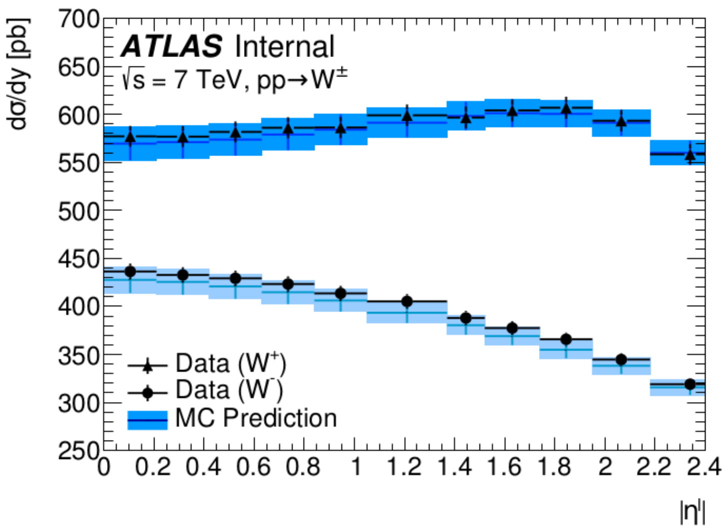

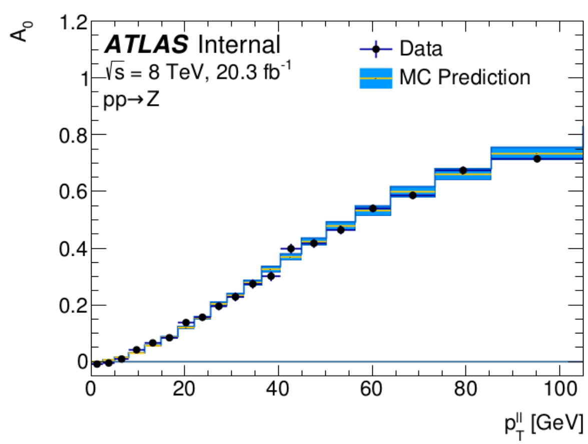

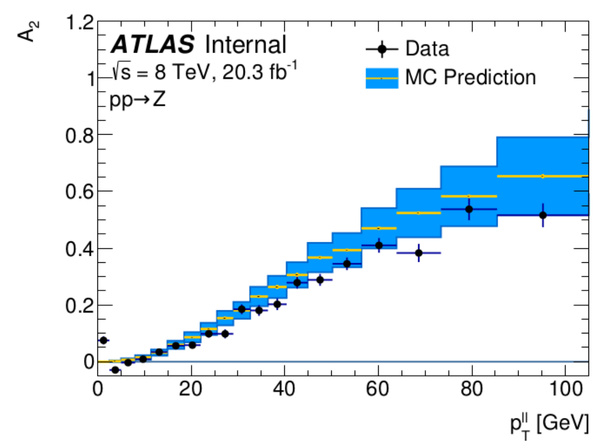

Lepton calibration overview

- General idea: use Z → ll events to calibrate lepton scale, resolution, efficiency
- For the lepton scale, use also E/p
- Electron-energy and muon-momentum scales determined with 10^{-4} relative uncertainty
- Lepton efficiencies evaluated with the tag-and-probe method
- Phi-dependent corrections are crucial for the Z to W extrapolation

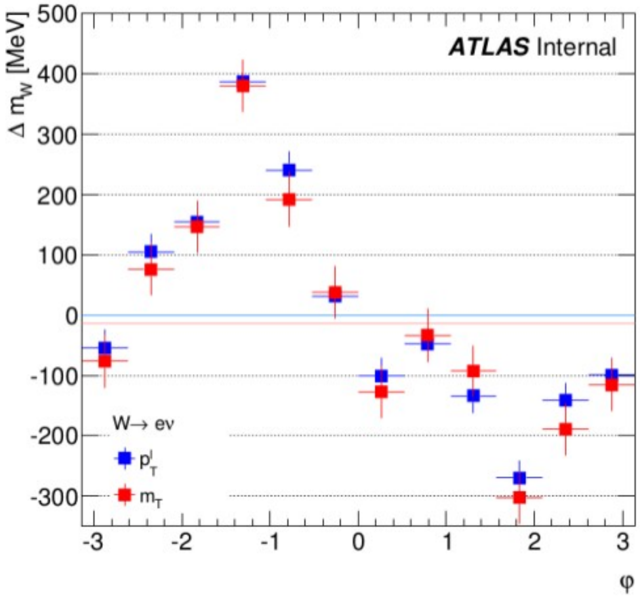

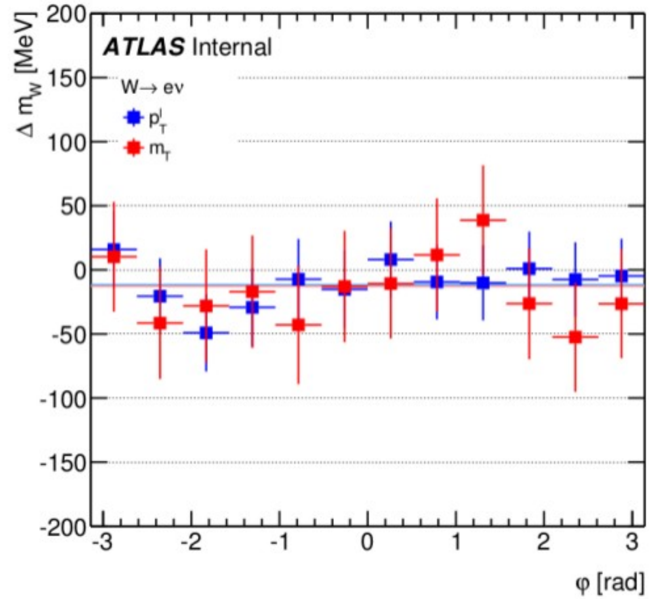

Recoil calibration overview

- $\langle\mu\rangle$ in the MC is corrected to match $SumE_T$ and u_T distributions in data
- Recoil corrections derived as a function of p_T and ($SumE_T$ - u_T), and applied with a Smirnov transform
  - Phi-dependent corrections are applied by projecting the recoil on the x and y axes and correcting the average values in the MC
  - Scale and resolution corrections are derived by comparing upar and uperp in data and MC

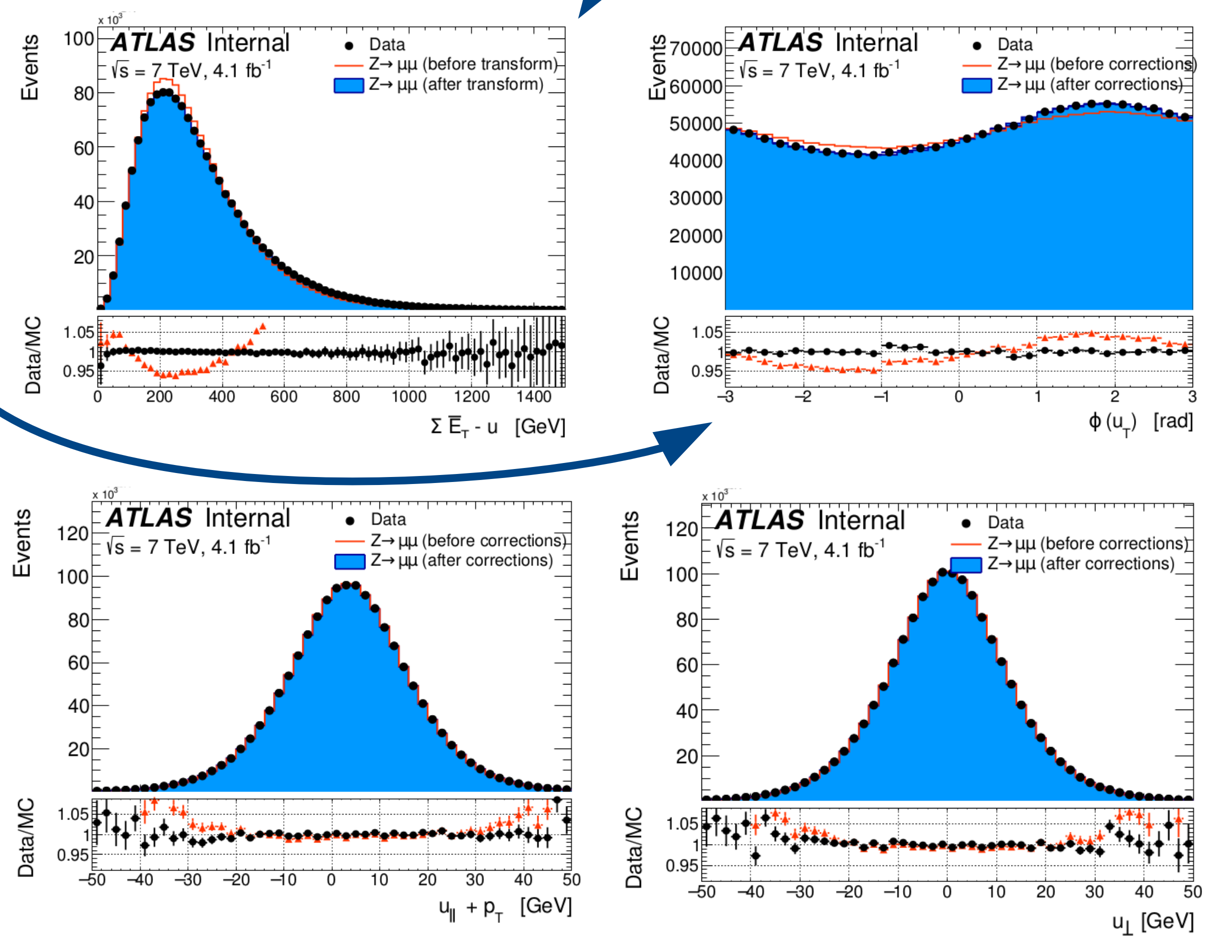

Compatibility of categories

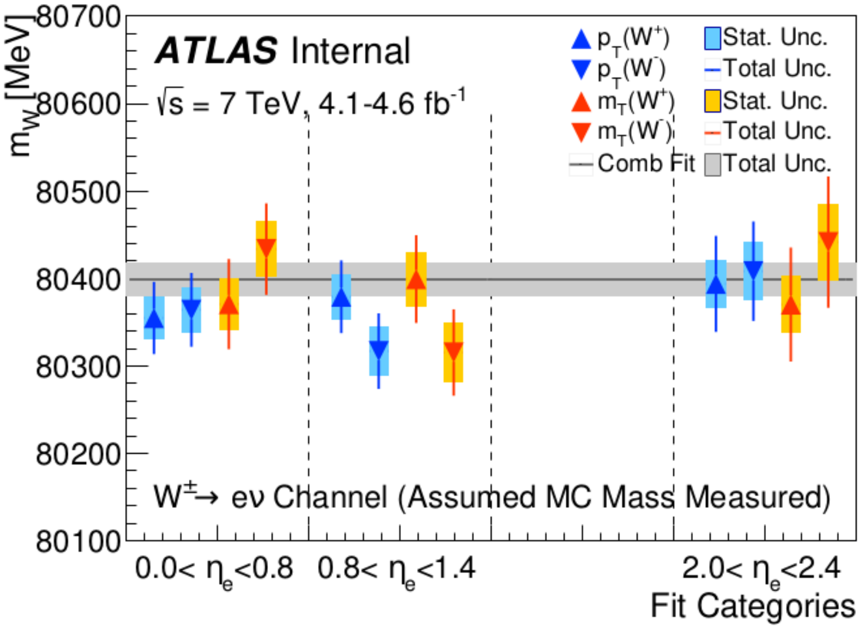

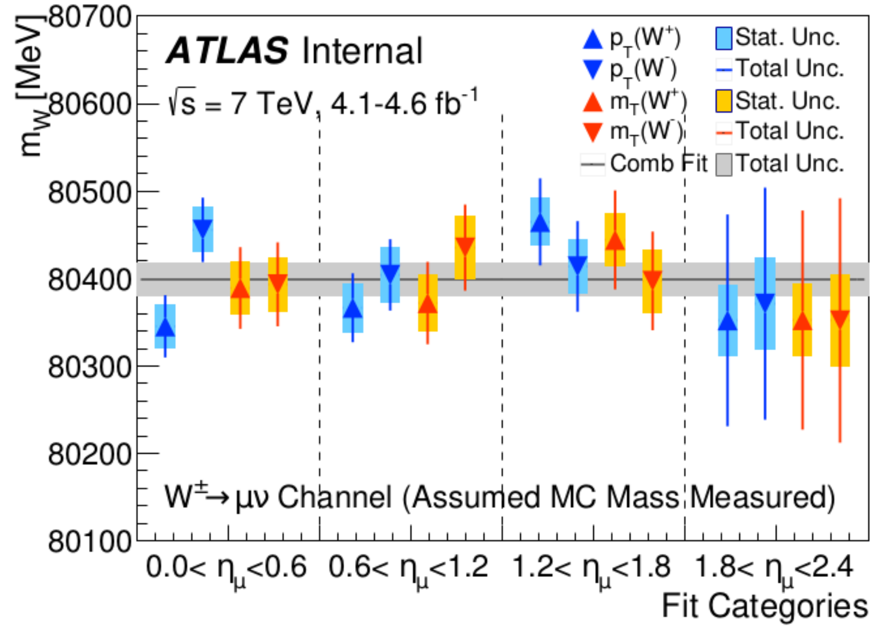

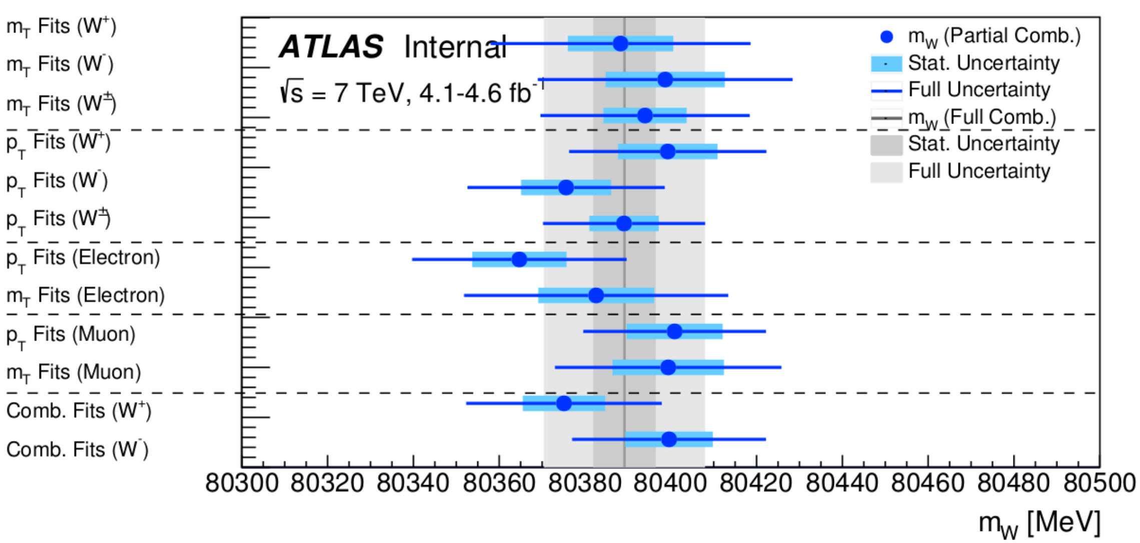

- All categories give consistent extractions of mW
- → Strong validation of physics modelling and detector calibration

Results

	Value [MeV]	Stat. Unc.	Muon Calib.	Elec. Calib.	Recoil Calib.	Back-grd.	QCD	EWK	PDF's	Total Unc.	χ^2/ndf of Comb.
Combined-Fit ($W^{\pm}$)	-9.8	7.1	7.0	6.2	2.9	3.9	10.5	5.3	6.9	18.6	28.1/27

Additional 3.5 MeV from the envelope of CT10, MMHT, CT14 PDF sets

$$m_W = 80xxx \pm 19.0 \text{ MeV}$$

m_W = 80xxx ± 7.1 (stat) ± 10.5 (exp.syst.) ± 14.1 (model.syst.) MeV

The dominant uncertainty is due to the physics modelling

Comparison of uncertainties with CDF

Better stat, worse recoil, similar PDF and p_T W

m_T fit uncertainties			
Source	$W \to \mu\nu$	$W \to e\nu$	Common
Lepton energy scale	7	10	5
Lepton energy resolution	1	4	0
Lepton efficiency	0	0	0
Lepton tower removal	2	3	2
Recoil scale	5	5	5
Recoil resolution	7	7	7
Backgrounds	3	4	0
PDFs	10	10	10
W boson p_T	3	3	3
Photon radiation	4	4	4
Statistical	16	19	0
Total	23	26	15

p_T^ℓ fit uncertainties			
Source	$W \to \mu\nu$	$W \to e\nu$	Common
Lepton energy scale	7	10	5
Lepton energy resolution	1	4	0
Lepton efficiency	1	2	0
Lepton tower removal	0	0	0
Recoil scale	6	6	6
Recoil resolution	5	5	5
Backgrounds	5	3	0
PDFs	9	9	9
W boson p_T	9	9	9
Photon radiation	4	4	4
Statistical	18	21	0
Total	25	28	16

Combination of	Value [MeV]	Stat. Unc.	Muon Calib.	Elec. Calib.	Recoil Calib.	Back-grd.	QCD	EWK	PDF's	Total Unc.	χ^2/ndf of Comb.
p_T-Fit (el)	-34.3	11.0	0	17.5	1.5	4.1	10.6	5.3	6.2	25.0	3.0/5
m_T-Fit (el)	-16.4	13.5	0	15.9	12.4	12.3	9.5	3.4	10.3	30.8	7.9/5
p_T-Fit (μ)	1.9	11.2	10.4	0	1.3	3.5	10.7	6.0	7.5	21.3	8.9/7
m_T-Fit (μ)	0.4	13.0	11.6	0	12.3	5.8	9.6	3.4	10.3	26.4	2.6/7

Comparison of uncertainties with D0

Source	Section	m_T	p_T^e	$\not\!\!E_T$
Experimental				
Electron Energy Scale	VII C 4	16	17	16
Electron Energy Resolution	VII C 5	2	2	3
Electron Shower Model	V C	4	6	7
Electron Energy Loss	V D	4	4	4
Recoil Model	VII D 3	5	6	14
Electron Efficiencies	VII B 10	1	3	5
Backgrounds	VIII	2	2	2
$\sum$(Experimental)		18	20	24
W Production and Decay Model				
PDF	VI C	11	11	14
QED	VI B	7	7	9
Boson p_T	VI A	2	5	2
$\sum$(Model)		13	14	17
Systematic Uncertainty (Experimental and Model)		22	24	29
W Boson Statistics	IX	13	14	15
Total Uncertainty		26	28	33

Combination of	Value [MeV]	Stat. Unc.	Muon Calib.	Elec. Calib.	Recoil Calib.	Back-grd.	QCD	EWK	PDF's	Total Unc.	χ^2/ndf of Comb.
p_T-Fit (el)	-34.3	11.0	0	17.5	1.5	4.1	10.6	5.3	6.2	25.0	3.0/5
m_T-Fit (el)	-16.4	13.5	0	15.9	12.4	12.3	9.5	3.4	10.3	30.8	7.9/5
p_T-Fit (μ)	1.9	11.2	10.4	0	1.3	3.5	10.7	6.0	7.5	21.3	8.9/7
m_T-Fit (μ)	0.4	13.0	11.6	0	12.3	5.8	9.6	3.4	10.3	26.4	2.6/7

Measurement of the W-boson mass - Details

- Physics modelling
- Recoil calibration
- Lepton calibration
- Z-boson mass cross checks
- Background subtraction
- Combination

Physics modelling

$$\frac{d\sigma}{dp_1\,dp_2} = \left[\frac{d\sigma(m)}{dm}\right]\left[\frac{d\sigma(y)}{dy}\right]\left[\frac{d\sigma(p_T, y)}{dp_T\,dy}\left(\frac{d\sigma(y)}{dy}\right)^{-1}\right]\left[(1+\cos^2\theta) + \sum_{i=0}^{7} A_i(p_T, y)P_i(\cos\theta, \phi)\right]$$

Breit-Wigner

NNLO pQCD

Parton Shower

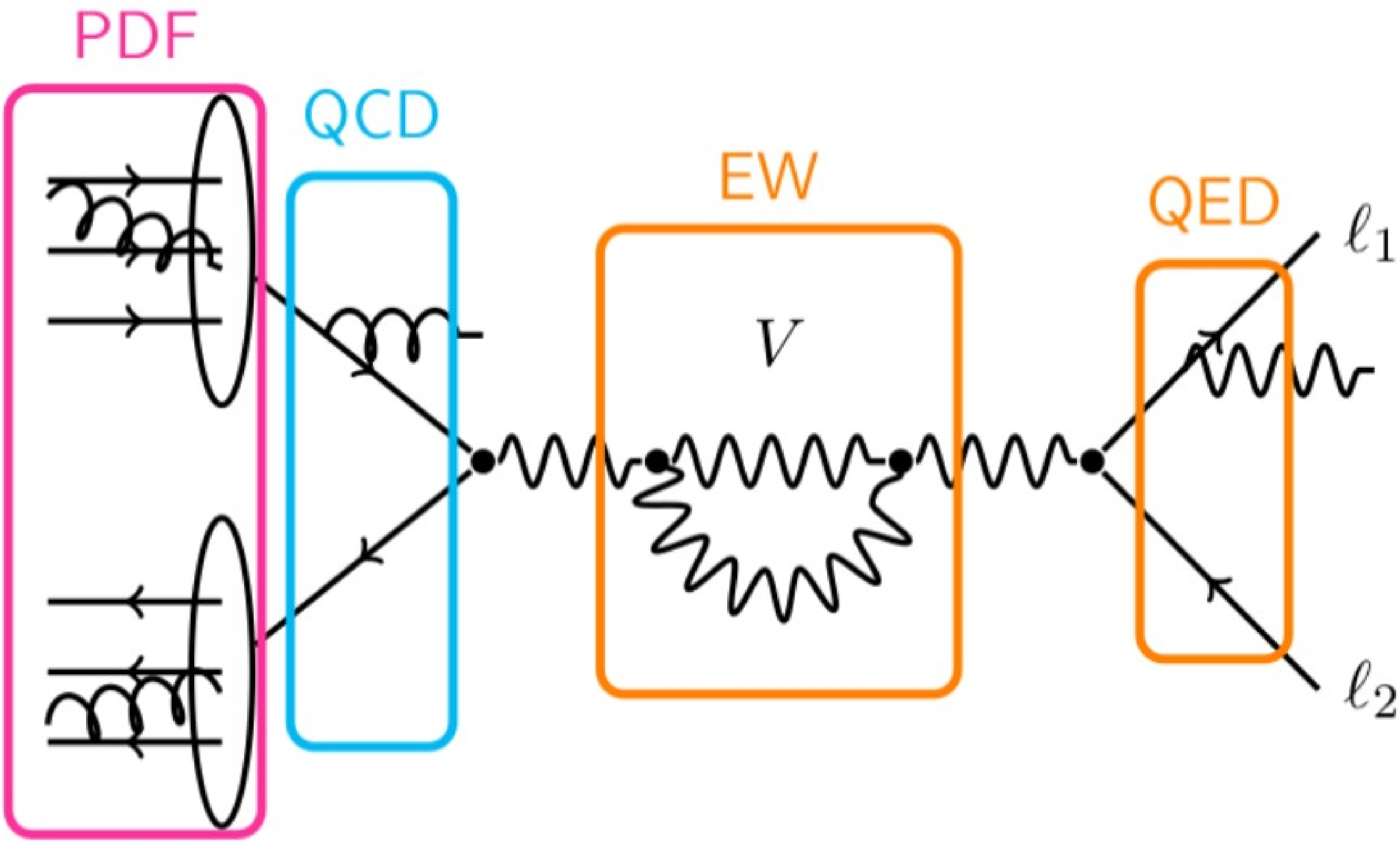

Physics modelling – electroweak corrections

- QED FSR: dominant correction, included in the MC with PHOTOS, uncertainty from comparison with YFS
- Running widths (and running of α for Z) included in the BW parametrisation
- NLO electroweak: pure weak corrections and ISR-FSR interference, estimated with WINHAC. QCD ISR included to predict a realistic ptW distribution
- FSR lepton pair production $\gamma^* \rightarrow$ ll : formally higher order (NNLO), but significant correction. Estimated and added as uncertainty

Kinematic distribution	p_T^e	$m_T^{e\nu}$	p_T^ν	p_T^μ	$m_T^{\mu\nu}$
δm_W [MeV]					
FSR (real)	< 0.1	< 0.1	< 0.1	< 0.1	< 0.1
FSR (pair production)	3.6	0.8	< 0.1	4.4	0.8
Pure weak and IFI corrections	3.3	2.5	0.6	3.5	2.5
Total [MeV]	4.9	2.6	0.6	5.6	2.6

Physics modelling – electroweak corrections

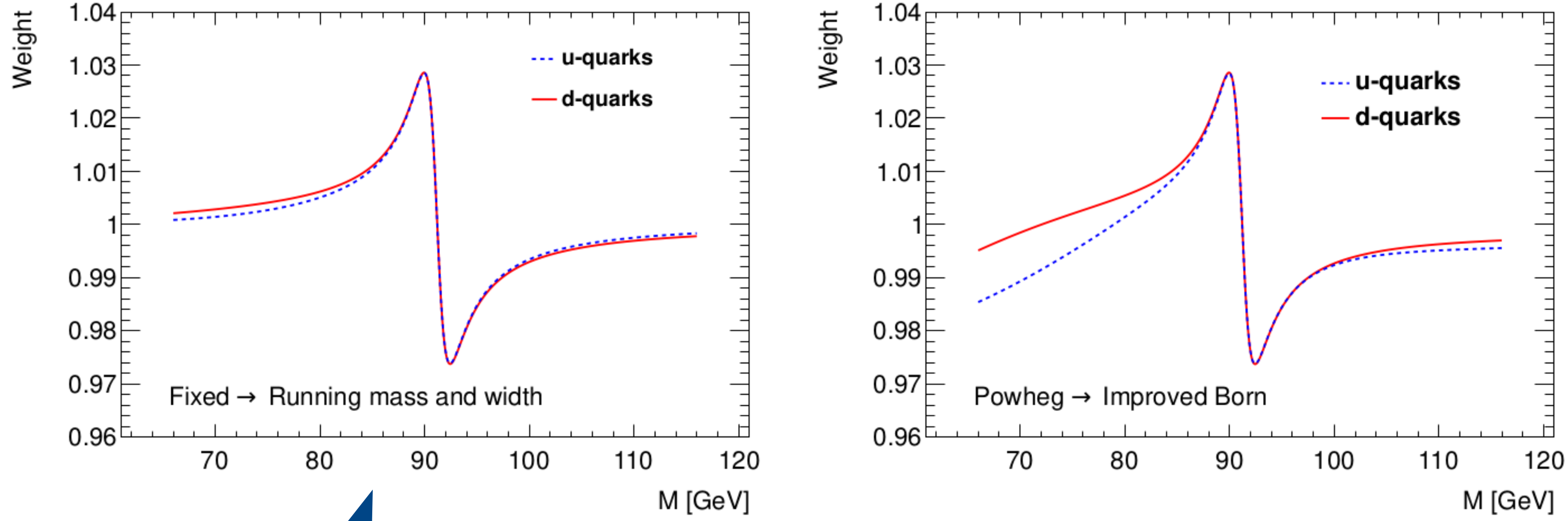

Running width

$$P'_{ij}(\hat{s}) = \hat{s}\,\frac{(\hat{s}-m'^2_i)(\hat{s}-m'^2_j) + \frac{\hat{s}^2}{m'_i m'_j}\Gamma'_i\Gamma'_j}{[(\hat{s}-m'^2_i)^2 + (\frac{\hat{s}}{m'_i}\Gamma'_i)^2]\,[(\hat{s}-m'^2_j)^2 + (\frac{\hat{s}}{m'_j}\Gamma'_j)^2]}$$

Running α

$$\alpha_{\text{em}}(s) = \frac{\alpha_{\text{em}}(0)}{1-\Delta\alpha(s)};$$

$$\Delta\alpha(s) = \frac{\alpha_{\text{em}}(0)}{3\pi}(13.4955 + 3\ln s) + 0.00165 + 0.00299\ln(1+s).$$

Physics modelling – pT W

- Pythia8 tuned to the pT Z measurement at 7 TeV

	PYTHIA8
Tune Name	AZ
Primordial k_T [GeV]	1.71 ± 0.03
ISR $\alpha_S^{ISR}(m_Z)$	0.1237 ± 0.0002
ISR cut-off [GeV]	0.59 ± 0.08
χ^2_{min}/dof	$45.4/32$

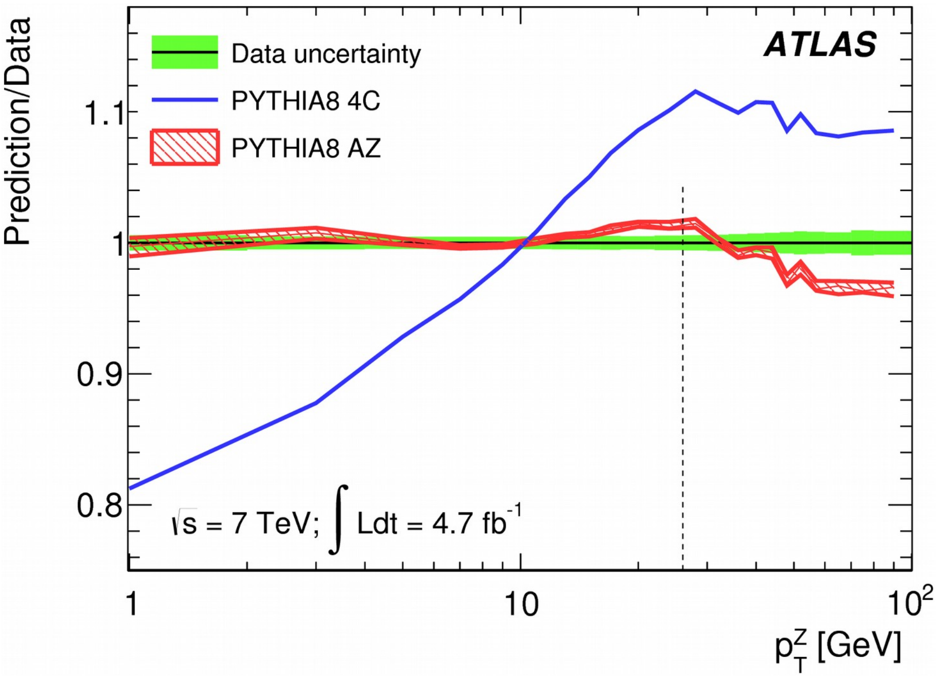

- The Pythia8 AZ tune describe the pT Z data within 2% inclusively and in rapidity bins

- Pythia8 is used to predict the pT W distribution and to evaluate uncertainties on pT W

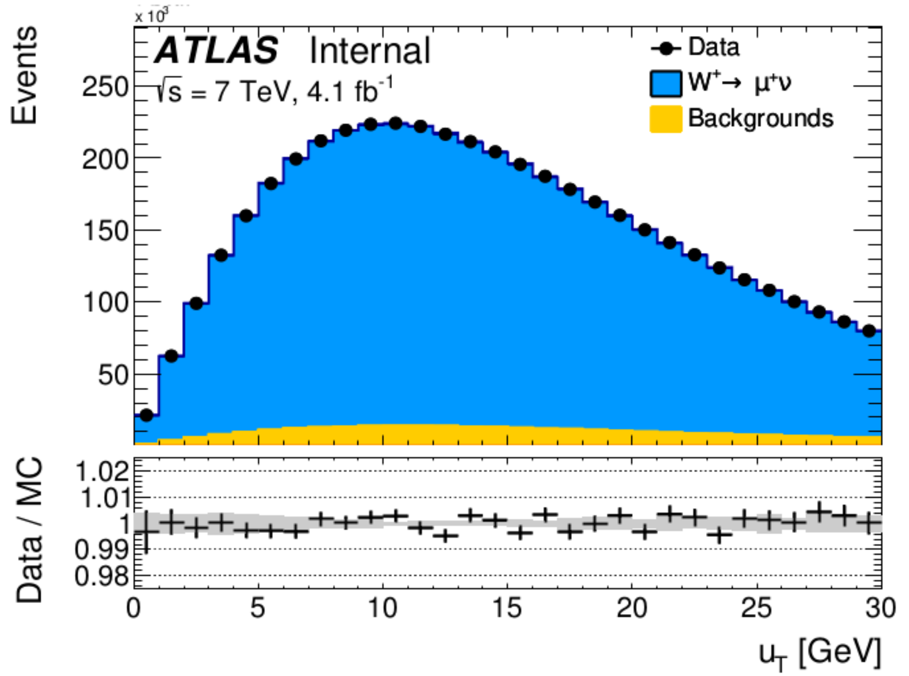

Physics modelling – pT W

Only Herwig, Pythia, and Powheg predict a monotonic falling W/Z pt ratio

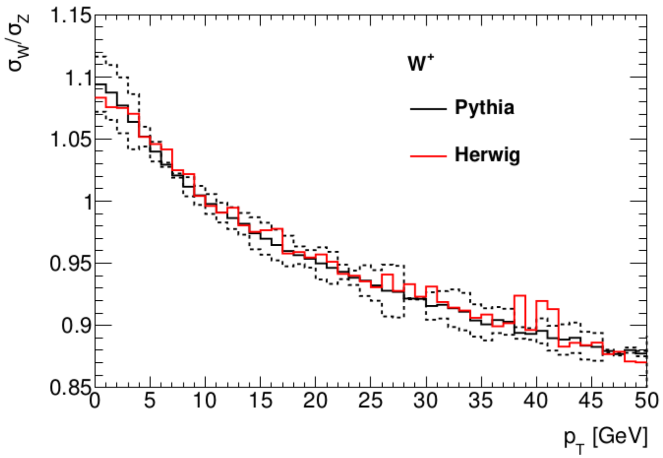

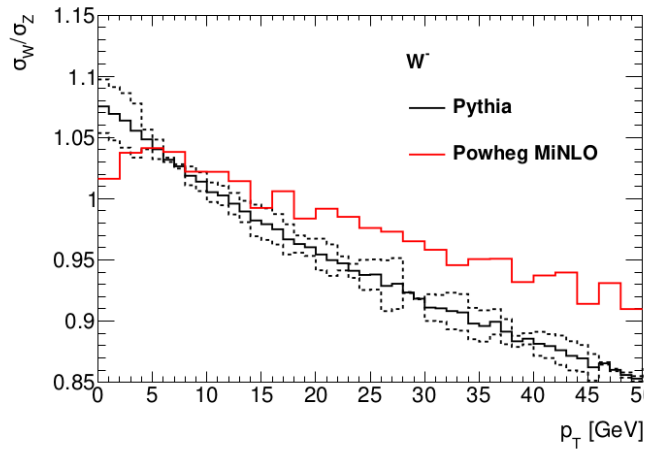

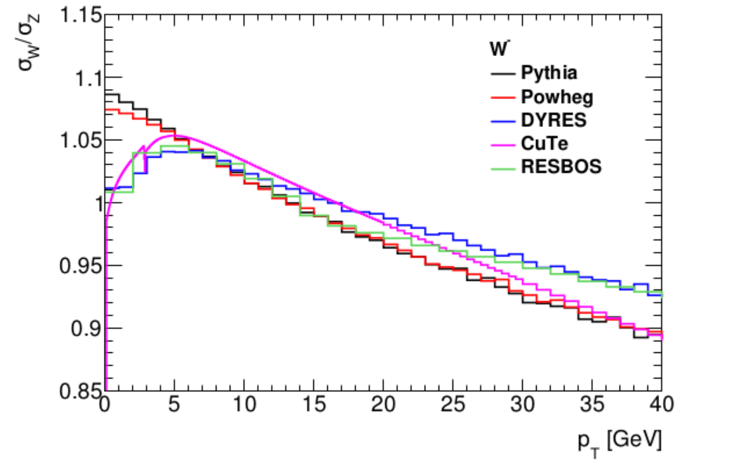

Resummed predictions strongly disfavoured by the data

PYTHIA8

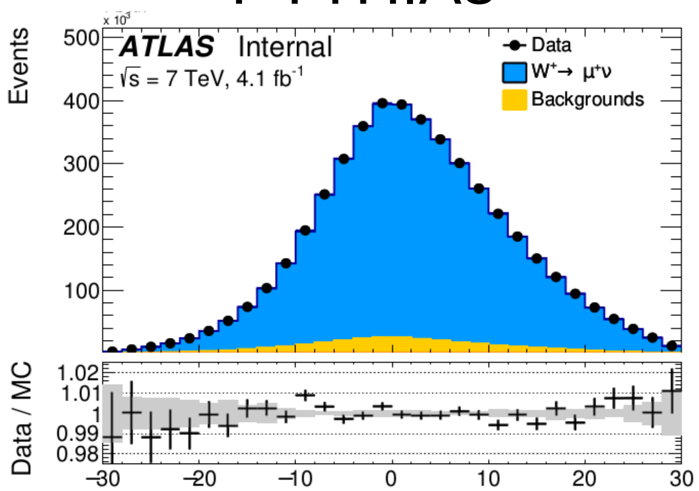

DYRES

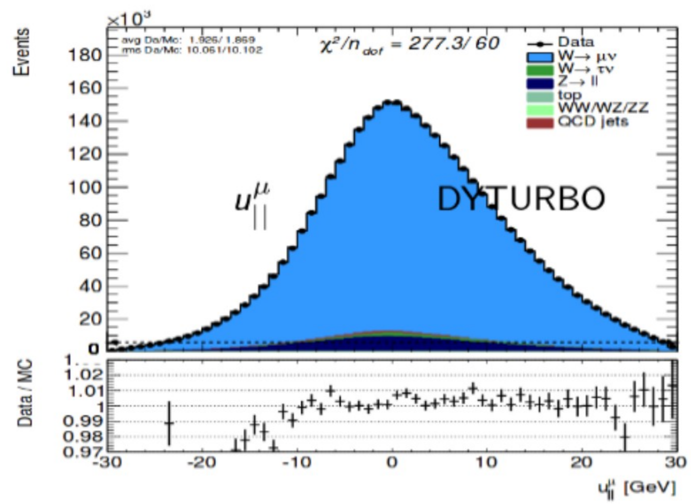

Powheg MINLO

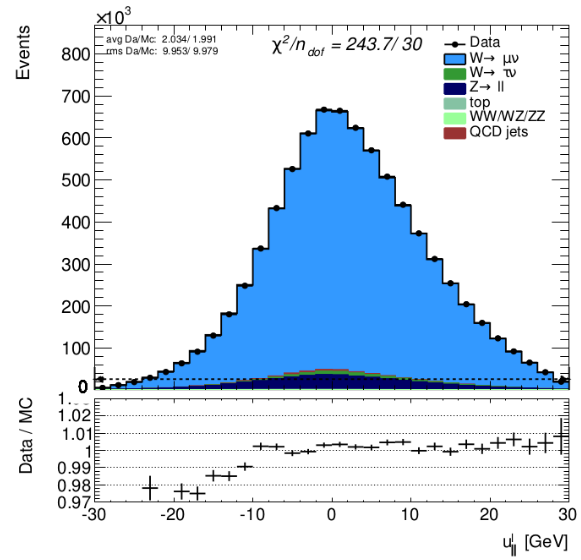

Physics modelling – rapidity and Ai

- Rapidity and angular coefficients are modelled with fixed order perturbative QCD at NNLO
- A fast prediction was developed, based on DYNNLO, which allows to evaluated correlated PDF uncertainties
- PDF choice and Ai predictions are validated by comparisons to ATLAS measurements
- Ai experimental uncertainties of Z measurement propagated to W predictions

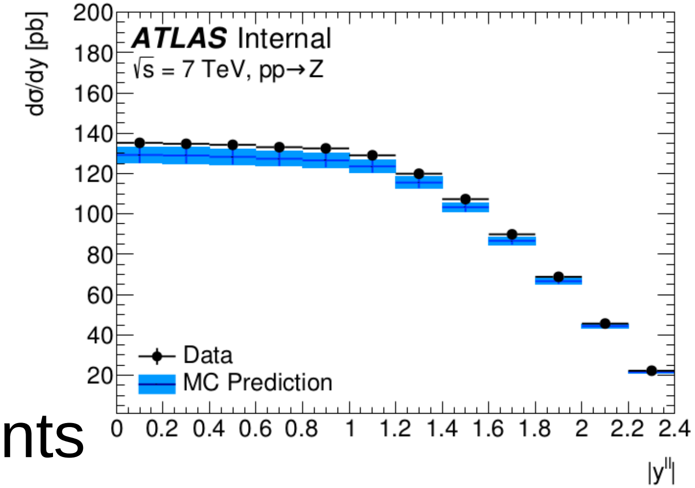

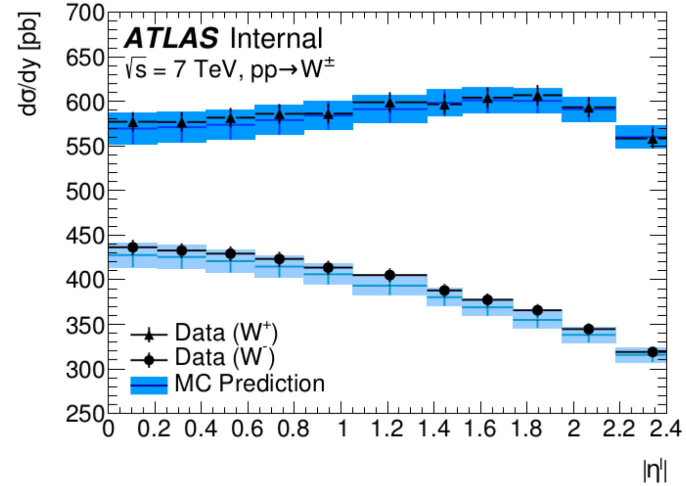

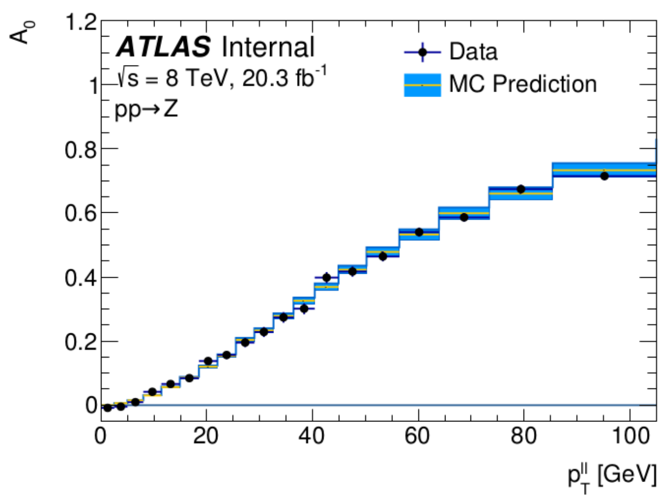

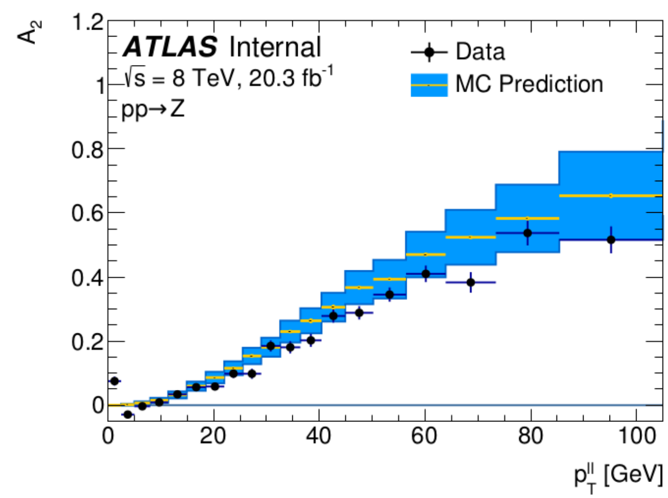

Heavy flavour and scale decorrelation

- Heavy-flavour-initiated production is a significant source of uncertainty, and introduce decorrelation between Z and W production. HF production has a harder boson pT spectrum
- cc → Z and bb → Z are 6% and 3% of Z production, cs → W is ~20% of W production
- Uncertainty addressed with charm mass variations, and by decorrelating muf between light and HF processes

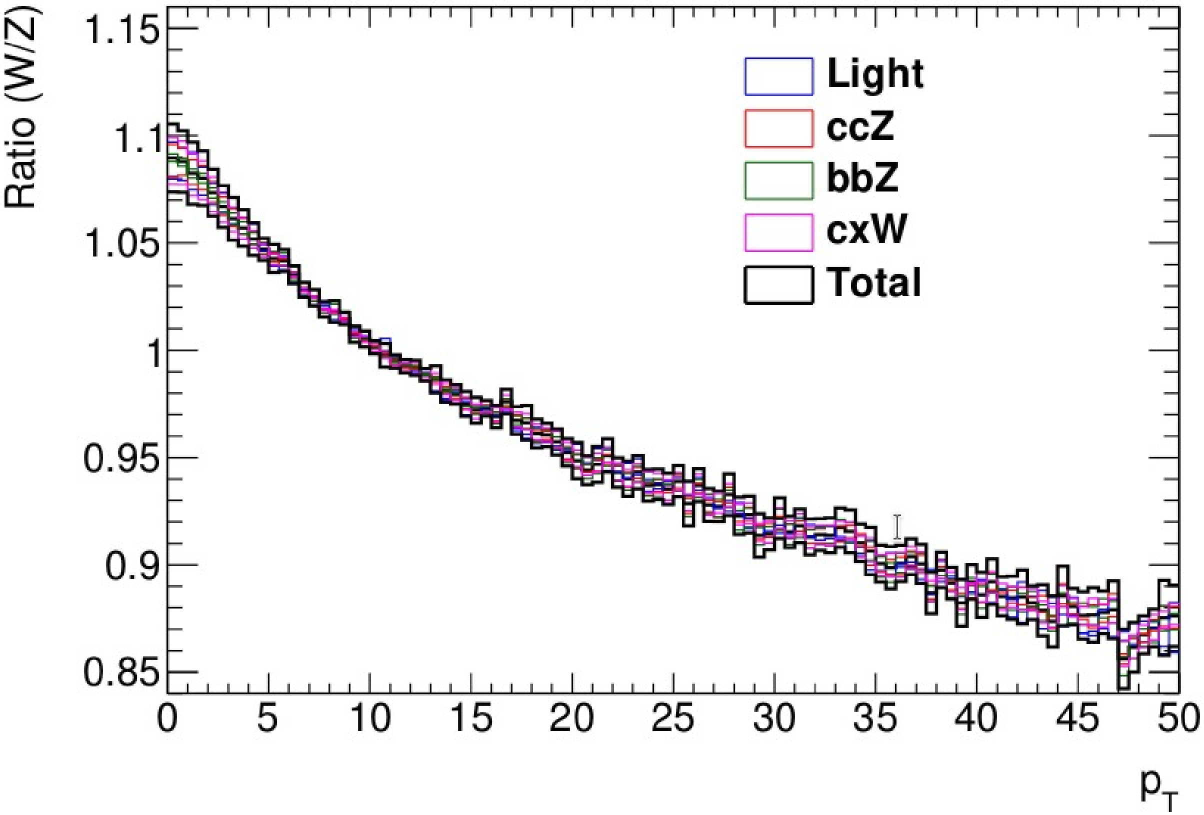

Physics modelling – QCD uncertainties

Kinematic distribution	p_T^e	$m_T^{e\nu}$	p_T^μ	$m_T^{\mu\nu}$
δm_W [MeV]				
PDF uncertainty (W^+)	14.2	14.1	15.8	16.0
PDF uncertainty (W^-)	12.7	13.8	15.0	14.7
AZ tune	(+5 -7)	(+1.5 -2)	(+5 -7)	(+1.5 -2)
Parton shower μ_F with heavy-flavour decorrelation	9.8	7.0	9.8	7.0
Charm-quark mass	2.5	0.8	2.5	0.8
Parton shower PDF uncertainty (W^+)	+7.5	+1.9	+7.5	+1.9
Parton shower PDF uncertainty (W^-)	-5.1	-1.3	-5.1	-1.3
Angular coefficients	6.4	5.4	6.4	5.4
Total (W^+) [MeV]	20.1	16.9	22.0	18.5
Total (W^-) [MeV]	19.1	16.6	20.7	17.3

Recoil calibration – <μ> scaling

- <μ> is scaled by a factor $\alpha = 1.10{+}0.04{-}0.03$

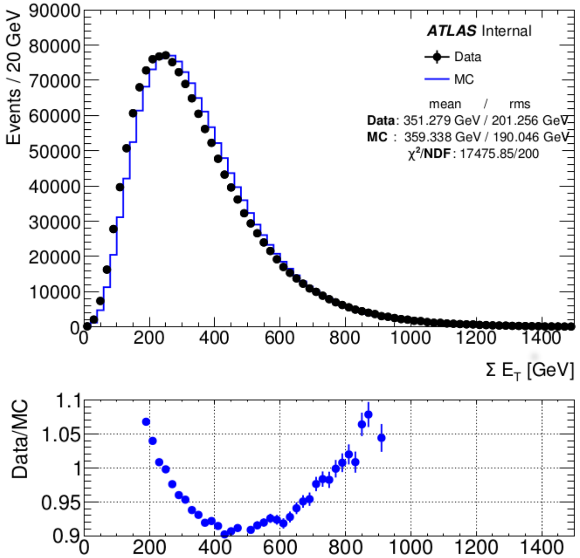

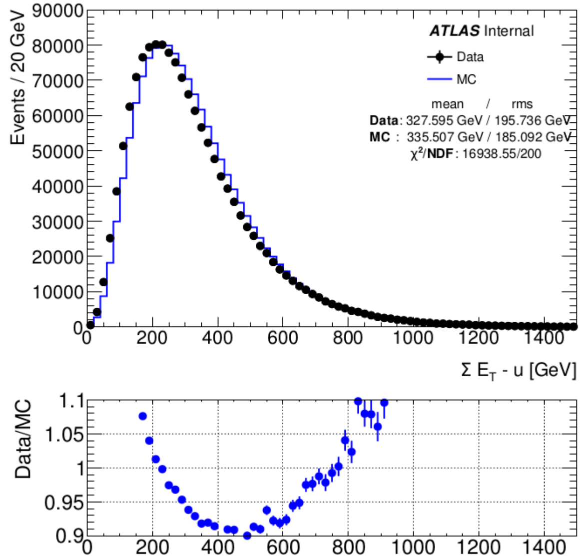

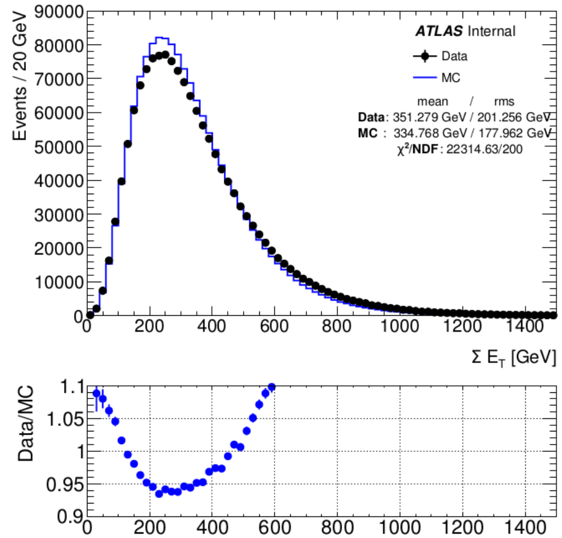

(c)

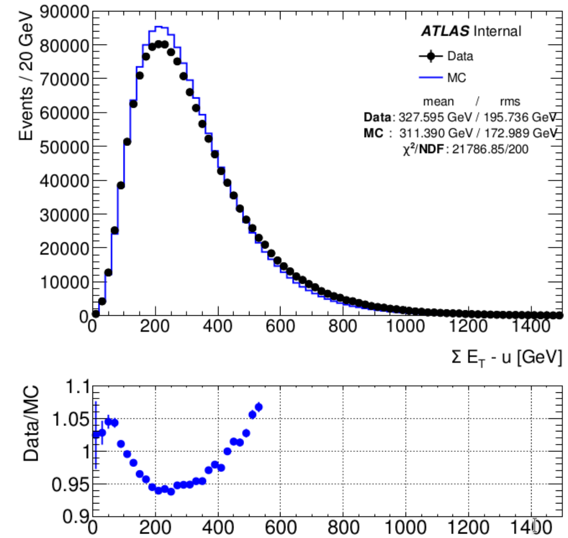

(d)

Recoil calibration

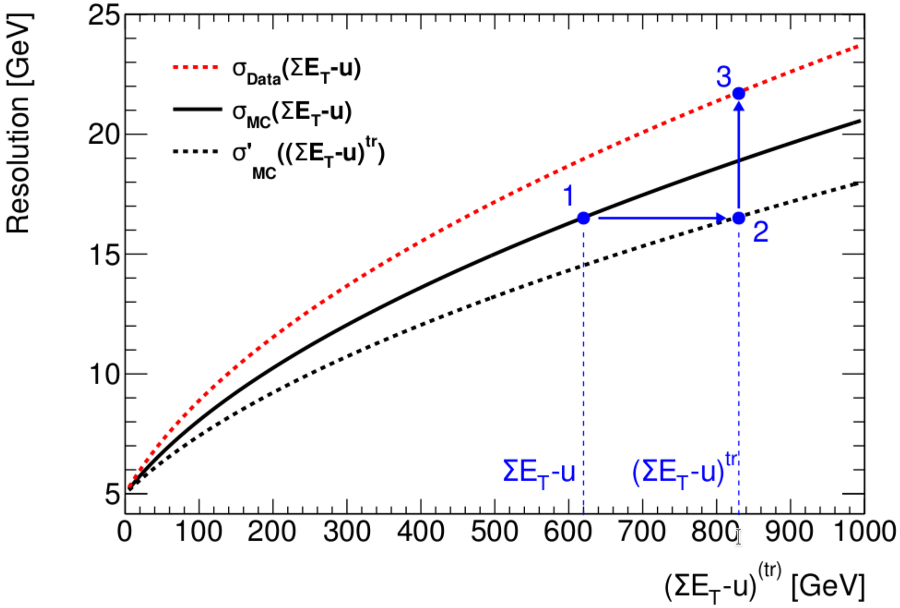

- SumE$_T$ Smirnov transform

$$h^W_{\mathrm{MC}}(\Sigma\bar{E}_{\mathrm{T}}; p_{\mathrm{T}}) \rightarrow h^W_{\mathrm{MC}}(\Sigma\bar{E}_{\mathrm{T}}'; p_{\mathrm{T}}) \equiv \tilde{h}^W_{\mathrm{data}}(\Sigma\bar{E}_{\mathrm{T}}; p_{\mathrm{T}}).$$

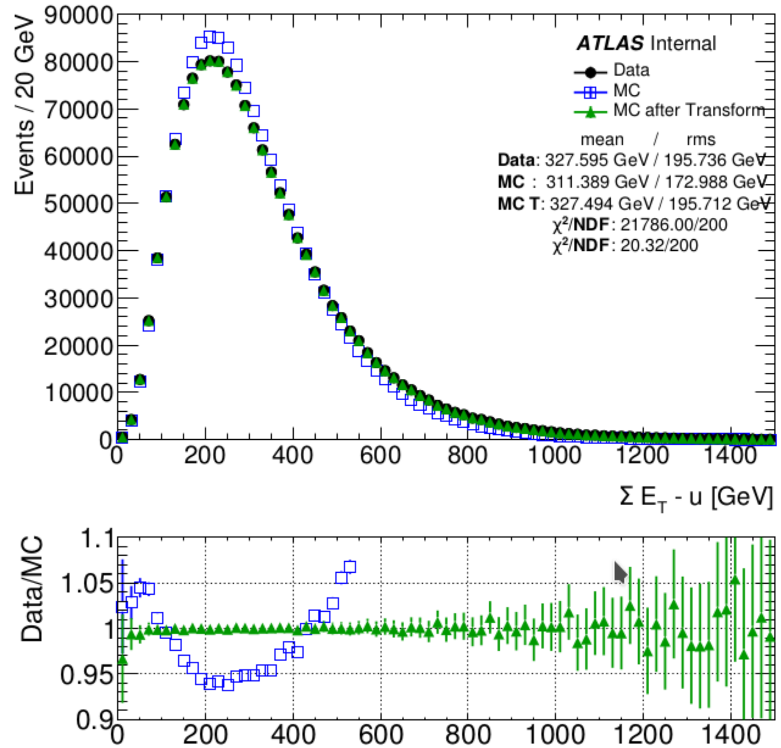

- Recoil scale and resolution correction

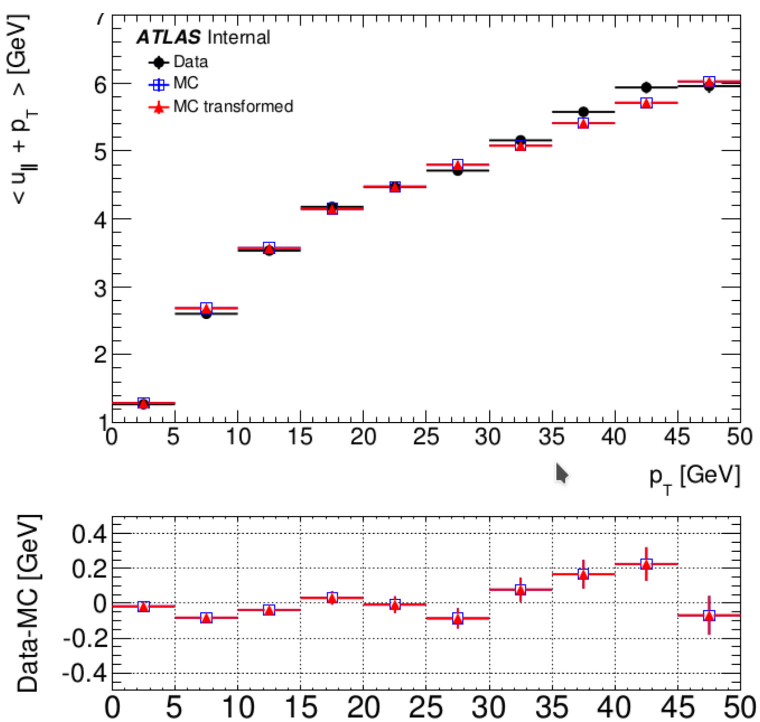

$$u_{\parallel}^{V,\mathrm{corr}} = u_{\parallel}^{V,\mathrm{MC}} + b(p_{\mathrm{T}}^{V}, \Sigma\bar{E}_{\mathrm{T}}') + (u_{\parallel}^{V,\mathrm{MC}} + p_{\mathrm{T}}^{V}) \cdot r(p_{\mathrm{T}}^{V}, \Sigma\bar{E}_{\mathrm{T}}');$$

$$u_{\perp}^{V,\mathrm{corr}} = u_{\perp}^{V,\mathrm{MC}} \cdot r(p_{\mathrm{T}}^{V}, \Sigma\bar{E}_{\mathrm{T}}'),$$

Recoil calibration

- pT dependence of the correction calibrated on Z data, and propagate to W with a pT-inclusive scaling

$$\tilde{h}^{W}_{\rm data}(\Sigma\bar{E}_{\rm T}, p_{\rm T}) \equiv h^{Z}_{\rm data}(\Sigma\bar{E}_{\rm T}, p_{\rm T}) \left(\frac{h^{W}_{\rm data}(\Sigma\bar{E}_{\rm T})}{h^{W}_{\rm MC}(\Sigma\bar{E}_{\rm T})} \Big/ \frac{h^{Z}_{\rm data}(\Sigma\bar{E}_{\rm T})}{h^{Z}_{\rm MC}(\Sigma\bar{E}_{\rm T})} \right)$$

- Recoil corrections evaluated as a function of <μ>

$\lvert\eta\rvert$ range	W^+		W^-		$W^\pm$	
Kinematic distribution	$p_{\rm T}^{\ell}$	$m_{\rm T}$	$p_{\rm T}^{\ell}$	$m_{\rm T}$	$p_{\rm T}^{\ell}$	$m_{\rm T}$
δm_W [MeV]						
μ scale factor	0.2	1.0	0.2	1.0	0.2	1.0
$\Sigma\bar{E}_{\rm T}$ correction	1.1	12.6	1.2	9.0	1.2	11.4
Effective corrections (stat.)	2.0	2.7	2.0	2.7	2.0	2.7
Effective corrections ($Z \rightarrow W$ extrap.)	0.1	5.8	0.1	4.3	0.1	5.1
Total	2.3	14.1	2.3	10.4	2.3	12.8

Muon calibration

$$p_{\mathrm{T}}^{\mathrm{corr}} = p_{\mathrm{T}}^{\mathrm{MC}} \times \frac{1 + \alpha(\eta,\phi)}{1 + q\cdot\delta(\eta,\phi)\cdot p_{\mathrm{T}}^{\mathrm{MC}}} \left[1 + \beta_{\mathrm{curv}}(\eta)\cdot G(0,1)\cdot p_{\mathrm{T}}^{\mathrm{MC}}\right]$$

- α: radial bias
- δ: sagitta bias
- β: resolution correction

- Charge dependent corrections
- Corrections derived form $Z \rightarrow \mu\mu$ line shape, and from E/p in $W \rightarrow e\nu$

$\lvert\eta^{\ell}\rvert$ range	$0.0< \lvert\eta^{\ell}\rvert <0.8$		$0.8< \lvert\eta^{\ell}\rvert <1.4$		$1.4< \lvert\eta^{\ell}\rvert <2.0$		$2.0< \lvert\eta^{\ell}\rvert <2.4$		Inclusive	
Kinematic distribution	p_{T}^{ℓ}	m_{T}	p_{T}^{ℓ}	m_{T}	p_{T}^{ℓ}	m_{T}	p_{T}^{ℓ}	m_{T}	p_{T}^{ℓ}	m_{T}
δm_W [MeV]										
Momentum scale	9.0	9.0	14.4	14.5	27.5	27.6	114.0	114.0	8.6	8.6
Momentum resolution	1.4	1.4	1.0	1.0	1.1	1.1	1.7	1.7	1.0	1.0
Curvature bias	1.0	1.2	2.8	2.8	3.8	1.7	4.8	10.5	1.8	1.8
Reconstruction and isolation efficiencies	4.0	3.6	5.1	3.7	4.8	3.5	6.4	5.5	4.3	3.6
Trigger efficiency	5.6	5.0	7.1	5.0	11.8	9.1	12.1	9.9	6.2	4.9
Total	11.5	11.0	17.1	16.1	30.6	29.3	114.9	115.0	11.6	10.7

Electron calibration

- Corrections derived form Z $\rightarrow$ ee line shape, and from E/p
- Energy scale determined with 10^{-4} relative uncertainty

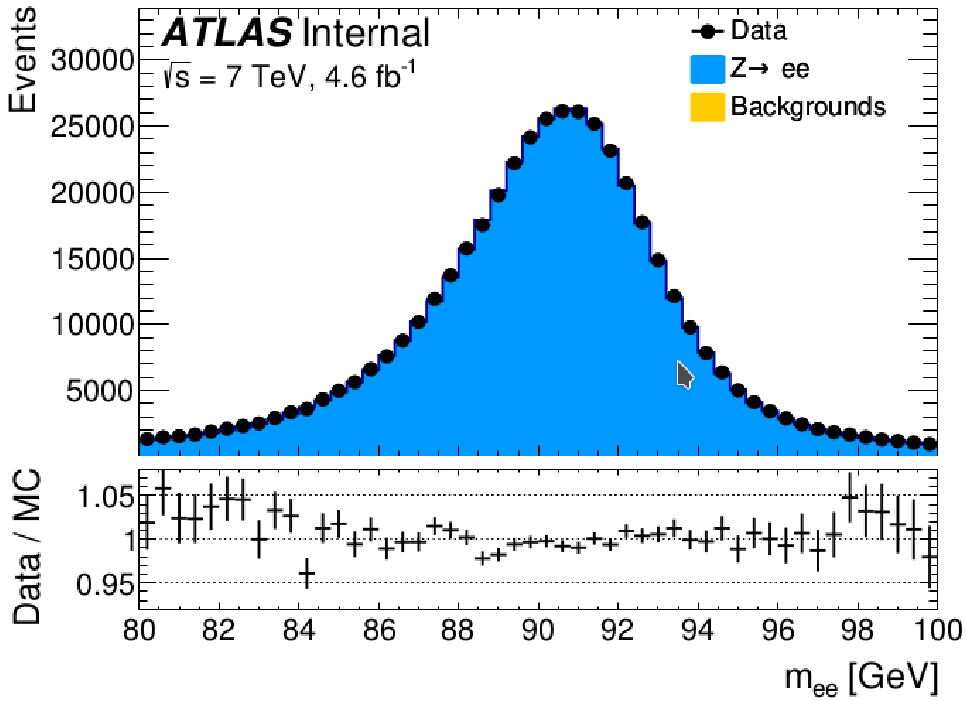

$\lvert\eta^\ell\rvert$ range	$0.0< \lvert\eta^\ell\rvert <0.6$		$0.6< \lvert\eta^\ell\rvert <1.2$		$1.82< \lvert\eta^\ell\rvert <2.4$		Inclusive	
Kinematic distribution	p_T^ℓ	m_T	p_T^ℓ	m_T	p_T^ℓ	m_T	p_T^ℓ	m_T
δm_W [MeV]								
Energy scale	10.3	10.3	10.9	10.9	16.0	16.0	8.0	8.0
Energy resolution	3.9	3.9	7.0	7.0	16.0	16.0	3.1	3.1
Energy linearity	4.9	5.4	7.4	7.2	4.6	5.1	4.2	4.5
Energy tails	2.3	3.3	2.3	3.3	2.3	3.3	2.3	3.3
Reconstruction efficiency	8.5	7.4	9.2	7.8	12.4	10.6	6.8	6.0
Identification efficiency	9.2	7.8	10.6	8.5	12.2	11.3	6.7	5.7
Trigger and isolation efficiencies	0.2	0.5	0.3	0.5	2.0	2.2	0.8	0.9
Total	17.5	16.6	20.6	19.1	29.1	28.2	13.7	13.2

Z cross checks

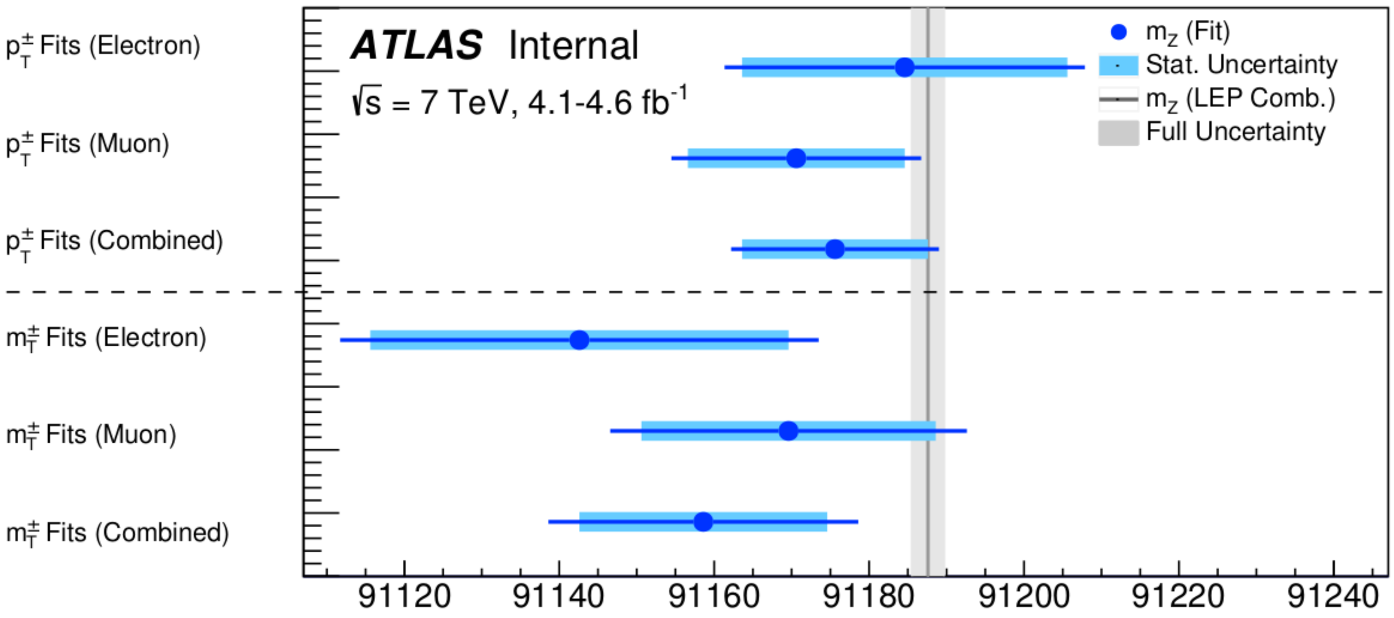

Distribution	$p_T^{\ell+}$	$p_T^{\ell-}$	$p_T^{\ell\pm}$	$m_T^{\ell+}$	$m_T^{\ell-}$	$m_T^{\ell\pm}$
δm_Z [MeV]						
Electron	$13 \pm 31 \pm 10$	$-20 \pm 31 \pm 10$	$-3 \pm 21 \pm 10$	$-93 \pm 38 \pm 15$	$4 \pm 38 \pm 15$	$-45 \pm 27 \pm 15$
Muon	$1 \pm 22 \pm 8$	$-36 \pm 22 \pm 8$	$-17 \pm 14 \pm 8$	$-35 \pm 28 \pm 13$	$-1 \pm 27 \pm 13$	$-18 \pm 19 \pm 13$
Combined	$5 \pm 18 \pm 6$	$-31 \pm 18 \pm 6$	$-12 \pm 12 \pm 6$	$-58 \pm 23 \pm 12$	$1 \pm 22 \pm 12$	$-29 \pm 16 \pm 12$

- mZ measured at LEP is an input for the lepton calibration
- The mZ fits provides a closure test of the lepton calibration, and a validation of the physics modelling and recoil calibration

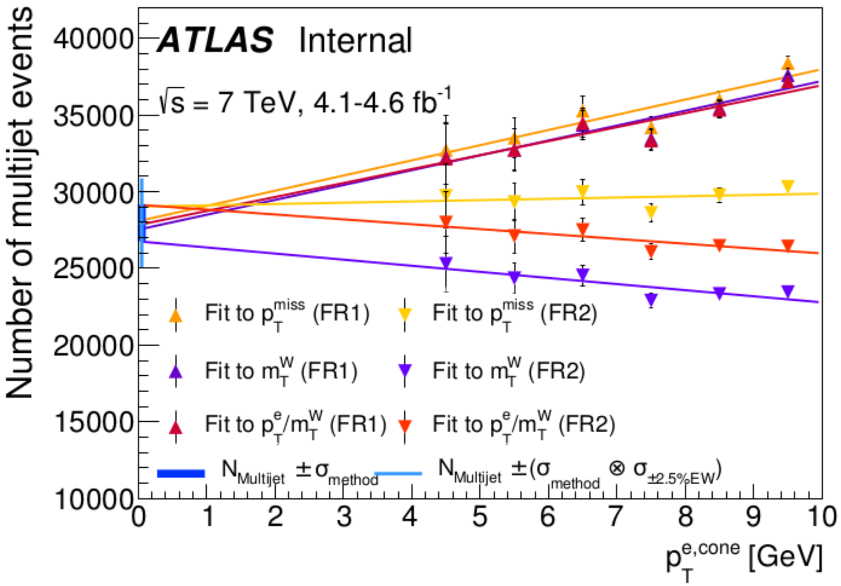

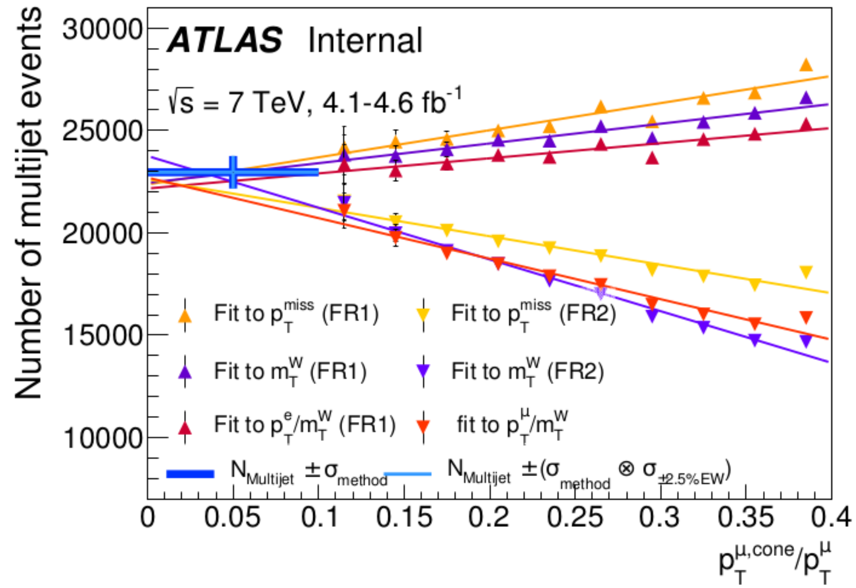

- The multijet background is determined with template fits, and by extrapolation of the lepton isolation to the signal region
- Both normalisation and shape are extrapolated
- Novel technique now adopted by other analyses

Background

Channel	$W^+ \to e^+\nu$	$W^- \to e^-\nu$	$W^+ \to \mu^+\nu$	$W^+ \to \mu^-\nu$
δm_W [MeV]				
$W \to \tau\nu$ (fraction)	2.2	2.2	2.2	2.2
$Z \to ee$ (fraction)	0.5	0.5	–	–
$Z \to \mu\mu$(fraction)	–	–	2.0	2.0
$Z \to \tau\tau$ (fraction)	0.5	0.5	0.5	0.5
WW, WZ, ZZ (fraction and shape)	0.2	0.2	0.2	0.2
Top (fraction and shape)	0.3	0.3	0.3	0.3
Multijet (fraction)	3.3	4.1	2.3	3.1
Multijet (shape)	5.6	7.3	2.1	2.8
Total				

Channel	$W^+ \to e^+\nu$	$W^- \to e^-\nu$	$W^+ \to \mu^+\nu$	$W^+ \to \mu^-\nu$
δm_W [MeV]				
$W \to \tau\nu$ (fraction)	2.2	2.2	2.2	2.2
$Z \to ee$ (fraction)	0.5	0.5	–	–
$Z \to \mu\mu$(fraction)	–	–	2.0	2.0
$Z \to \tau\tau$ (fraction)	0.5	0.5	0.5	0.5
WW, WZ, ZZ (fraction+shape)	0.2	0.2	0.2	0.2
Top (fraction+shape)	0.3	0.3	0.3	0.3
Multijet (fraction)	8.2	8.7	3.6	4.7
Multijet (shape)	8.0	11.4	2.5	3.5
Total				

Combination

- The combination is performed with BLUE, and cross checked with HERAverager
- Statistical correlation between p_T lepton and m_T are evaluated with the Boostrap method

Combination of	Value [MeV]	Stat. Unc.	Muon Calib.	Elec. Calib.	Recoil Calib.	Back-grd.	QCD	EWK	PDF's	Total Unc.	χ^2/ndf of Comb.
m_T-Fit (W^+)	-10.7	12.3	8.6	7.2	13.8	8.8	9.4	3.4	16.5	30.3	2.0/6
m_T-Fit (W^-)	-0.3	13.9	9.0	7.1	11.1	8.7	9.7	3.4	15.8	29.7	6.7/6
m_T-Fit ($W^\pm$)	-5.0	9.7	8.0	5.8	12.2	7.8	9.6	3.4	9.4	24.4	11.3/13
p_T-Fit (W^+)	0.3	11.6	7.3	8.1	1.3	3.6	10.4	5.7	11.0	23.0	9.7/6
p_T-Fit (W^-)	-23.4	10.5	7.0	8.3	1.3	3.7	10.7	5.7	11.8	23.0	4.7/6
p_T-Fit ($W^\pm$)	-9.9	8.1	6.7	6.7	1.3	3.5	10.6	5.8	6.5	18.9	17.3/13
p_T-Fit (el)	-34.3	11.0	0	17.5	1.5	4.1	10.6	5.3	6.2	25.0	3.0/5
m_T-Fit (el)	-16.4	13.5	0	15.9	12.4	12.3	9.5	3.4	10.3	30.8	7.9/5
p_T-Fit (μ)	1.9	11.2	10.4	0	1.3	3.5	10.7	6.0	7.5	21.3	8.9/7
m_T-Fit (μ)	0.4	13.0	11.6	0	12.3	5.8	9.6	3.4	10.3	26.4	2.6/7
Combined-Fit (W^+)	-23.9	9.6	7.1	7.8	2.8	4.3	10.6	5.4	12.1	22.8	6.3/13
Combined-Fit (W^-)	0.6	10.2	7.6	7.8	2.8	4.3	10.3	5.3	11.3	22.6	15.2/13
Combined-Fit ($W^\pm$)	-9.8	7.1	7.0	6.2	2.9	3.9	10.5	5.3	6.9	18.6	28.1/27

Fitting range optimisation

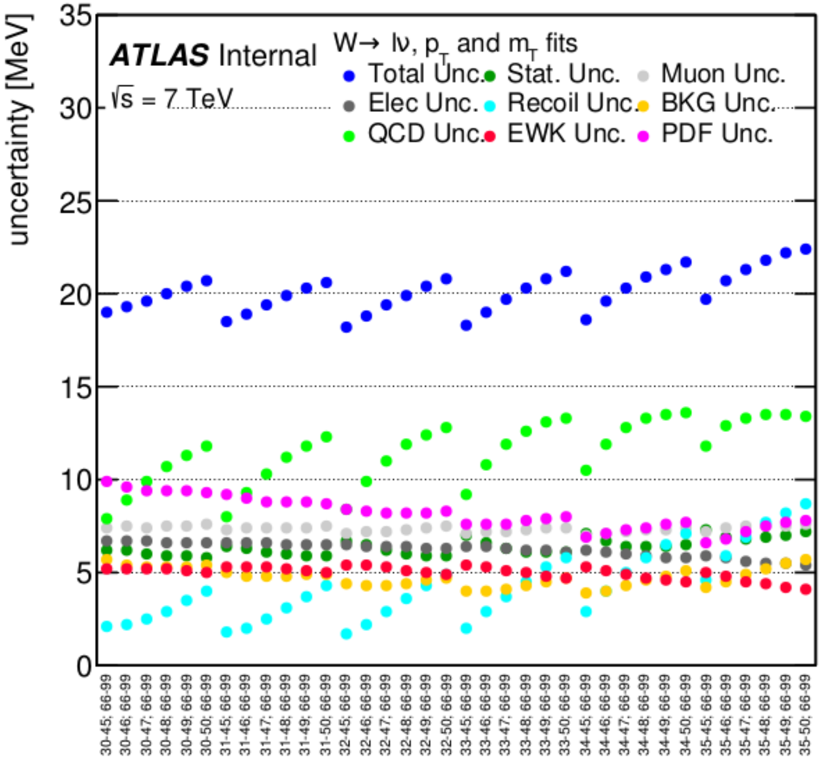

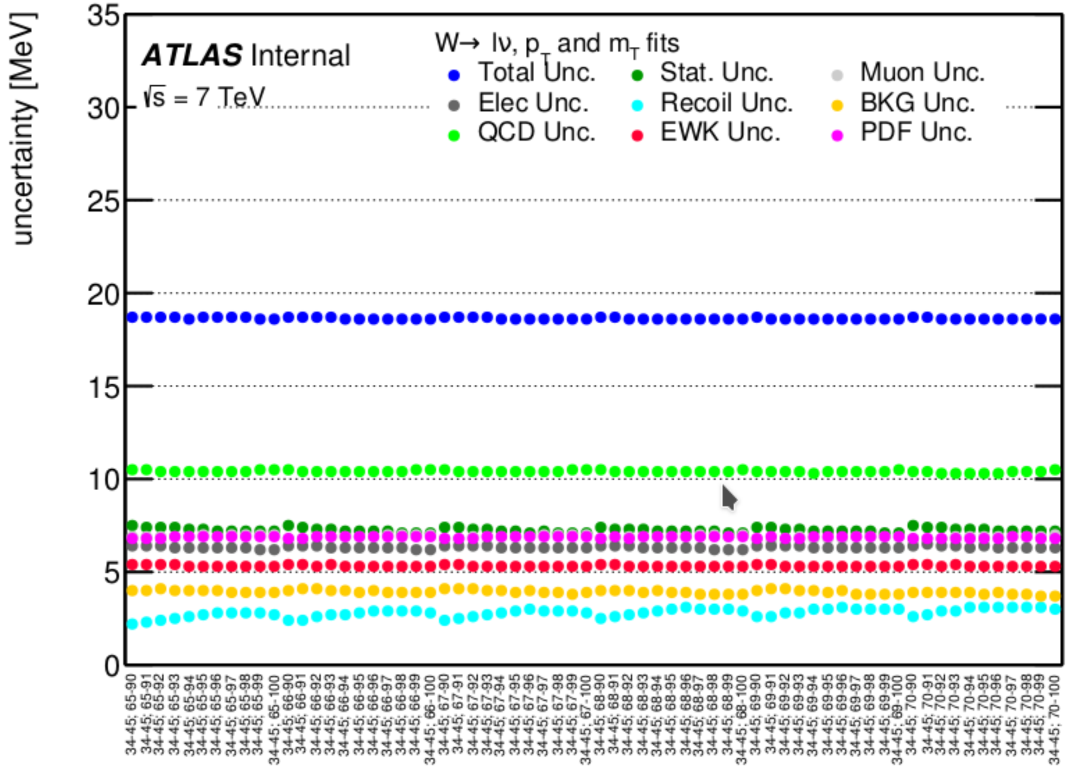

- Nominal range: p_Tl 30-50, m_T 65-100, δm_W = 20.8
- Optimal range: p_Tl 34-45, m_T 66-99, δm_W = 18.6

Final combination

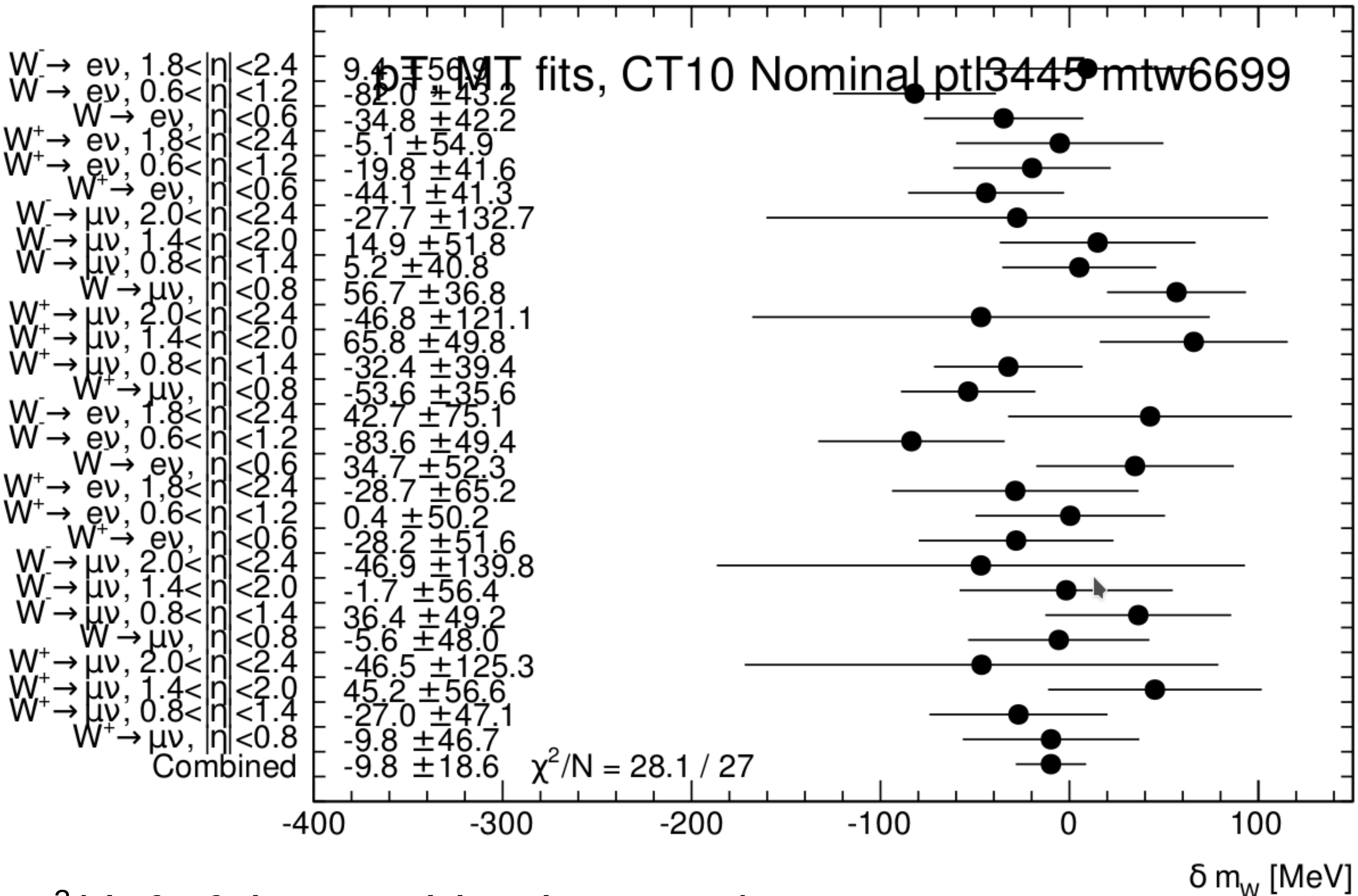

- χ^2/dof of the combination 28.1/27

Fitting range stability and cross checks

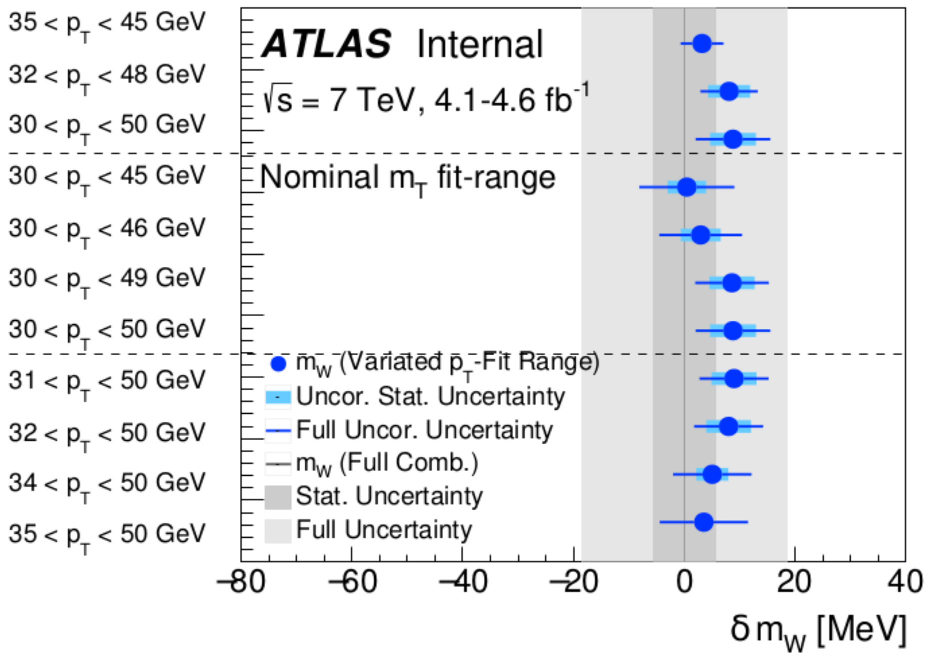

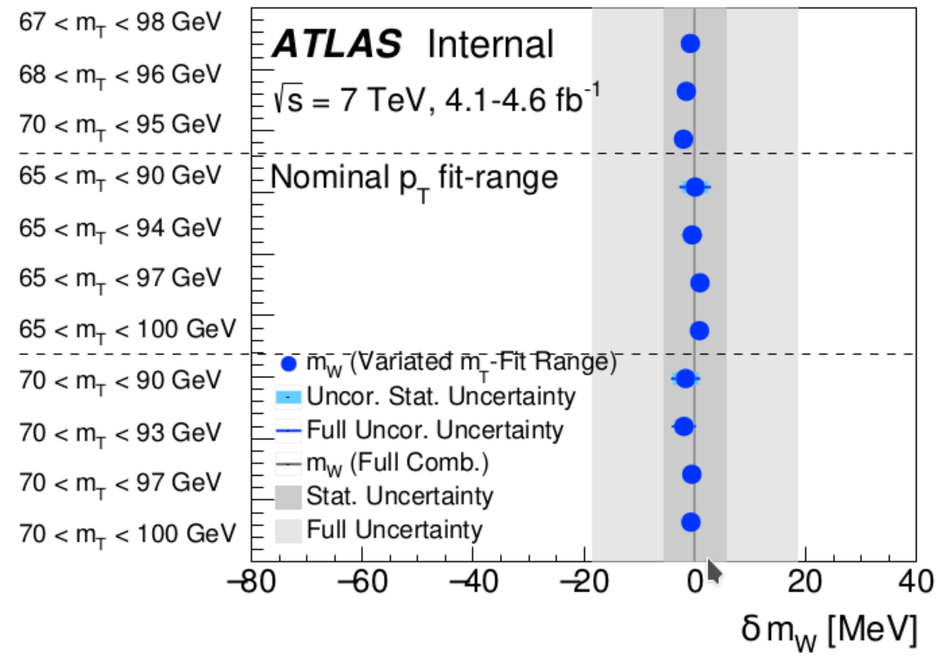

Measurement Category	$W \to e\nu$ p_T^ℓ-Fit Δm_W [MeV]	$W \to e\nu$ m_T-Fit Δm_W [MeV]	$W \to \mu\nu$ p_T^ℓ-Fit Δm_W [MeV]	$W \to \mu\nu$ m_T-Fit Δm_W [MeV]
$< \mu >$ in [2.5, 6.5]	8 ± 11	14 ± 12	-21 ± 9	0 ± 11
$< \mu >$ in [6.5, 9.5]	-6 ± 11	6 ± 19	12 ± 13	-8 ± 18
$< \mu >$ in [9.5, 16]	-1 ± 13	3 ± 22	25 ± 14	35 ± 23
$0 < p_T(W) < 15$ GeV	0 ± 3	-8 ± 3	5 ± 6	8 ± 5
$15 < p_T(W) < 30$ GeV	10 ± 12	0 ± 20	-4 ± 11	-18 ± 18
$u_{\parallel} < 0$ GeV	8 ± 11	20 ± 11	3 ± 10	-1 ± 11
$u_{\parallel} > 0$ GeV	-9 ± 5	1 ± 5	-12 ± 6	10 ± 6

- Compatible within statistical uncertainty

Summary

- The indirect determination of m_W from the global fit of the SM parameters has an uncertainty of 8 MeV which sets a natural target for the precision of the measurement of m_W
- We have achieved an uncertainty of 19 MeV on m_W which equal the uncertainty of the current best measurement by CDF
- The measurement relies on a thourough detector calibration, and on innovative strategy for the physics modelling, which combines theory predictions and fits and validation to experimental data
- Theoretical uncertainties, in particular PDF and pT W uncertainties, are the dominant uncertainties for the W mass

Prospects on physics modelling

- PDF uncertainties can be reduced by the inclusion of our precise W, Z inclusive rapidity measurement with 2011 data
- pT W uncertainties can be reduced by using higher-order predictions based on analytical resummation, and with fits to Z pT 8 TeV measurement, which is more precise than the 7 TeV measurement, and has low- and high-mass distributions which can constrain heavy-flavour-initiated production
- Much work was already done on the two points above, and there are plans to update the 7 TeV measurement with updated physics modelling
- Thanks to the precise measurement at 8 TeV, uncertainties on the angular coefficients are currently not a limiting factor. In the future they can be reduced with more precise predictions and more precise measurements.

Prospects on 8 and 13 TeV

- Larger data samples allow (in principle) more precise calibration, provided material, alignment, geometry, etc… are all well understood.
- However, larger data samples come with higher pile-up, which deteriorates recoil resolution. This could compromise the mT measurement, and reduce our ability to control and validate modelling uncertainties through uT and upar distributions.
- In order to benefit from the larger 8 and 13 TeV data samples, it is crucial to improve the methodology used for the recoil calibration.
- For the vaidation and constraint of the physics modelling, we need to perform precise measurements of W pT, either with low pile-up runs, or with new methodologies.

Recoil calibration

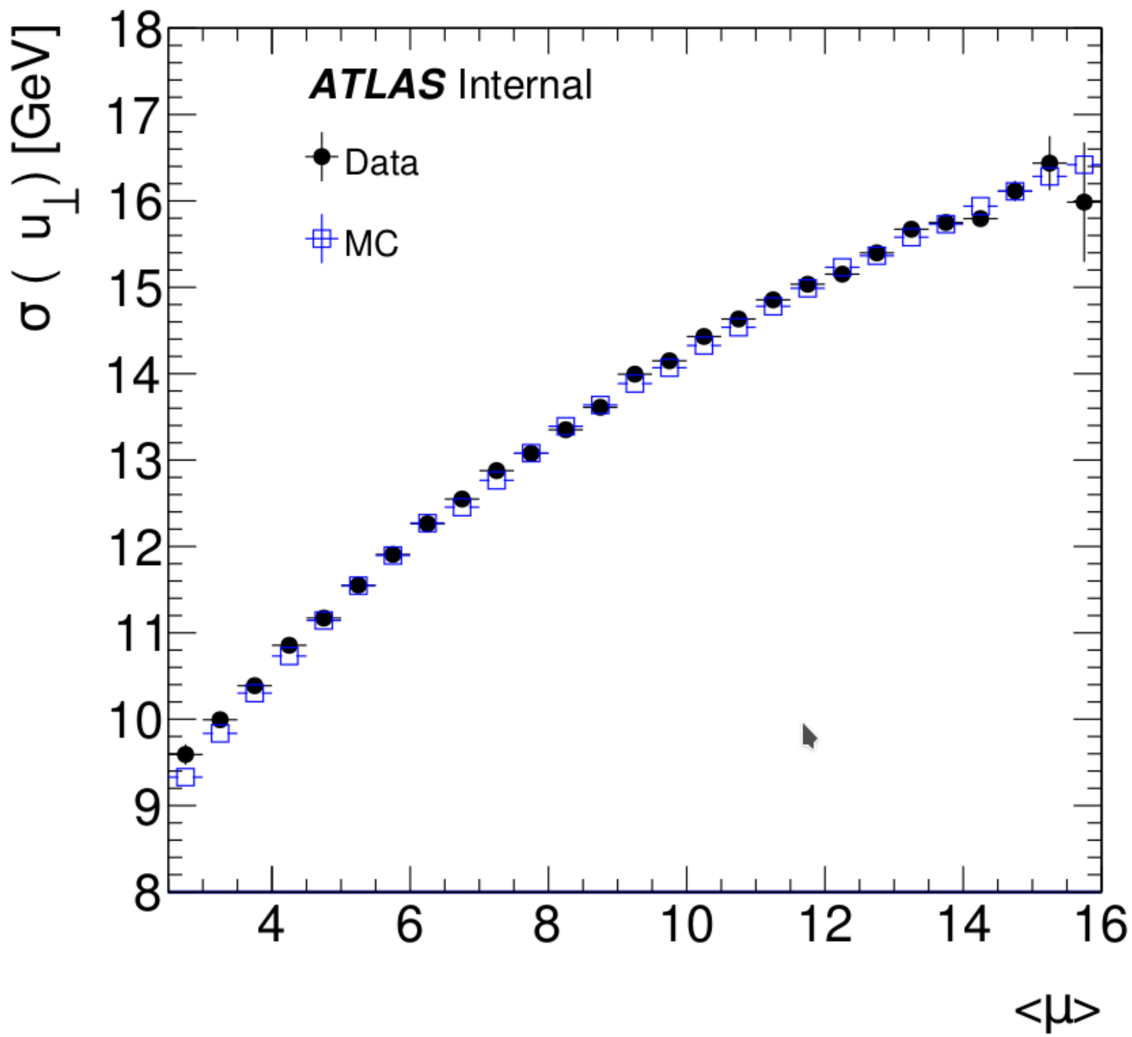

- The recoil resolution rapidly deteriorates with increasing pile-up conditions

BACKUP

Control plots

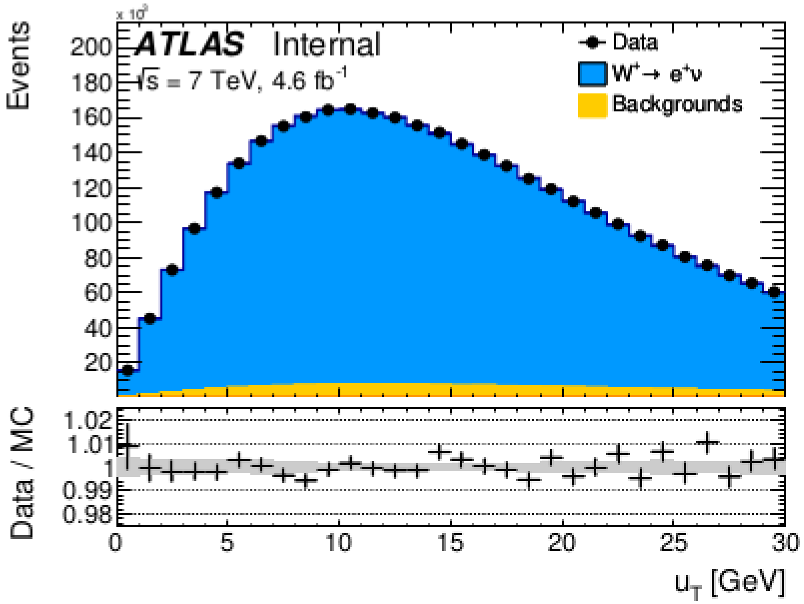

(c)

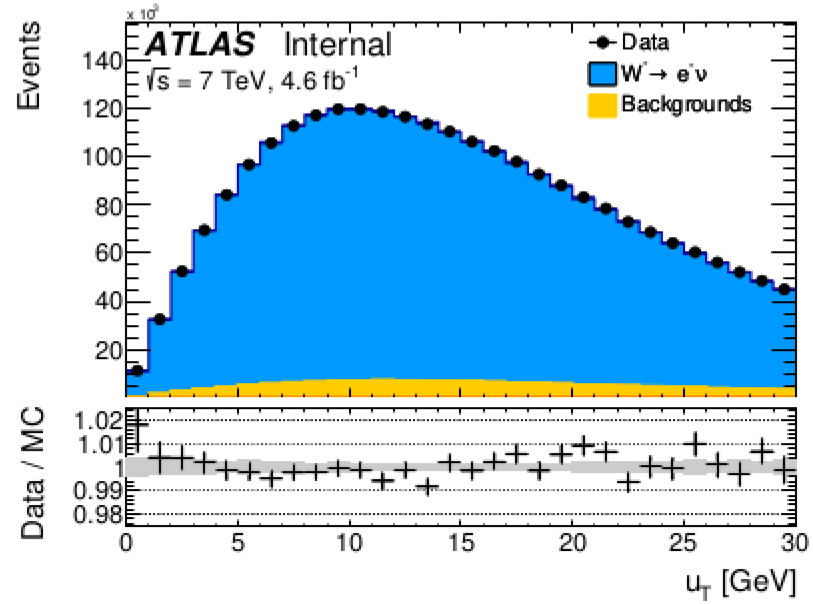

(d)

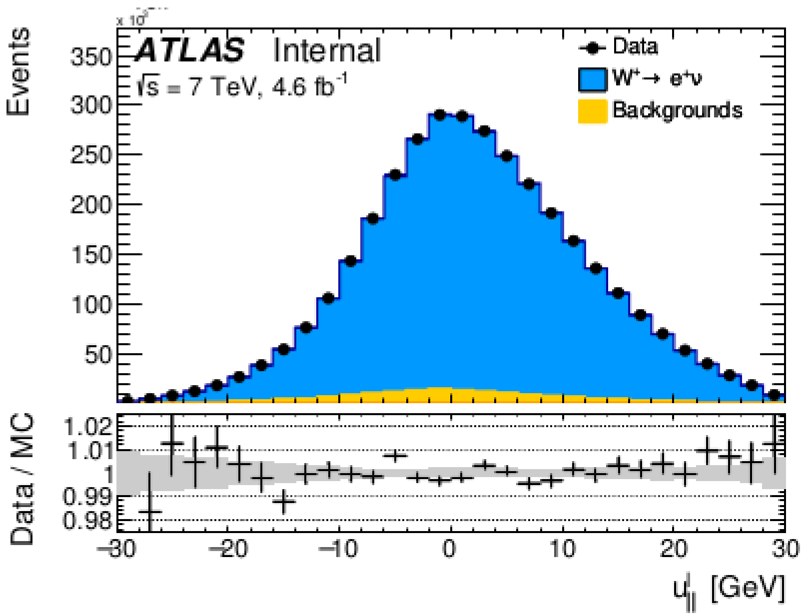

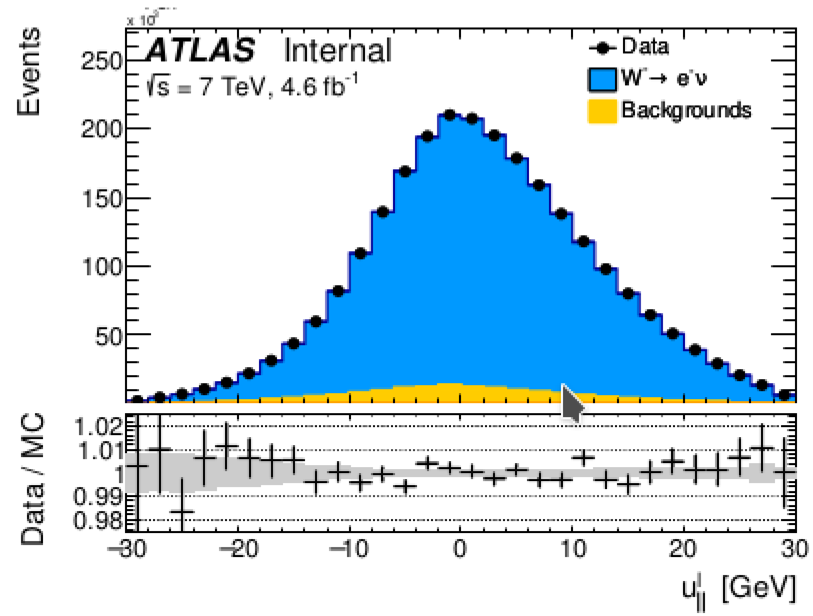

Control plots

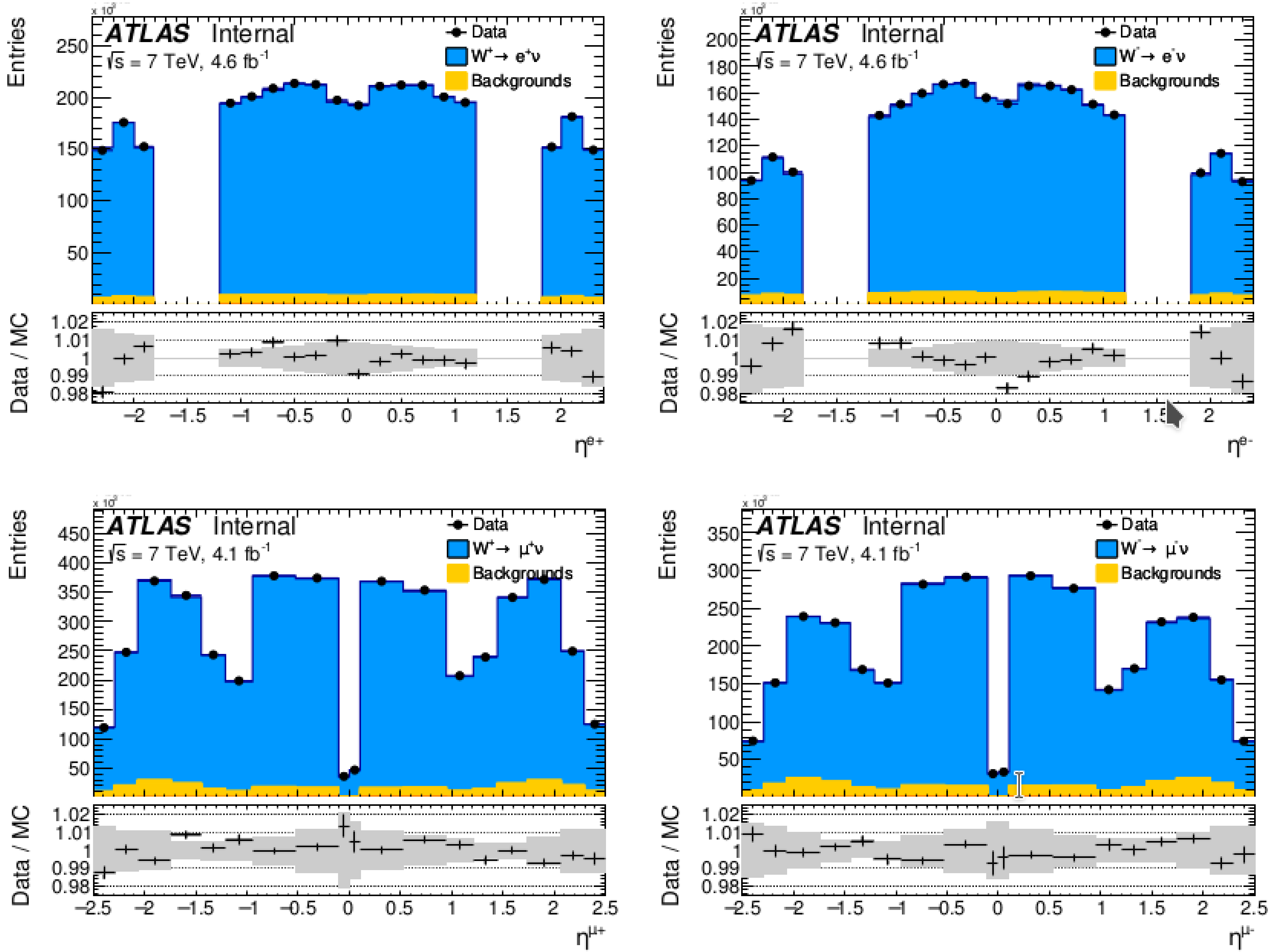

χ^2 table – muon

Distribution	Category	Stat.	Stat+Syst (diag.)	Full	n_{dof}	Full (opt.)	n_{dof} (opt.)
p_T^μ	Inclusive, W^+	36.3	16.2	21.9	39	14.4	21
	Inclusive, W^-	29.8	16.8	28.8	39	14.2	21
	$0 < \|\eta\| < 0.8$, W^+	44.0	32.1	35.4	39	25.0	21
	$0 < \|\eta\| < 0.8$, W^-	41.4	31.0	38.7	39	19.5	21
	$0.8 < \|\eta\| < 1.4$, W^+	29.8	23.5	27.6	39	17.4	21
	$0.8 < \|\eta\| < 1.4$, W^-	24.4	19.4	23.5	39	16.2	21
	$1.4 < \|\eta\| < 2.0$, W^+	36.0	26.9	25.7	39	17.2	21
	$1.4 < \|\eta\| < 2.0$, W^-	34.2	28.0	32.0	39	20.6	21
	$2.0 < \|\eta\| < 2.4$, W^+	40.5	27.8	33.4	39	23.5	21
	$2.0 < \|\eta\| < 2.4$, W^-	44.1	30.3	42.1	39	19.8	21
m_T	Inclusive, W^+	76.5	62.1	71.6	79	57.8	65
	Inclusive, W^-	71.2	61.1	68.2	79	62.7	65
	$0 < \|\eta\| < 0.8$, W^+	86.5	78.5	84.6	79	58.1	65
	$0 < \|\eta\| < 0.8$, W^-	75.3	71.0	74.7	79	57.1	65
	$0.8 < \|\eta\| < 1.4$, W^+	70.2	64.6	68.0	79	61.3	65
	$0.8 < \|\eta\| < 1.4$, W^-	106.1	101.3	105.4	79	87.8	65
	$1.4 < \|\eta\| < 2.0$, W^+	61.4	56.0	58.4	79	46.3	65
	$1.4 < \|\eta\| < 2.0$, W^-	74.1	70.5	73.3	79	64.0	65
	$2.0 < \|\eta\| < 2.4$, W^+	76.1	61.3	71.4	79	49.6	65
	$2.0 < \|\eta\| < 2.4$, W^-	71.0	63.8	69.2	79	60.8	65

χ^2 table – electron

Distribution	Category	Stat.	Stat+Syst (diag.)	Full	n_{dof}	Full (opt.)	n_{dof} (opt.)
p_T^e	Inclusive, W^+	74.4	39.5	39.6	39	26.9	21
	Inclusive, W^-	41.0	25.6	31.7	39	20.2	21
	$0 < \|\eta\| < 0.6$, W^+	58.6	43.1	47.1	39	32.3	21
	$0 < \|\eta\| < 0.6$, W^-	38.4	28.3	32.0	39	20.2	21
	$0.6 < \|\eta\| < 1.2$, W^+	38.8	28.2	30.2	39	19.9	21
	$0.6 < \|\eta\| < 1.2$, W^-	40.3	31.9	29.1	39	19.8	21
	$1.8 < \|\eta\| < 2.4$, W^+	60.7	36.6	31.6	39	17.2	21
	$1.8 < \|\eta\| < 2.4$, W^-	49.1	36.9	39.5	39	28.5	21
m_T	Inclusive, W^+	72.2	62.4	69.5	79	53.8	65
	Inclusive, W^-	78.5	70.4	77.1	79	55.7	65
	$0 < \|\eta\| < 0.6$, W^+	95.6	89.6	93.7	79	76.4	65
	$0 < \|\eta\| < 0.6$, W^-	69.9	65.7	66.2	79	44.8	65
	$0.6 < \|\eta\| < 1.2$, W^+	60.9	56.3	58.9	79	50.8	65
	$0.6 < \|\eta\| < 1.2$, W^-	87.1	82.3	80.3	79	58.9	65
	$1.8 < \|\eta\| < 2.4$, W^+	84.6	73.9	80.8	79	71.7	65
	$1.8 < \|\eta\| < 2.4$, W^-	90.3	83.5	87.1	79	66.1	65

Post fit plots

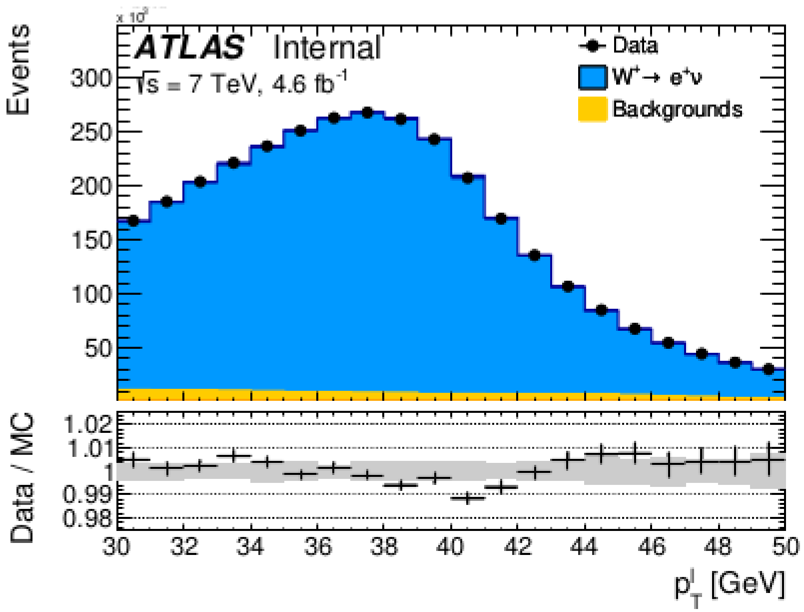

(a)

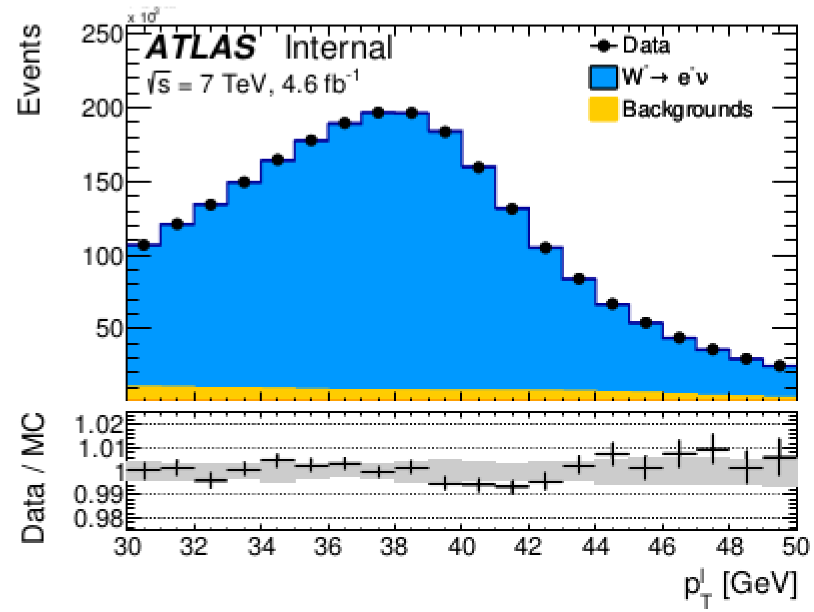

(b)

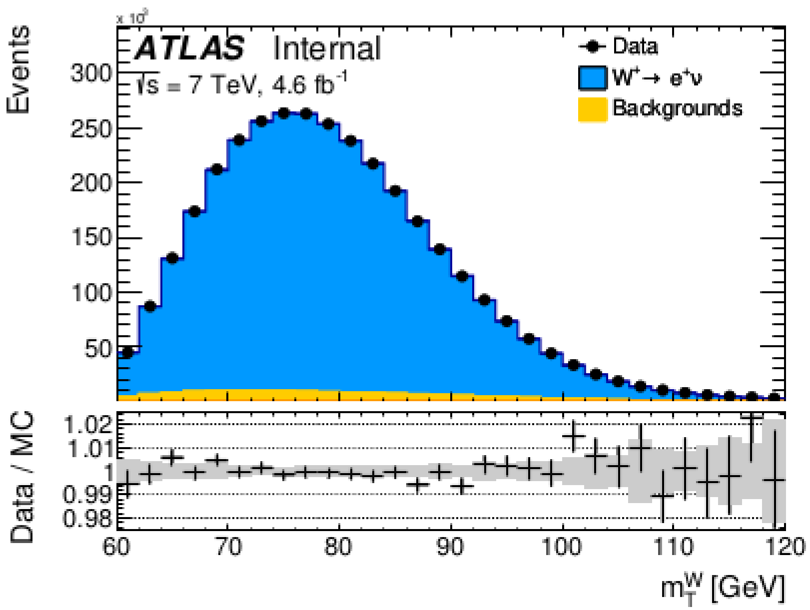

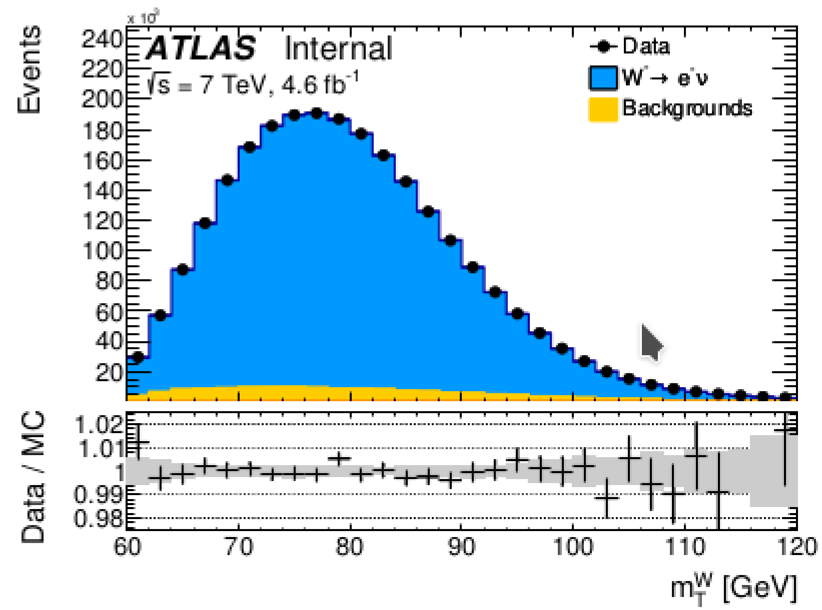

Post fit plots

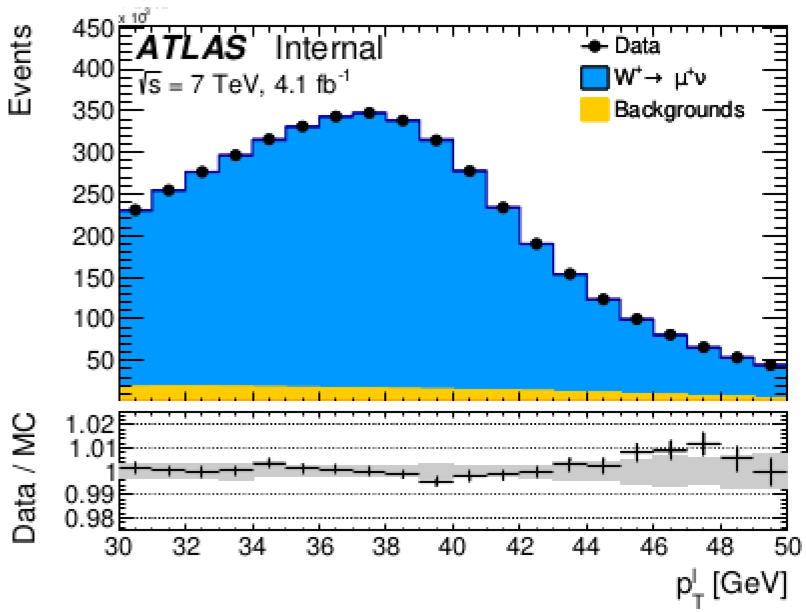

(a)

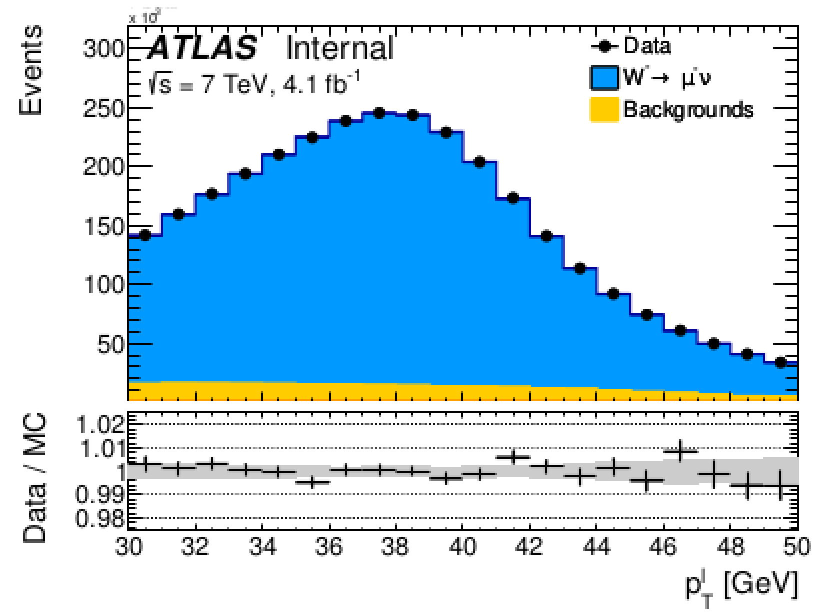

(b)

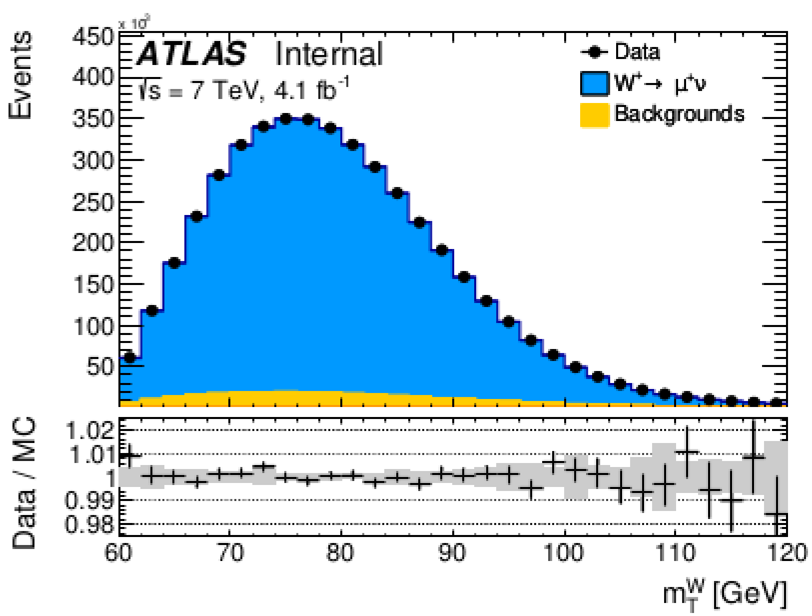

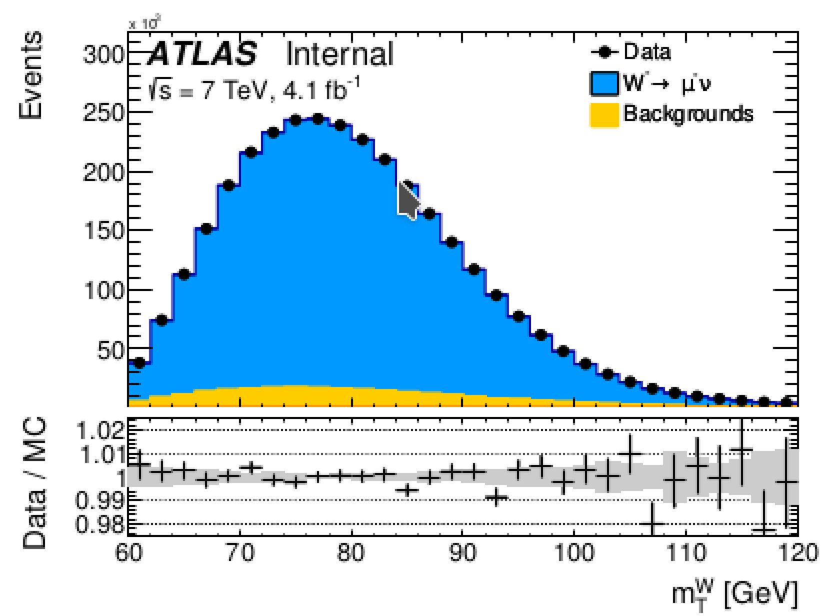

Fitting range stability

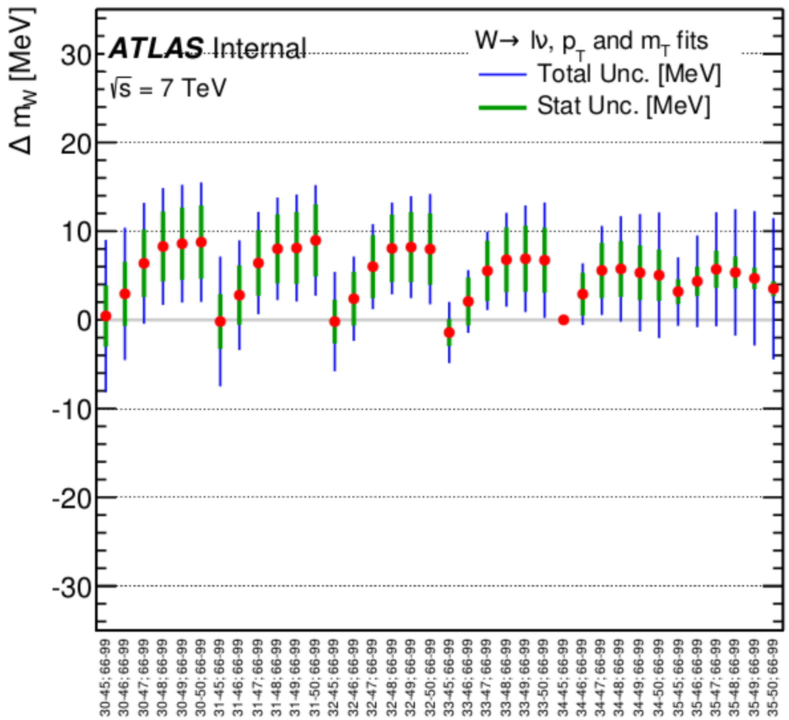

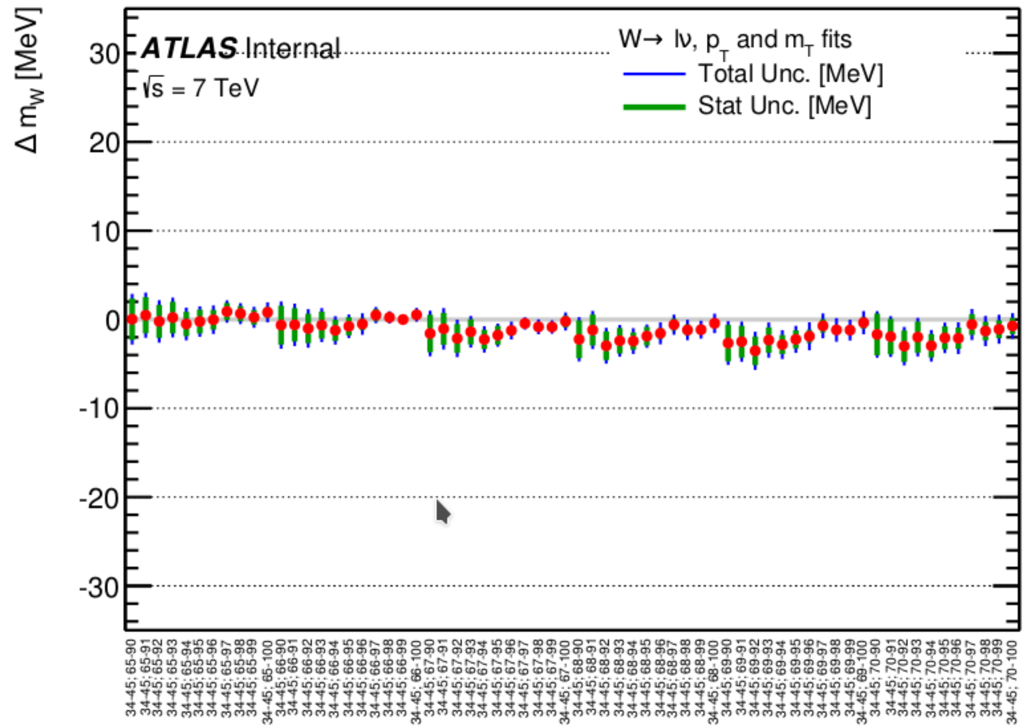

Methodology for the W mass extraction

- Event selection: W leptonic decay
  $W \rightarrow l\,\nu,\ l = e,\ \mu$
- The full kinematic of the W decay cannot be reconstructed, since the longitudinal momentum of the neutrino is unknown

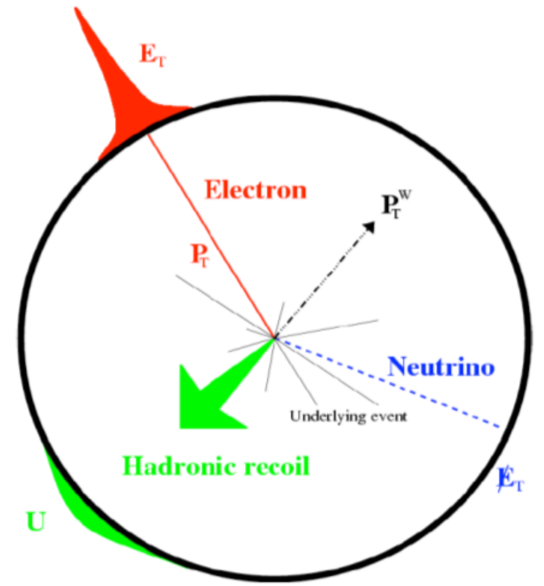

The analysis is based on a template fit extraction from observables sensitive to M_W

Lepton transverse momentum	p_T^l
W transverse mass	$M_T = \sqrt{2 \cdot p_T^l p_T^\nu \cdot (1 - \cos\Delta\phi(l,\nu))}$
Neutrino transverse momentum (from hadronic recoil)	p_T^ν (Not used)

A key ingredient of the W mass measurement is to use $Z \rightarrow ll$ events to constraint both experimental and theory systematics

Theoretical uncertainties

List of theoretical uncertainties:

1st generation quarks (u,d)

2nd generation quarks (charm,strange)

3rd generation quarks (bottom)

PDF

Higher order corrections to the W boson polarisation

Soft-gluon resummation

Non-perturbative Sudakov form factor (or primordial kT)

QCD

Higher order EW corrections

QED ISR and FSR

EW

PDF uncertainties for the W mass

- Sea quarks composition of protons is charge symmetric

  → same amount of q_s and $\bar{q}_s$ from sea
- Valence quarks determines a charge asymmetry in the proton:

$u = u_v + u_s \qquad \bar{u} = \bar{u}_s$

$d = d_v + d_s \qquad \bar{d} = \bar{d}_s$

What is the effect of this valence asymmetry for Charged Current Drell-Yan (W-boson) production?

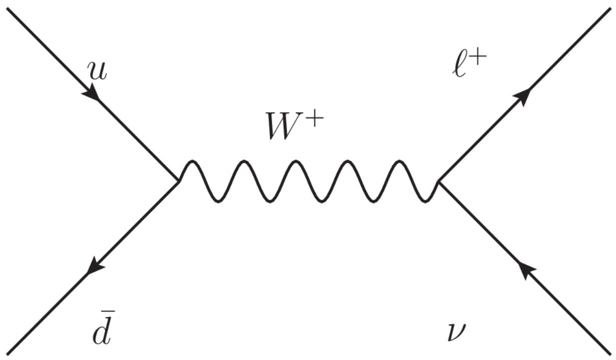

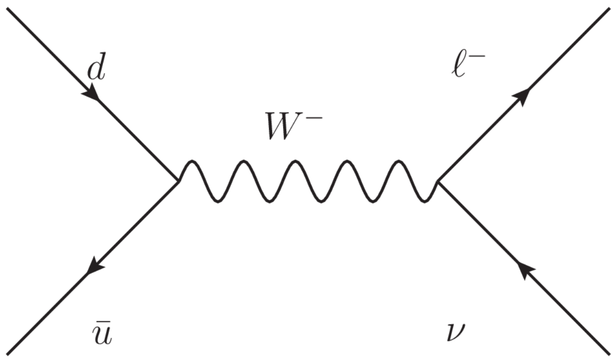

PDF uncertainties for the W mass

- In proton-antiproton collision
- Asymmetry of the W rapidity
- Same cross section for W+ and W-
- Valence-dominated production
- Very small ambiguity for the incoming parton: quark from proton, antiquark from antiproton

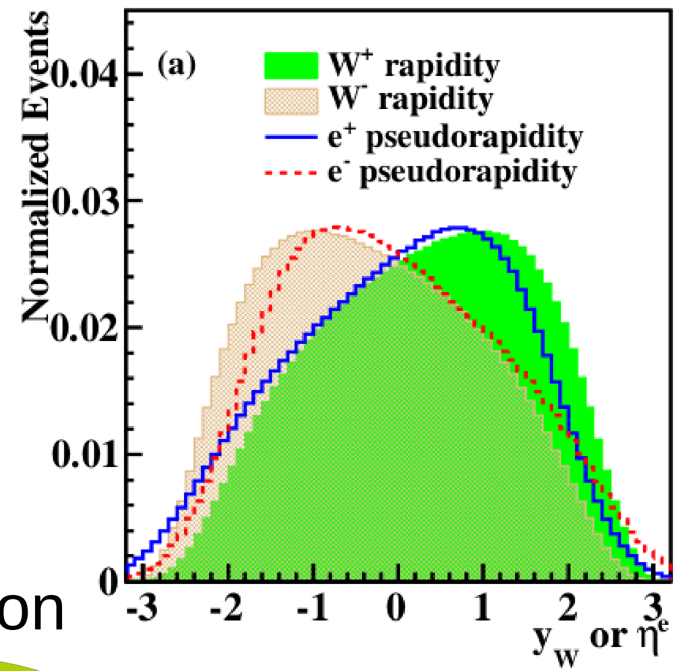

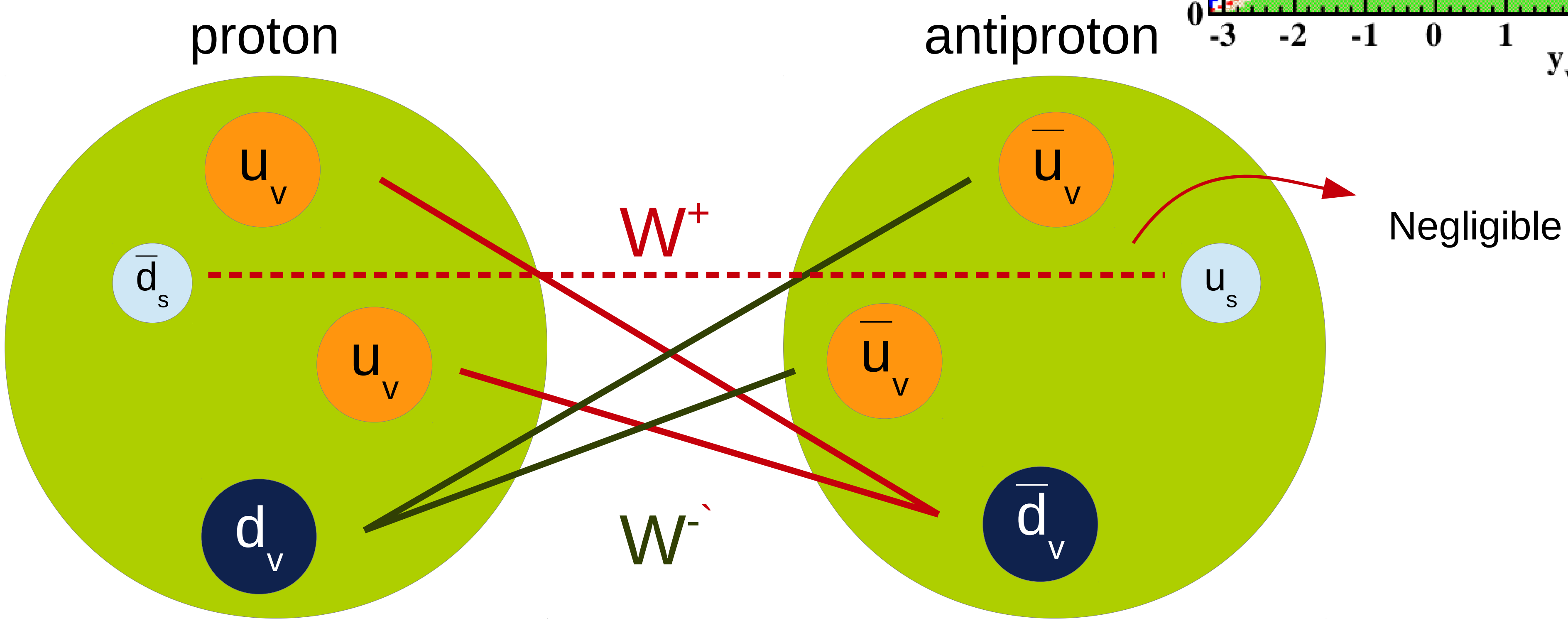

PDF uncertainties for the W mass

- In proton-proton collision
- Different cross section for W+ and W-
- Large ambiguity in the direction of the incoming quark

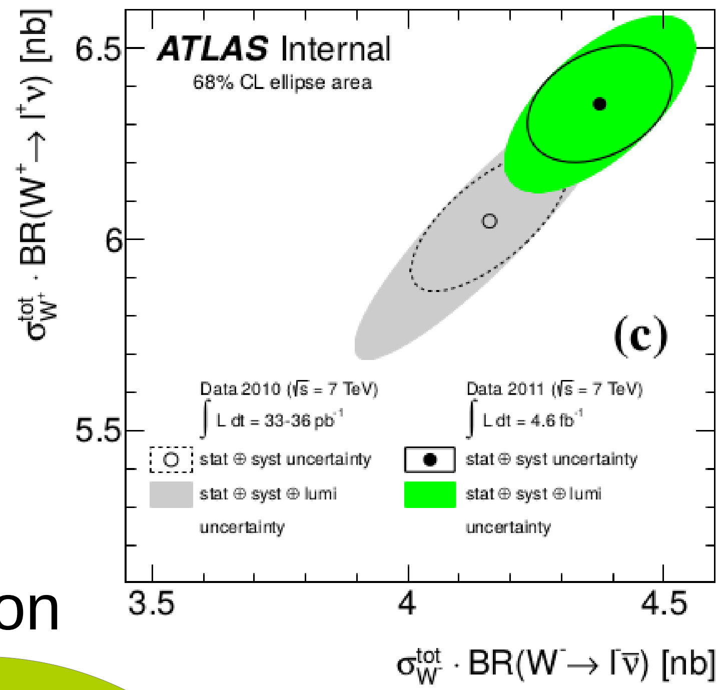

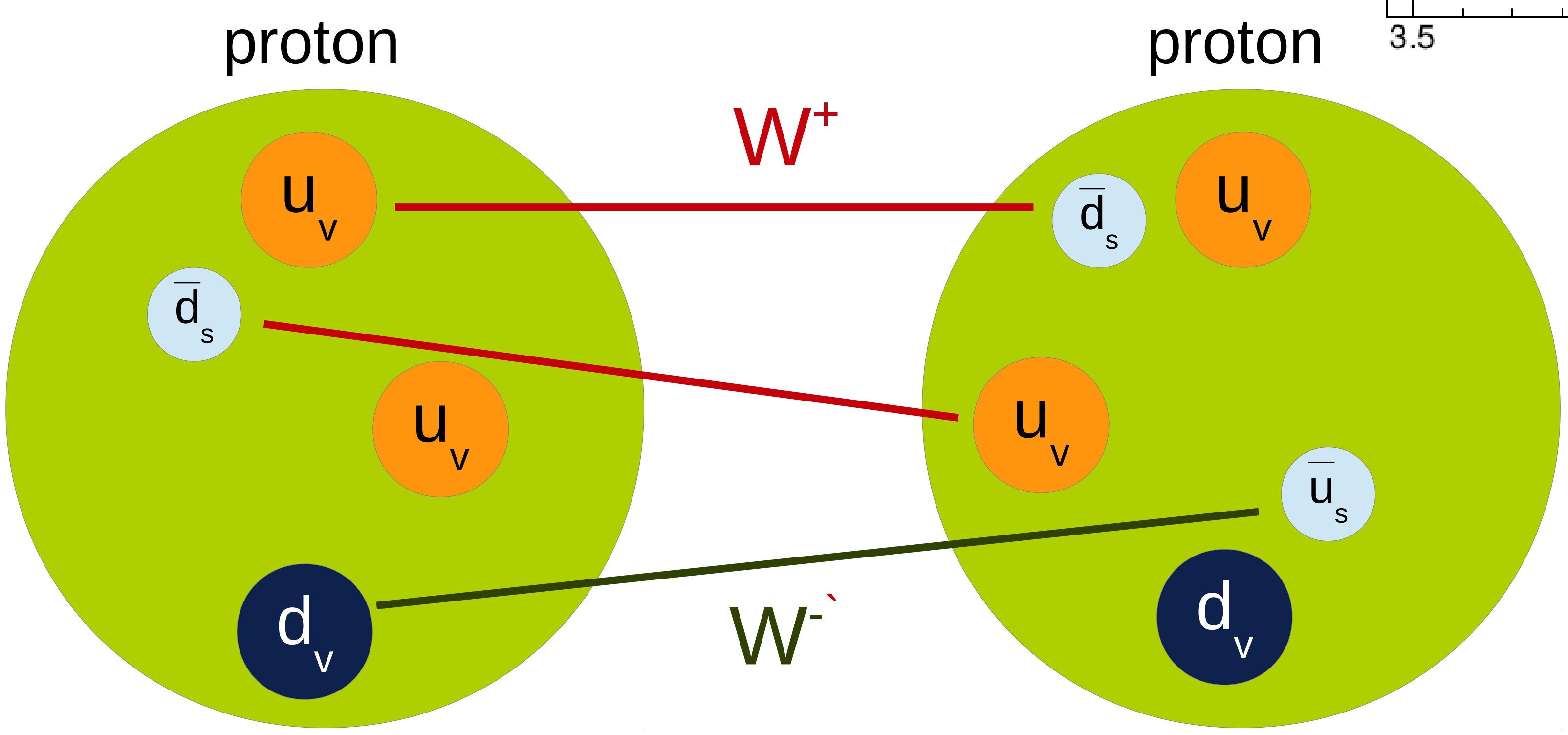

PDF uncertainties for the W mass

- What is the consequence of the ambiguity in the direction of the incoming quark?

$$\sigma_{W^+}(y) \propto u(x_1) \cdot \bar{d}(x_2) + \bar{d}(x_1) \cdot u(x_2)$$
$$\sigma_{W^-}(y) \propto d(x_1) \cdot \bar{u}(x_2) + \bar{u}(x_1) \cdot d(x_2)$$

- The helicity is the projection of the spin on the momentum axis
- The W is a spin 1 particle, with 3 possible helicity states: λ = +1,0,-1
- Ambiguity in the average helicity of the W (polarisation)

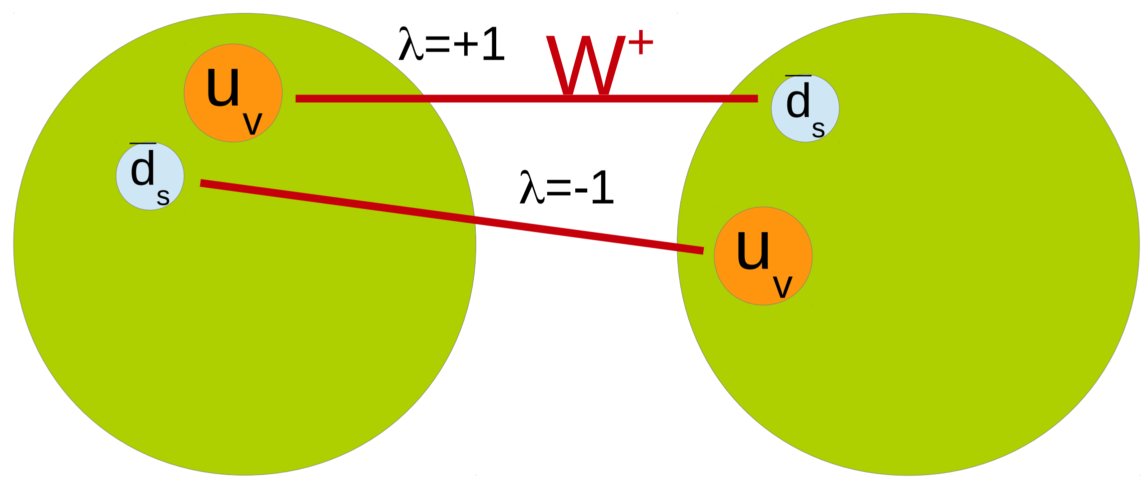

PDF uncertainty → polarisation uncertainty

W polarisation

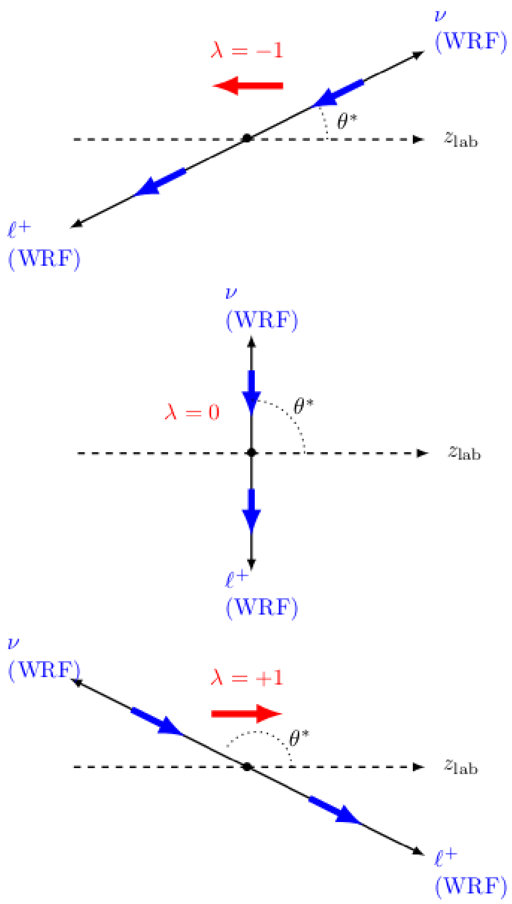

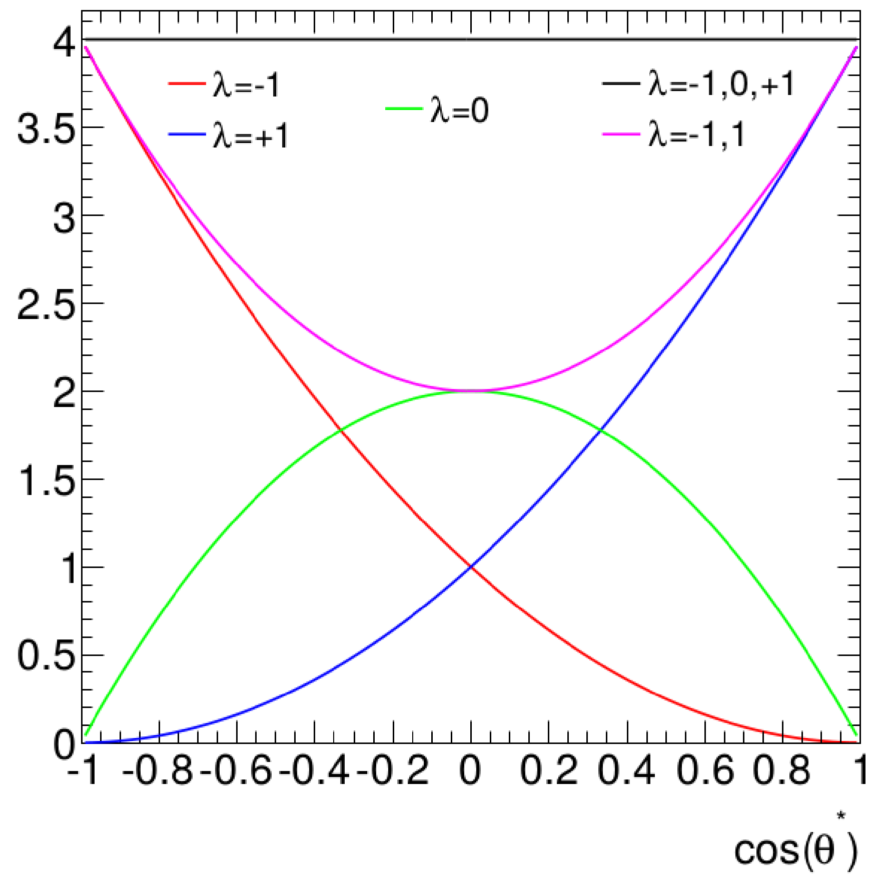

- The 3 helicity states have very different decay polar angles
- The average polarisation heavily affects the lepton kinematic

W polarisation

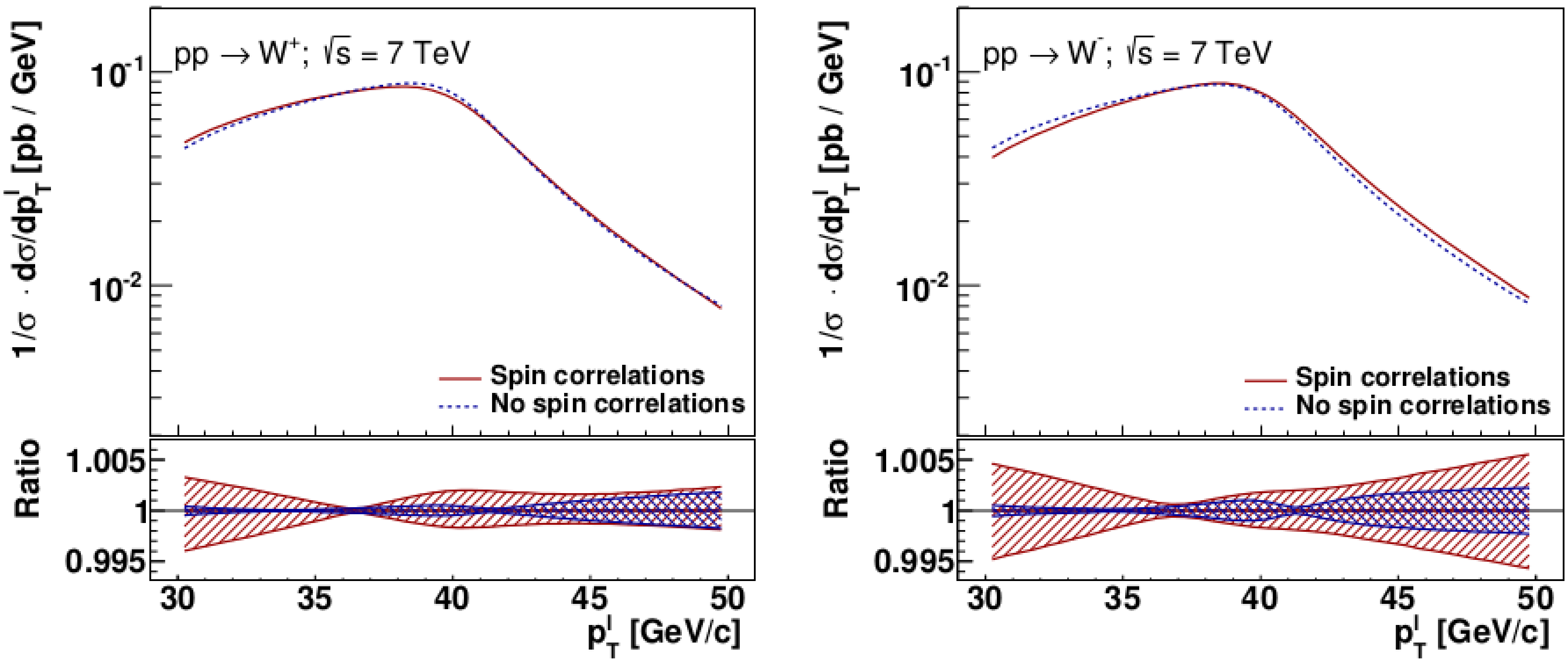

- We can artificially remove the ambiguity in the W helicity by removing spin correlations → Unpolarised W
- Dramatic effect on PDF uncertainties of lepton p_T distribution

Propagate PDF uncertainties to W mass

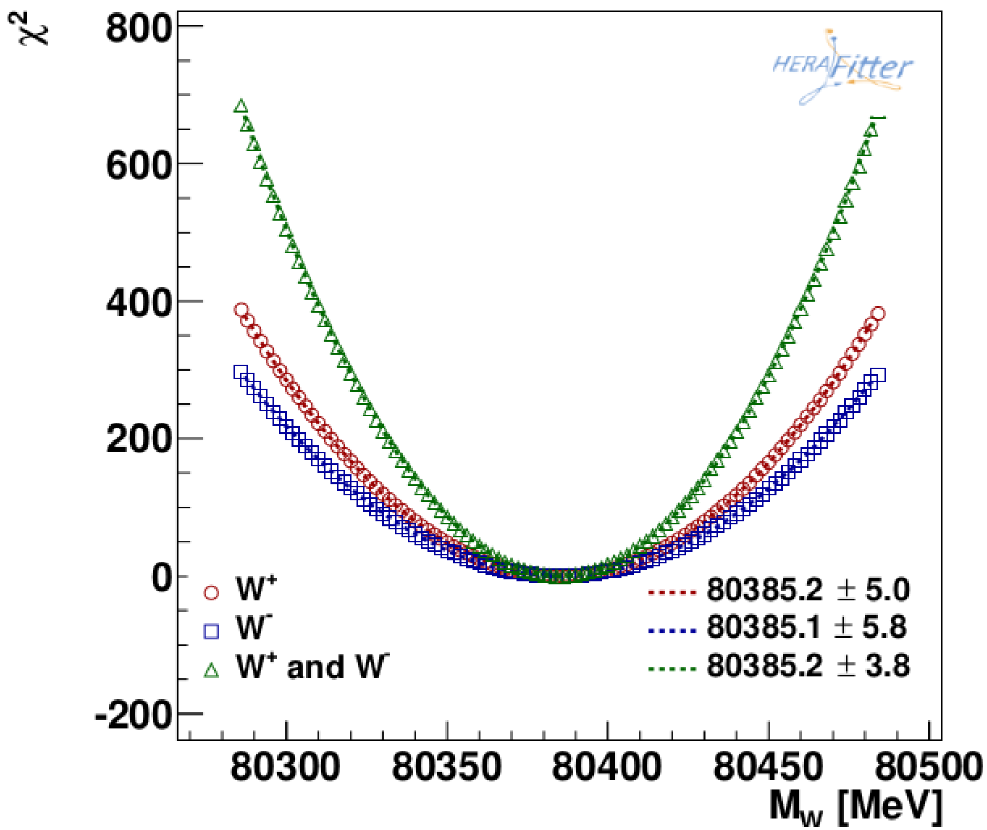

- Template fit of lepton p_T
- Fit the χ^2 profile with a parabolic function to find minimum and sigma at $\Delta\chi^2 = 1$
- Extract the minimum for each hessian or MC-replica PDF variation
- Calculate PDF uncertainty from the difference between the minimum for the central PDF and each PDF variation

W polarisation

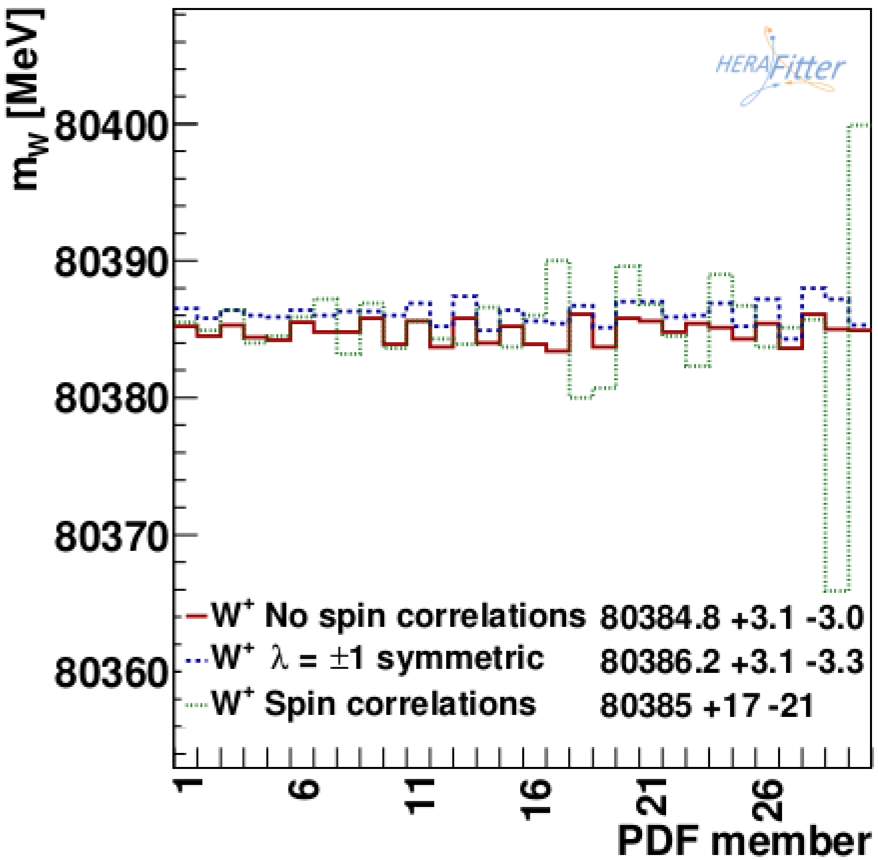

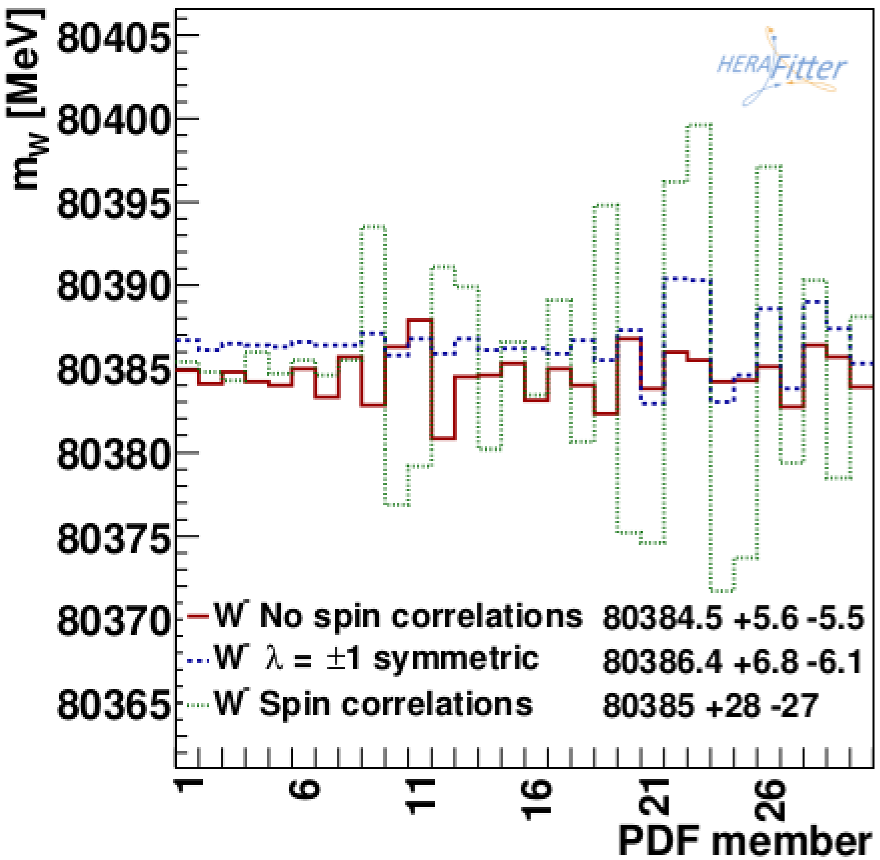

- This effect accounts for 20 (30) MeV uncertainty to the W mass extracted from W+ (W-) lepton p_T

The effect of the charm mass

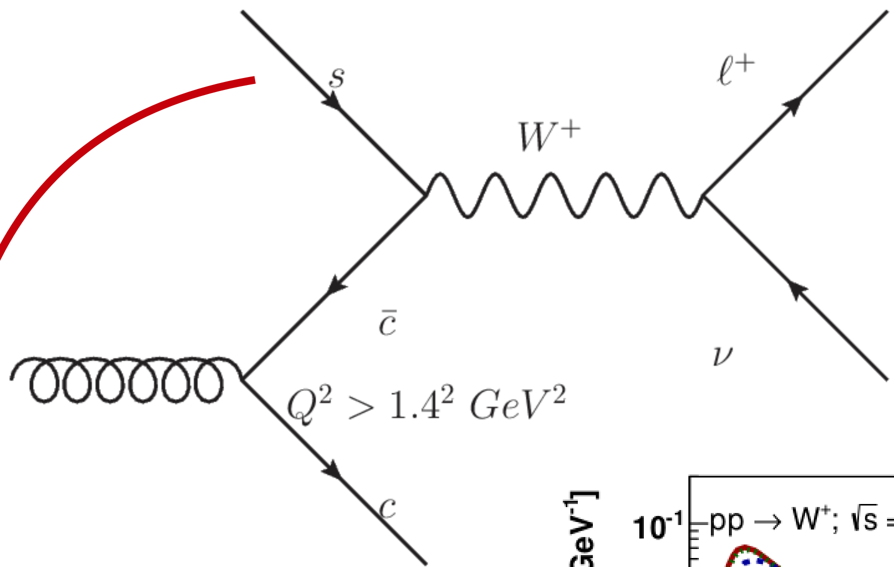

- A charm in the initial state must have come from a gluon splitting above the charm mass
- Additional recoil of about 1 GeV, harder p_T spectrum

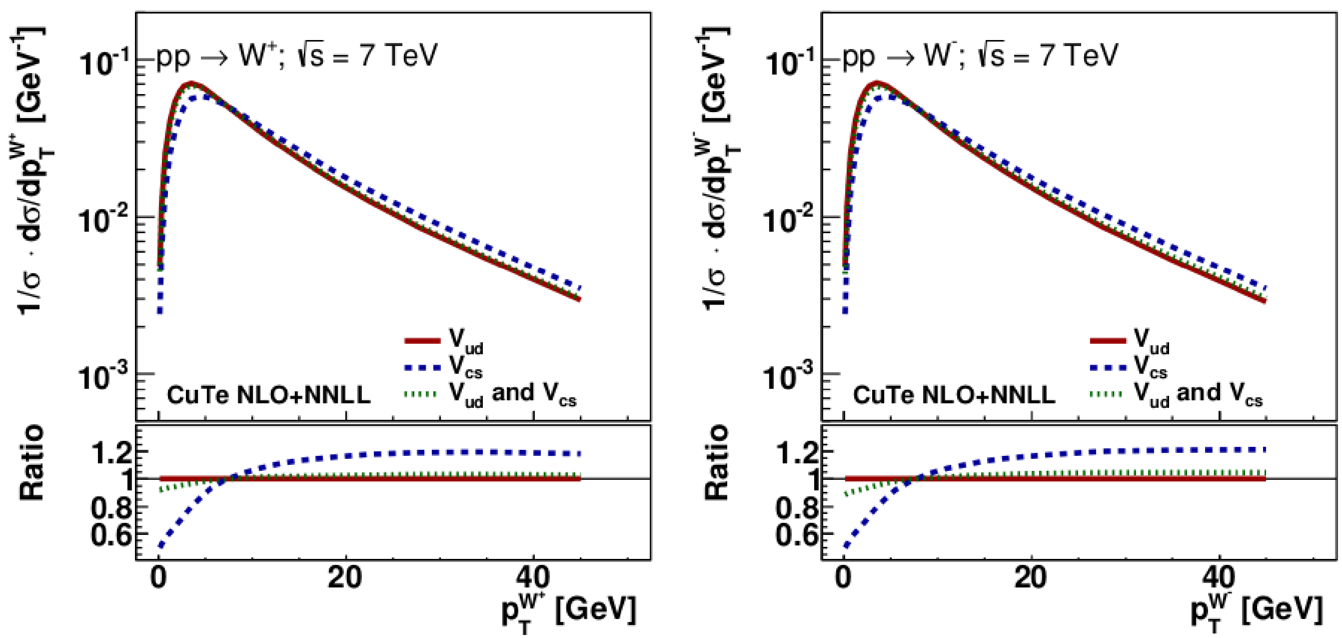

- The uncertainty on the strange PDF translates into an uncertainty on the charm-initiated W production

The effect of the charm mass

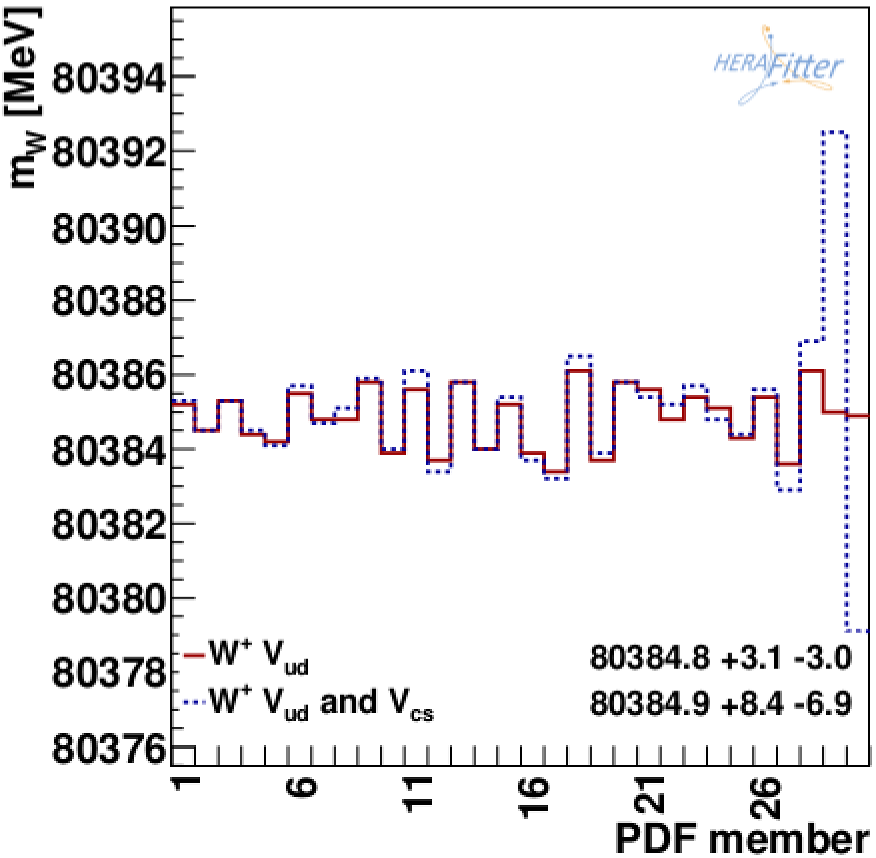

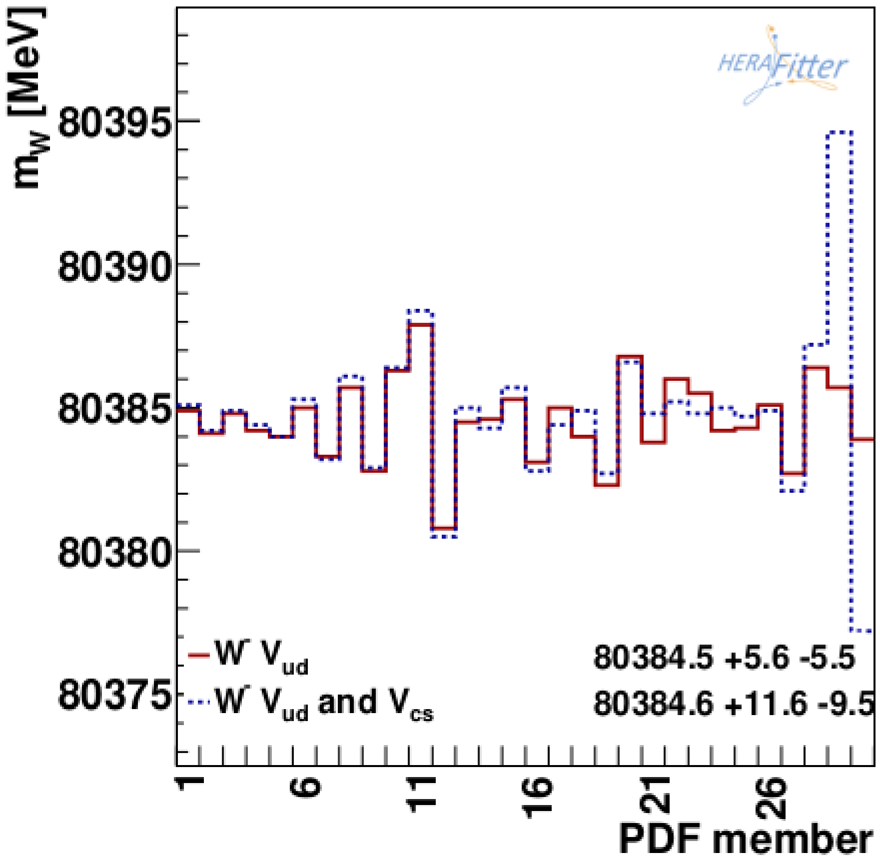

The uncertainty on the strange PDF accounts for 7-9 MeV on the W mass extracted from the lepton p_T

Prospects for M_W at ILC and TLEP

M_W can be measured at e^+e^- colliders through an energy scan of the WW production threshold

Near threshold, the WW cross section is proportional to the non-relativistic W velocity

$$\sigma(WW) \propto \beta_W$$

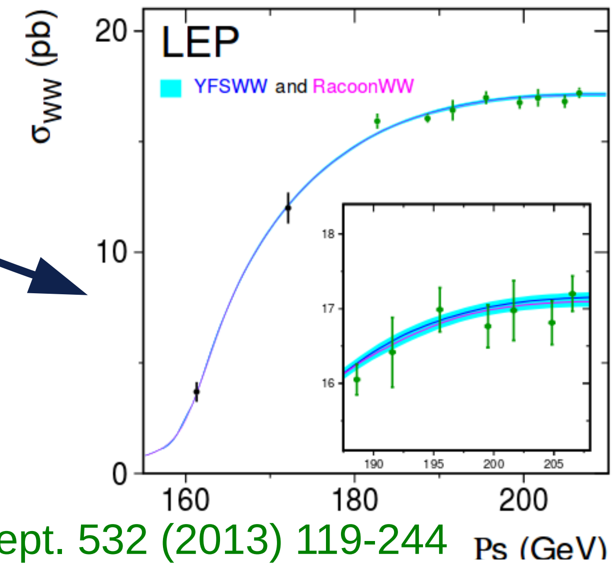

Phys.Rept. 532 (2013) 119-244

arXiv:1306.6352

ILC Giga-Z program

- Energy scan 160 to 170 GeV
- δM_W = 6-7 MeV

JHEP 1401 (2014) 164

TLEP OkuW program

- δM_W = 0.5 MeV

  → dominated by statistical uncertainty

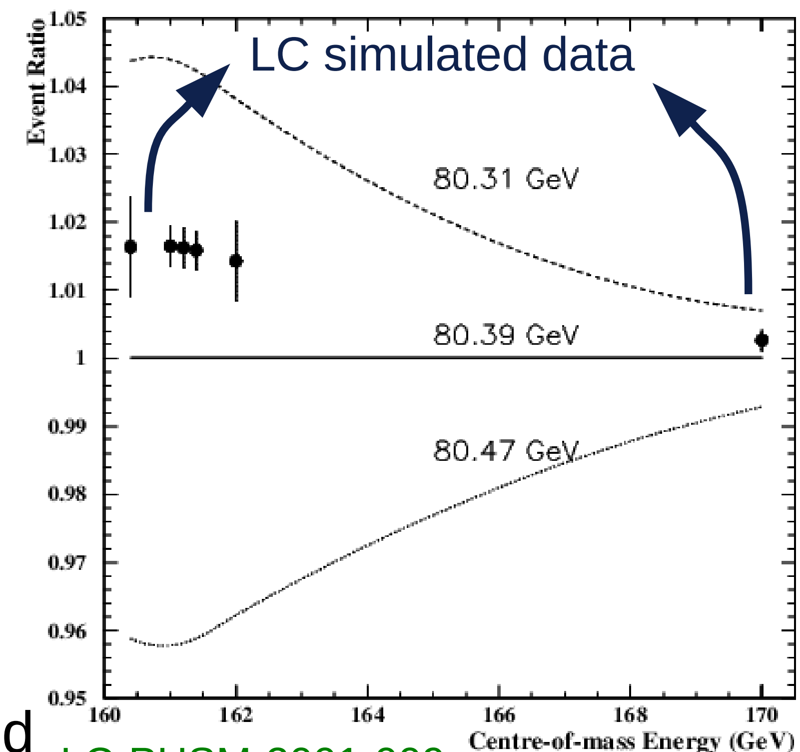

LC-PHSM-2001-009

Dominant theory uncertainties

- Initial state QED corrections
- Parametrization of cross section near threshold